MODELLING RAINFALL-RUNOFF PROCESSES IN KABUL RIVER BASIN USING ARCSWAT MODEL

A Thesis Submitted to
the Graduate School
İzmir Institute of Technology
in Partial Fulfilment of the Requirements for the Degree of

MASTER OF SCIENCE

in Civil Engineering

by
Hamidullah TANI

September 2020
İZMİR

ACKNOWLEDGEMENTS

Thanks to almighty Allah for giving me the strength and energy to perform such a complex task. I would like to express my gratitude to **Prof. Dr. Gökmen TAYFUR** for taking me under his wing and providing insightful guidance and mentoring. I would like to thank our prestigious **IYTE** and their staff especially our librarians who had provided me with all the necessary materials on time to write this thesis. I cannot express my gratitude in word for Turkey and their people for their hospitality and providing me opportunity upon opportunity to study Bachelors and Masters at one of their prestigious Institute, a favor I fear I cannot return.

I would like to thank my family especially my father whose resolute support kept me going through all this. My mother's late night prayers have finally been answered, my brothers Taj Mohammad, Siraj Mohammad and Dr. Shams Ur Rehman have always been supportive and believed in me for which I am grateful. I cannot express my love in words to my daughter Aneesa as she had been the inspiration for me to accomplish this task, even during difficult periods her laughter had rejoiced me and had given me new hope and inspiration.

Ministry of Energy and Water Afghanistan has been a big help in providing all the relevant data for my research for which I am forever in their debt.

I would like to acknowledge the help of my dear friend Mr. Feda M. Tanai for his help in organizing my research thesis.

ABSTRACT

MODELLING RAINFALL-RUNOFF PROCESSES IN KABUL RIVER BASIN USING ARC SWAT MODEL

SWAT model is applied to Kabul River Basin (KRB) located in Afghanistan to assess the runoff. KRB is located between latitudes 33 ˚ N and 37 ˚ N, and longitudes 67 ˚ E and 74 ˚ E, with a drainage area of 72000 km^2. This study (1) determines the most sensitive parameters that affect the catchment flow, (2) estimates monthly and daily flows of the basin from the available meteorological stations data, (3) calibrates and validates the simulated and observed flow data for different hydrological stations located in the basin, and (4) determines the total amount of surface runoff and water yield in the basin.

SWAT-CUP is applied for the sensitivity analysis. Initially 27 different sensitive parameters effecting the runoff are tasted and 20 most sensitive ones are found. Among these, GWQMN.gw (Treshold depth of water in the shallow aquifer required for return flow to occur), SMTMP.bsn (Snow melt base temperature), CN2.mgt (SCS runoff curve number II), PLAPS.sub (Precipitation lapse rate), and HRU_SLP.hru (Average slope steepness) are found to be the most sensitive parameters.

The predicted flow is calibrated and validated against the measured flow for seven different Hydrological Stations both on a monthly and daily time scales. The performance of the model is checked by applying R^2, NSE, and the RSR. Overall, the model's monthly simulation flow is superior to the daily simulation.

Keywords: Rainfall-Runoff modelling, SWAT model, SWAT-CUP, Kabul River Basin

ÖZET

KABUL NEHİR HAVSAZINDA YAĞIŞ-AKIŞ OLAYLARININ ARC SWAT MODELİ KULLANILARAK MODELLENMESİ

SWAT modeli USDA-ARS tarafından geliştirilmiş olan bir modeldir. Bu çalışmada SWAT modeli Kabul River Havzasına (KRB) uygulanmıştır. KRB 33° N ve 37 ° N enlem, ve 67 ° E ve 74 ° E boylamda bulunmakta ve yaklaşık 72000 km^2 drenaj alanıne sahiptir. Bu çalışmanın ana amaçları: (1) önemli parametrelerin belirlenmesi ve optimize edilmesi, (2) Havzada oluşabilecek yüzeysel suyun tahmini, (3) aylık ve günlük akımların tahminleri, (4) modelin kalibrasyonu ve velidayonunu yapmak, ve (5) düşük ve yüksek akımların tahminleridir. SWAT-CUP programı ile model paramterelerin kalibrasyonu yapıldı. 20 tane duyarlı paramtrenin yağış-akış olayını etkilediği belirlenmiştir. Bu parametrelerden en önemlilerinin GWQMN.gw (su tablası lokasyonu), SMTMP.bsn (kar erime sıcaklığı), CN2.mgt (eğri numarası), PLAPS.sub (yağış şiddeti), ve HRU_SLP.hru (eğim) oldukları ortaya konmuştur. Modelin kalibrasyonu ve velidasyonu 7 istasyondan elde edilen ölçümlerle hem günlük hem de aylık periyotlar için ayrı ayrı gerçekleştirilmiştir. Modelin performansı Korrelasyon katsayısı (R^2), Nash-Shutcliffe parametresi (NSE) ve RMSE hata ölçüm değerleri kullanılarak yapılmıştır. Genel olrak, modelin aylık akımları daha iyi modelleyebildiği ortaya konmuştur.

Anahtar Kelimeler: Yağış-akış modellemesi, SWAT modeli, SWAT-CUP, Kabul Nehir Havzası

TABLE OF CONTENTS

LIST OF FIGURES

Figure **Page**

Figure **Page**

LIST OF TABLES

LIST OF ABBREVIATIONS

KRB	Kabul River Basin
SWAT	Soil and Water Assessment Tool
SWAT-CUP	SWAT Calibration and Uncertainty Program
GIS	Geographic Information System
AIMS	Afghanistan Information Management Service
FAO	Food and Agriculture Organization
NEPA	National Environmental Protection Agency
DEM	Digital Elevation Model
LULC	Land Use Land Cover
USGS	United States Geological Survey
MoEW	Ministry of Energy and Water
WMO	World Meteorological Organization
USDA-ARS	United States Department of Agriculture and Agriculture Research Service
HRUs	Hydrological Response Units
TRMM	Tropical Rainfall Measuring Mission

CHAPTER 1

INTRODUCTION

1.1 Overview

Afghanistan is one of the non-coastal countries with a total area of around 652,000 km^2 located in South Central Asia. The country is surrounded by Uzbekistan, Tajikistan, and Turkmenistan from the north, China to the north-east, Pakistan to the east and south, and Iran to the west (see Figure 1.1). It is a rugged land with an average elevation of 1100 m above mean sea level varying from 150 m to 8000 m. One-quarter of the country 's land lies, 2500 m above mean sea level. About three-quarters of the country's land is covered by mountains and hills, while wetlands, including river valleys, are located in the north, and south and mostly desert areas of the country are located in the south-eastern part. Hindu Kush mountains and Himalayan-Pamir mountain divided the country from west to east. The southern part of the country is covered by the mountains of Suleiman and Karakoram, which are the main source of water, and even most farming lands are located in this specified area (Bob, 2008).

In 2009, the populated area was expected to be around 7.91 million hectares, 7.79 million hectares of which were under temporary production, and approximately 0.12 million hectares of land under permanent production. The main populated areas are located in the northern and western parts of the country.

In 2011, the total population was approximately 32 million, of which 77% of the total population was rustic and the population density was found to be 50 residents per km^2 . From 2001 until now, most Afghan refugees have returned from Pakistan and Iran to Afghanistan, and the population growth rate has increased by 3.2%. Due to the increase in population, the water demand for water has also increased. In 2010, the majority of the population had access to developed water sources, about 78% of the total population in the municipal area, and 42% in the rural area.

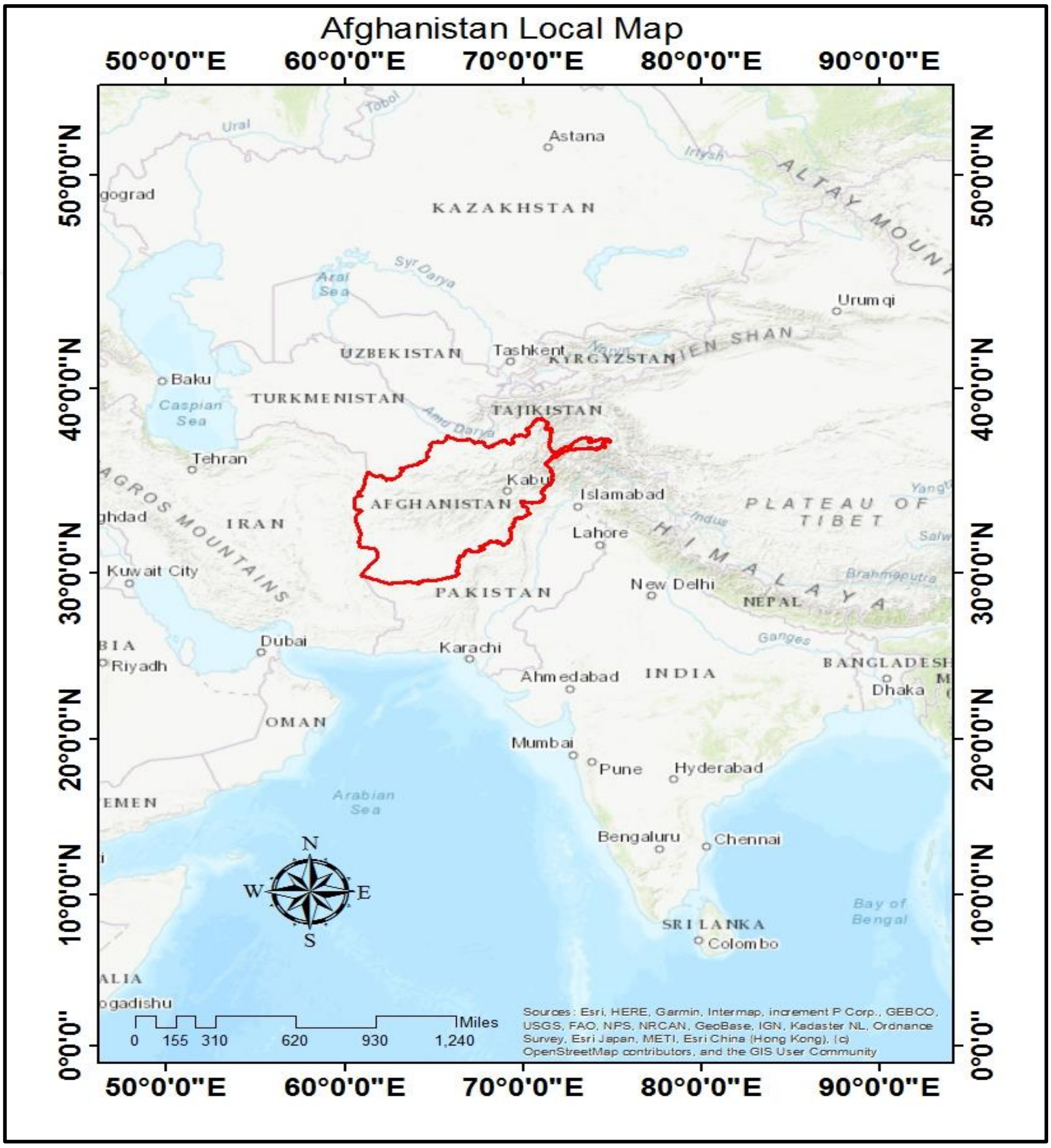

Figure 1. 1 Afghanistan Local Map (Source: GIS Global Map)

1.2 Afghanistan River Basins

Although Afghanistan is located in the aridity region this country has enough water resources mainly due to the high mountain series, such as Hindu Kush and Baba Mountains, which are lined with snow. From the present amount of water, more than 80 percent of water emanates from Hindu Kush mountains at an altitude of 2 000 m. These mountains are a function of the inherent storage of water in the form of snow during the winter season and snowmelt during the summer season, which therefore promotes the perpetual flow of water in all rivers during the summer season (ICARDA, 2002).

According to the reports provided by Aini (2007) and the Ministry of Energy and Water, 80 percent of Afghanistan's water resources are dependent on rain and snow melting in the upland above 2000 m. The amount of water coming from the snow melting is approximately 150,000 million cubic meters and the amount of water coming from the precipitation is 30000 million cubic meters and the total amount of water which received from both rainfall and snow is 180,000 million cubic meters. From the total amount of runoff, just 15 percent of Afghanistan's overall precipitation contributes to the country groundwater recharge (Abdullah Aini, 2007). Based on the geographical characteristics of Afghanistan, the country is divided into five major river basins shown in Figure 1.2.

1) Kabul River Basin
2) Helmand River Basin
3) Hari Rod Murghab River Basin
4) Northern River Basin
5) Panj Amu River Basin

Kabul River Basin with a total length of 700 km and with a catchment area of 72000 km^2 emanates from the central part of Hindu Kush Mountain located approximately 100 km in the west of Kabul. From the total length of the river, 560 km is located in Afghanistan (Qureshi, 2002). The storage capacity of the Kabul River Basin is estimated 22 billion cubic meters. Kabul River moves from the eastern direction toward Kabul and finally, the river flows to Pakistan and joins to Indus River in the east of Peshawar city. Its key river branches are Laghman Alingar, Panjsher, Logar, and Kunar rivers.

Helmand River with a total length of 1300 km and storage capacity of 6.5 billion cubic meters (Qureshi, 2002), originates from the central area of Hindu Kush Mountain next to the headwaters of Kabul River. The river moves in the southwest direction and after entering Iran from the west, the river reaches to Sistan Swamp. Helmand River flow is usually supplied from Upper Helmand Region and it is exposed to heavy snowstorms in the winter. The main tributaries of Helmand River Basin are Arghandab, Harut Rut, Farah Rut, and Khask Rut rivers (FAO, 2012).

Hari Rod River is another main source of water covering an area of 40 000 km^2, which is approximately 6% of the total country area. The river flow runs westward from the main source located 250 km to the west of Kabul. The river passing through the Heart City in Afghanistan, and after entering Iran , the river is heading northwards, and eventually reaching to Turkmenistan.

The Northern River Basin with a total catchment area of 75 000 km^2 is another major source of water, accounting for 12% of the country's total area. The Northern River originates from Hindu Kush mountains and moves in the northward until joining with Amu Darya River. Before reaching to Amu Darya River, the flow of the river disappears on Turkistan deserts. The important tributaries of the Northern River Basin are Shirin Tagab, Balkh, Khulm, and Sarepul rivers.

Amu Draya River is one of the largest rivers in Central Asia, covering an area of approximately 309 000 km^2 with a storage capacity of 24 billion cubic meters. The total length of the river is approximately 2540 km and it divides the water between Afghanistan, Kyrgyzstan, Tajikistan, Turkmenistan, and Uzbekistan. Of the total basin area, approximately 72.8, 14.6, and 8.5 percent of the catchment area covered by Amu Darya are located in Tajikistan, Afghanistan, and Uzbekistan, respectively. The main branches of Amu Draya river are Sherabad, Surhandary, and Kafirnigan.

The Northern basin has the lowest amount of yearly flow among the five main river basins, (about two percent of the total yearly flows in Afghanistan), unlike the other transboundary watershed of the country, the whole volume of water produced in the Northern river basin is being used inside the country.

Afghanistan is a drought-prone country where severe drought in two sequential years would usually cause low amounts of rain in winter. The region's weather records indicate that low winter rainfall occurs at least once in every 10 to15 years in two sequential years. The last under-average years ordered across the country were 1963-1964, 1966-1967, 1970-1972, 1999-2001, and partly 2002. Besides, many droughts have been recorded over the period from 2002 to 2011 that have had a major effect on the agriculture and livestock sector (Favre and Kamal, 2004). Controlling the long term drought, which is part of extensive water management policies, while updated data on water resources can facilitate better designing for drought management within the future. Droughts like that of 2004, effected cereal crops which decreased 43 present, about 3.06 million tons related to the high cereal production yield in 2003.

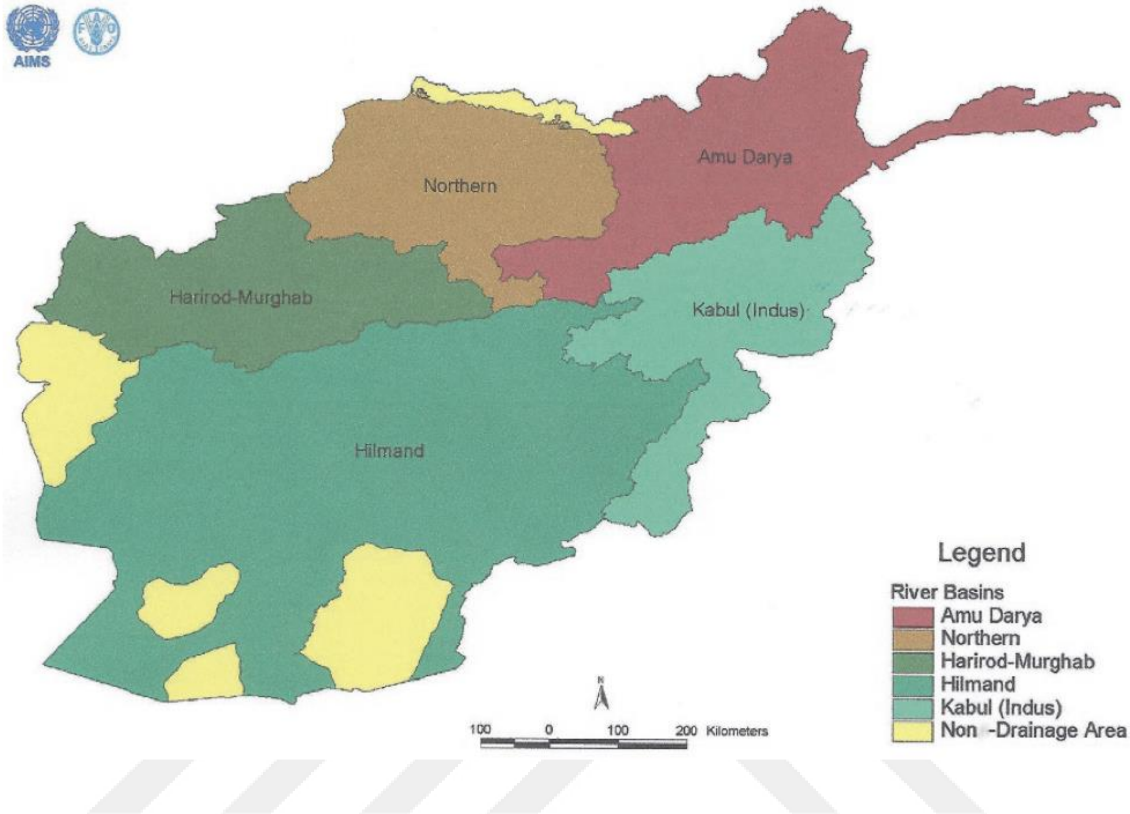

Figure 1. 2 Afghanistan River Basins (Source : AIMS)

1.3 Accessibility of Water Resources

Afghanistan's climatic conditions range from arid to semi-arid, receiving irregular rainfall over the year. The rainfall ranges from 75 mm in Farah to 1170 mm in the South Slang, with heavy rainfall during the winter months from February to April. The moistest seasons are concentrated in winter and spring once the vegetation cover is low. At high altitudes, the rainfall falls within the type of snow that is extremely crucial for streamflow and irrigation during the summer. Afghanistan has a relatively low amount of rainfall from June to October. These precipitation patterns are highly dependent on snow melting for irrigation.

The less amount of rainfall occurs in the south of Bust and Farah, with annual precipitation of less than 100 mm. The southern part of the country, starting from Herat to Ghazni, has an annual precipitation of about 300 mm, while the central and northern parts of the country have annual precipitation of between 300 and 400 mm. The north-east and eastern parts of the Hindu Kush mountains have an annual rainfall of over 400 mm (Favre and Kamal, 2004).

Based on (FAO) data, the country generates 65.3 km^3 of renewable water resources per year. Of the total renewable water resources, 10.65 km^3 is groundwater and 55.5 km^3 is surface water. Out of the total amount of surface water, 37.5km^3 / year produced internally and approximately 18.18 km^3 / year produced externally. The portion to internal water supplied from the Kabul River Basin is approximately 11.5 km^3, from Helmand, Hari Rod, Amu Darya, and the Northern River Basins 9.3 km^3, 3.1 km^3, 11.7 km^3, and 1.9 km^3 respectively. Similarly, from the total amount of groundwater provided internally, Kabul, Helmand, Western, Northern, Murghab, Amu Darya, and Hari-Rod river basins contribute about 1.92km^3, 2.98km^3, 2.14km^3, 2.97km^3 and 0.64km^3 respectively (FAO, 2016).

In 1987, the total annual water intake was about 26.11km^3, of which approximately 99 percent (25.8km^3) intended for agricultural purposes. However, the latest water withdrawal was in 1998 and the total annual volume of water withdrawn for irrigation purposes was estimated to be around 20 km^3.

It is clear that there is a high degree of uncertainty in the information available on water withdrawals throughout the country without offering a specific explanation for the variations found over a short period of about 10 years. Accordingly, it highlights the need for major water supply and demand studies to be conducted to promote overall water management throughout the country.

1.4 Climate Regions of Afghanistan

Because of the geographical diversity of the country, National Environmental Protection Agency (NEPA) separated the country into five main climate regions as shown in Figure 1.3 based primarily on altitude, annual rainfall, and land cover.

The following are the main characteristics of these regions.

1) Hindu Kush region: It is Afghanistan's highest and most hilly area, which is located in the northwest of the country. It has peak rainfall and it is thus the main source of water feeding rivers of central Asia significance such as the Amu Darya.

2) Northern Plains (North): This area is covered by grass and has an average height of about 600 m. Even though the area is relatively dry, it is still important for agriculture, especially due to the agronomy of almond trees and the provision of sheep and goat pastures.

3) Central Highlands: These uplands are typically situated in the center of the country and are known for their deep valleys and mountains ranges of up to 6400 m.

4) Eastern Highlands: This is a small area that occupies 11 percent of the country's total area of 72,000 km^2, and a large number of forests are also situated in this region. Eastern Highlands is the only area that is heavily influenced by the warm air masses of the Indian monsoon, causing heavy rainfall in the covered areas, which can lead to floods and landslides (Aich et al., 2017).

5) Southern Plateau: It is the largest desert region which covers around 215,000 km^2 area of the country. The only area considered for agricultural purposes is along the riversides and marshlands. Helmand River which is located in this region divides the area and feeds the Helmand Lake. This region is often vulnerable to sand and dust storms, mostly associated with winds from the north (Aich et al., 2017).

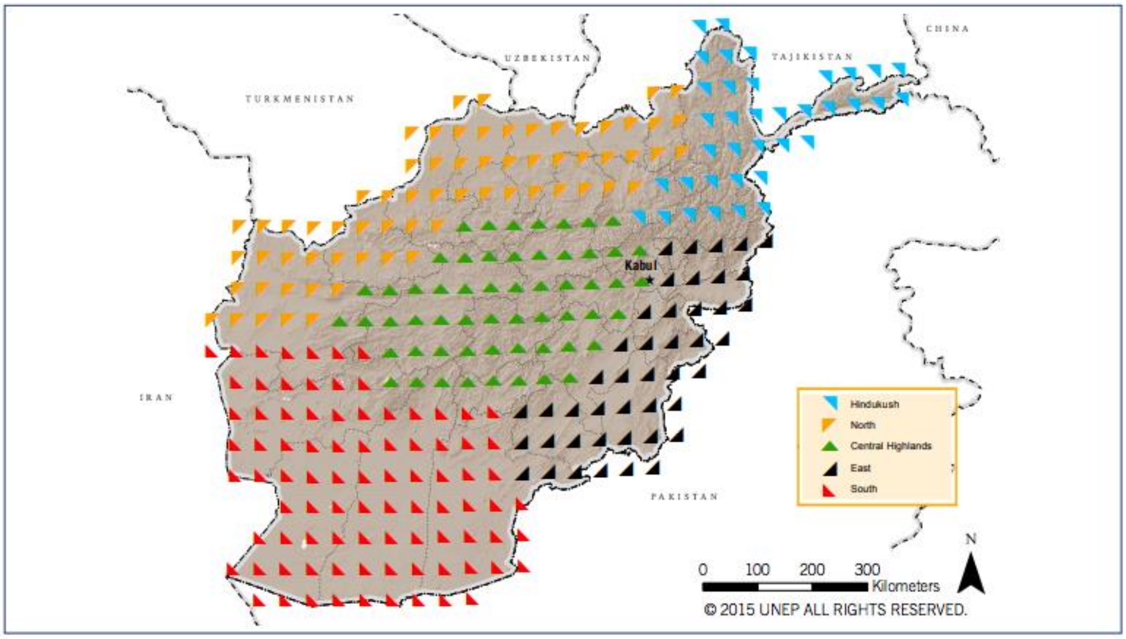

Figure 1. 3 Climate regions of Afghanistan (Source: NEPA, 2016)

1.5 Objecive of The Study

The main objective of this study is to apply soil and water assessment tool (SWAT) model, with limited meteorological, land use land cover, and soil data to estimate overall flow yield of Kabul River Basin, and to find average monthly hydrology components of the study area over the period 2009 to 2017. Some specific objective of the study are as follows:

1) To determine the most sensitive parameters that affect the catchment flow.
2) To estimate monthly and daily flows of the basin from the available meteorological stations data.
3) To calibrate and validate the simulated and observed flow data for different hydrological stations located in the basin, in order to check the performance of the SWAT model.
4) To determine the total amount of surface runoff and water yield in the basin.

1.6 Structure of The Thesis

This thesis contains eight chapters and organized as follows:

Chapter 1: Introduction

This chapter provides general information about Afghanistan's river basins, accessibility to water resources, Afghanistan's climatic regions, and also the objective of the current study are presented in this chapter.

Chapter 2: Literature review

This chapter provides reviews of relevant literature on rainfall-runoff processes, runoff prediction, hydrological modeling, rainfall-runoff modeling, and the application of the SWAT model to various hydrological modeling.

Chapter 3: Description of the study area

This chapter mainly describes the location of the study area, climate, uses of water, sub-basin of the main watershed, and water resources of the basin are discussed in this chapter.

Chapter 4: Materials and dataset

This chapter covers the input data required for the SWAT model such as DEM, land use land cover, meteorological, and hydrological data sets.

Chapter 5: Soil and water assessment tool (SWAT) model

This chapter deals with the theoretical background of the Soil and Water Assessment Tool (SWAT) model and the mathematical relationships used to simulate various hydrological processes.

Chapter 6: Soil and water assessment tool (SWAT) model setup

This chapter basically describes the model setup, including watershed delineation, hydrological response unit (HRU) analysis, model simulation, sensitivity analysis, calibration and validation, and model performance evaluation.

Chapter 7: Result and discussion

This chapter figures out the results obtained by the SWAT and auto-calibrated SWAT-CUP models, including the processes of watershed delineation, sensitivity analysis, and model calibration and validation analysis.

Chapter 8: Conclusion and recommendation

This section summarizes the contribution of this study and outlines relevant future research issues.

CHAPTER 2

LITERATURE REVIEW

2.1 Hydrological Cycle and Rainfall-Runoff Processes

The hydrologic cycle reflects the incessant flow of water across the different components of the climate system on Earth. Water is gathered in the seas, atmosphere, and under the surface of the earth. Water forwarding between these basins, during different stages, plays a key role in the climate system.

Water evaporates into air from both seas and earth surface, where it is circulated as water vapor over the face of the earth. The water vapor is gradually compressed into the atmosphere and returns to the earth in the form of sleet, snow, hail, and rain. This rainfall can drop on open water sources, be captured and absorbed by plants, and then becomes surface runoff or groundwater recharge. Water that has penetrated the surface of the land may seep into the profound areas to become a portion of groundwater storage, finally reappearing as streamflow or mixing in coastal areas with saltwater. In this last step, the water enters the ocean again and finally evaporates again, completing the water cycle (Thomas Pagano and Soroosh Sorooshian, 2002).

Each year, the yield of water on the earth's surface is measured to be around 577,000 km^3 of water. The volume of water that evaporates from land and seas is roughly 74,200km^3, and 502,800km^3 respectively. The same quantity of water drops as atmospheric rainfall, 119,000km^3 on the land, and 458,000km^3 on the seas. The rivers water capacity, which defines the difference between rainfall and evaporation from the land is 44,800km^3/year, from this amount of water 42,700km^3/year is rivers water and, the remaining 2100km^3/year is groundwater runoff to the ocean. These are the primary freshwater sources to sustain human life's needs and economic activity.

The most essential steps, linked to the hydrological cycle are shown in Figure 2.1. From the hydrology knowledge, it can be seen that precipitation is one of the most important key element in the hydrological cycle and that it is the foremost contribution of water to the surface of the earth. Precipitation is no longer completely captured by vegetation before reaching the Earth's surface.

The amount of precipitation caught by floras, trees, etc., does not rely only on their types, growth stage, and vegetation cover density, but also on rainfall intensity and period of the precipitation.

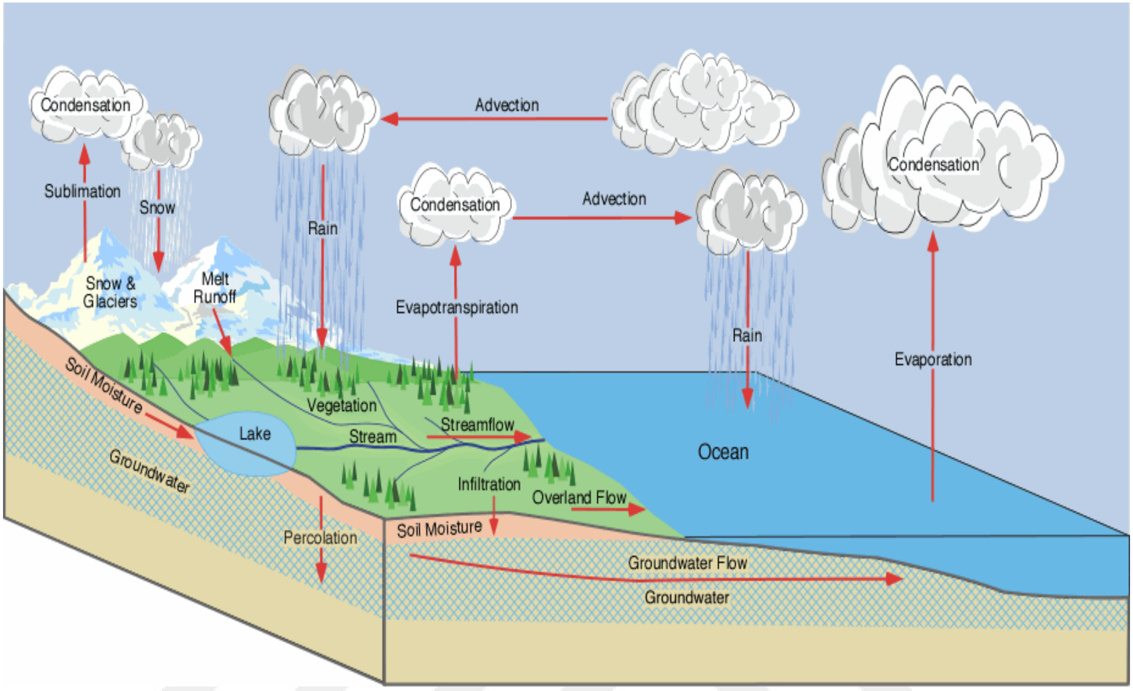

Figure 2. 1 Hydrological Cycle (Source: Arba Minch, 2015)

In the actual world, the processes of rainfall-runoff in a catchment is one of the most difficult tacks to comprehend because it includes hydrological domains (saturated, unsaturated, overland, etc). In fact, it is possible to distinguish many flow processes, such as Horton overland flow, which occurs when the precipitation intensity is more than soil infiltration capacity, because of this water is collected on the surface of the ground. Horton overland flow generally occurs in arid and semiarid regions, when rainfall is heavy and the vegetation is poor. Another type of flow is saturation overland flow, which occurs when the soil is fully saturated due to the rise of the groundwater level to the surface of the land. In moist areas, saturated overland flows are typical. Stream flows happen when the water flow at the land surface is slowly converted into a small stream. Eventually, once water enters the catchment drainage system, channel flow occurs.

The flow process occurs not only on the ground but also underground. In fact, water infiltrates into the subsurface as unsaturated underground flow in the form of a matrix or Macro pore flow. If the saturation conductivity of a specific layer is low related to the upper layer, perched subsurface flow is generated. In saturated zones, groundwater flow can be speedy or slow. All these processes are shown in Figure 2.2.

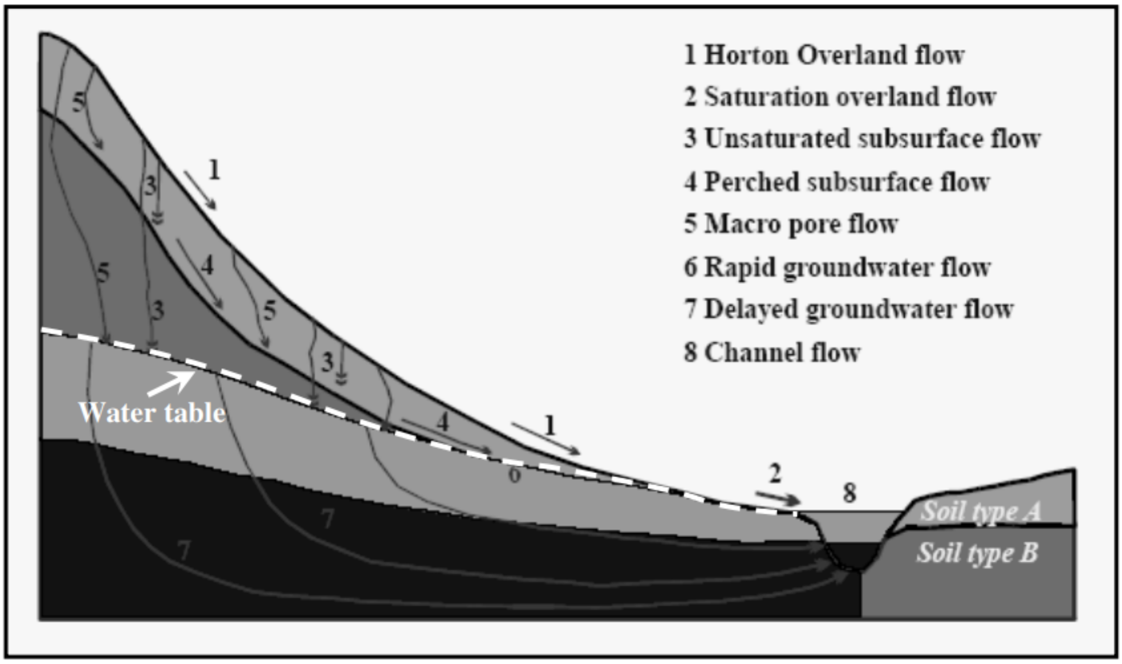

Figure 2. 2 Flow Processes on a hillslope (Source: Rientjes, 2004)

2.2 History of Runoff Prediction

Early hydrologists used limited data and basic mathematical methods to quantify surface runoff. The Rational Method which was published in 1851 by Thomas Mulvaney, was the first broadly used runoff method at that time, in which most hydrologists were using the Rational method for surface runoff calculation. The Rational method is mostly based on precipitation intensity, runoff coefficient, and drainage area to define the maximum discharge in a drainage basin. The coefficient that specifies the correlation between the quantity of runoff and precipitation was severely studied and resulted in a graphical method for estimating the quantity of runoff. The graphical method uses a series of graphs showing prior rainfall, soil water maintenance index, week of the year, and rainfall over the last six hours to measure the quantity of runoff.

Recently, the idea of unit hydrograph was presented and the catchment reaction to storm event was conceptualized based on the principle of superposition. The unit hydrograph can be applied to detached base flow and storm event runoff from streamflow.

Due to increasing computing power and deeper knowledge about hydrological processes, runoff models have become more developed.

2.3 Hydrological Modeling

The hydrological models are defined as a mathematical or symbolic representation of expected or recognized functions which represent the various components of a hydrological cycle (Beven et al, 1979). Based on the Schultz (1993) definition, hydrological modeling is a vigorous hydrological system analysis tool for practicing water resource engineers and hydrologists who are involved in the creation and preparation of assimilated methods for water resources management. For nearly 40 years, hydrological modeling techniques have been commonly used for many aims, but nearly all modeling tools have been established mainly for moist area uses. There are specific challenges in dry and semi-dry regions that have obtained slight consideration.

Model development is closely linked to computational power growth. Event-based models began in the 1930s and the model was used with hand calculation, but the first hydrologic model for incessant simulation of rainfall-runoff processes appeared in the 1960s when there was enough computing power to signify all land stage processes in an easy theoretical way. In 1970 and 1980, due to the increases in power physically based models were developed. These models are able to solve a set of partial differential equations to signify underground, overland, and transport processes, along with evaporation from the surface of land and water.

Presently, global climate models are capable to denote the global hydrological cycle with simpler physics-based models. At the same time, recent advances in computer power affords an opportunity to identify ambiguities connected with hydrological simulation, using gradually powerful methods for model performance analysis. So far, a wide range of hydrological models have been established, which are categorized in various ways. These models can be predictive (to get an exact answer to a particular question) or exploratory (for a better understanding of the hydrological process).

Based on the world metrological organization report which was published in 1990, hydrological models are classified into two groups as deterministic and stochastic models. The deterministic model is defined in which for specific input values the models can generate precisely the same output values and the stochastic model is defined in which the input values generally do not generate the same output values due to the random components of the models.

An important basis for modeling tasks is to define the relationship between data and models. Today's technology and computer capabilities offer mighty preprocessors and postprocessors for hydrological models via geographic information system, connecting with digital data sets to offer a sociable modeling environment for users. New sources of information are being generated by global advances in remote sensing, combined with modeling and data integration.

2.4 Rainfall-Runoff Modeling

Knowing the relationship between rainfall and runoff has been a longstanding topic in hydrological research. The studies which were carried out by Betson and Marius (1969), and Ragan (1968) mentioned that runoff happens because of composite interplay between surface, saturated, and unsaturated flow. At the same time, most of the researchers in the field of hydrology concentrated on modeling rainfall-runoff processes. The model is defined as representing the real world into a theoretical world. Obviously, modeling simplifies the flow processes that occur in the real world. Nevertheless, these models must be capable to record the prevailing processes at various space and time scale in a basin.

For rainfall-runoff analysis, models are generally classified into three groups; lumped, distributed, and semi-distributed models. The lumped models generally disregard the heterogeneities and represent the catchment area in the form of a single homogeneous unit. The model inputs and outputs are averaged and taken a single value for the whole basin. Such models are mostly used in the simulation of rainfall-runoff and averages can be obtained empirically or physically. In addition, the lumped model can be applied for total runoff and streamflow simulation at the outlet point, not particular flow inside the catchment. Therefore the lumped model sufficiently simulates average runoff conditions with fast computational times (David Pullar and Darren Springer 2000, Jan Sitterson et al., 2017).

The distributed model is one of the most complex models for rainfall-runoff calculation this is because it takes into account the spatial variability of inputs and parameters. The distributed model defines the hydrological processes of a catchment at each point. Fully distributed models divide the model process into small uniform grid cells to decrease the time interval and memory for modeling. Calculations are carried out on individual cells and then accrued in order to predict entire values for a catchment (David Pullar and Darren Springer 2000).

The Semi-distributed model adopts a lumped model with the characteristics of a distributed model. The semi-distribution model contains a set of lumped factors that can be applied in the manner of a quasi-spatial distribution model. During the application of the semi-distribution model, the model divides the total catchment area into sub-areas. Each sub-area has various factors. The sub-area shows the key elements of the catchment area and shows the benefits of a combination of lumped and distributed models. Another classification of rainfall-runoff models is known as the Event-Based and continuous models. The event-based model mainly focuses on a single runoff event and generate output only for a specific time period and, generally, this model is inclined to a lumped model. The continuous model is generally used to estimate flow during a storm event.

2.5 Application of Soil and Water Assessment Tool (SWAT) in Hydrological Modeling

SWAT model has been designed for watershed hydrology, prediction of water, pesticide yield, and sediment for long run. This model is used by various scholars in large and complex catchments with variant land use, land cover, and soil conditions. The model is helpful in the determination of effect of land activities on sediment yield and water.

R.L. Binger et al., (1997) utilized the SWAT model in Goodwin Creek Basin to look at the impacts of basin subdivision on simulated runoff and fine sediment yield. They recorded that the annual yield of fine sediment resulting from highland areas was highly sensitive to the watershed subdivision level but annual runoff was not sensitive. They concluded that the level of detail does not enhance SWAT's ability to improve basin runoff simulation.

J.R. Peterson and J.m. Hamlett (1998) used SWAT model for simulation of base flow in Ariel Creek basin with a catchment area of 39.4km^2 including fragipan soils. The researchers of this study indicated that the SWAT model is more appropriate for long-term simulation of hydrologic yield, and recommended that extra testing should be carried out using SWAT model with longer simulation periods, and that, it can adequately handle estimation of flow rate on a monthly or yearly basis.

H.B. Manguerra and B.A Engel, (1998) focused on the key parameterization issues of runoff prediction using SWAT model, concentrating on how to enhance model performance without restoring time-consuming and arbitrary parameter calibration. The findings of the study offered valuable information to enhance the efficiency of SWAT in terms of stream runoff prediction in a way that is especially useful for modeling ungauged watersheds where observational data for calibration is not available.

Michael W. Van Liew and Jurgen Garbrecht, (2003) utilized SWAT model to assess runoff in the Little Washita River Experimental Watershed under changeable climatic conditions (average, dry, and wet) in order to check the abilities of model. For calibration and validation, rainfall and streamflow data for 8 and 15 years, respectively, were used. The result indicates that the model calibrated result under wet climatic conditions was suitable and that, it was useful for predicting streamflow responses over average, wet, and dry climatic conditions selected for model validation. The study concluded that the SWAT model can provide a suitable simulation for hydrological studies linked to the effects of climate changes on water budget and water availability.

M.P. Tripathi et., (2004) applied SWAT model together with generated rainfall data to analyze runoff and sediment yield in a small agrarian catchment in India. The model's ability for generating rainfall was evaluated for 18 years. The results of this study have shown that the SWAT model can provide satisfactory monthly average precipitation which produces monthly average surface runoff and sediment yields close to the observed values and that, it can be used to develop multi-year plans for a small watershed.

Jugen D. Garbrech et al., (2006) used the SWAT model to simulate monthly runoff reaction to rainfall predictions in a small basin located in central Oklahoma for rainy, average, and dry predicted rainfall, respectively under rainy, average, and dry preceding rainfall conditions. The results of this study concluded that the preceding hydrological conditions and precipitation forecasts make a wide range of runoff responses that indicates excellent potential for water resource uses.

Rokhsare Rostamian et al., (2008) applied the SWAT model for sediment and runoff modeling in two different watersheds, Beheshtabad and Vakan in central Iran with covering areas of 3860km2 and 3198km2 respectively. Collected Sediment and Runoff data from four different Hydrometric stations were used for the calibration and validation purposes in each basin. The study mentioned that the predicted runoff values were close enough to the actual values compared to the sediment. In that study, the authors also draw attention to the weakness of the model that can be due to poor characterization of snowmelt processes in these mountainous watersheds, lack of adequate discharge data, lack of input data for the simulation of groundwater recharge, groundwater–river interaction, inadequate peak runoff simulation and the nature and accuracy of the measured sediment data. The relationship was found between estimated runoff and discharge that shows a better performance of the model. According to them, SWAT is a useful tool to predict soil erosion and the impact of climate change on soil erosion.

Soil and Water Assessment Tool (SWAT) model was used once again with a theoretical context and numerical methods for a selected portion of the River Drina basin with a covered area of 20.000km^2. The SWAT model was applied on a daily and hourly basis in order to calculate cumulative runoff on the outlet profile of the basin which was used for multi-year simulations. The authors of this study found that the result obtained by the SWAT model was particularly suitable during rainy and dry seasons and that it can be used positively for rainfall-runoff transformation in yearly and multi-year simulations. The study also presented that the quality of the rainy season simulation results is straightly linked to the input data such as rainfall, temperature, etc (Z. Simić et al., 2009).

M.T. Vu et al., (2011) computed runoff in Dak Bla river watershed in Vietnam with the help of five high-resolution rainfall gridded datasets (APHRODITE, TRMM, PERSIANN, GPCP, GHCN2) through SWAT model, where possible accessible station data were also used for the comparison. Bilinear interpolation was used for the gridded datasets to insert rainfall data at the nearest grid points to the station site. The results of this study mentioned that the simulated discharge result on a daily scale, obtained from the APHRODITE dataset was better compared to the four other datasets. According to the authors of this research work, the SWAT model can be used properly for gridded data set to simulate runoff in the regions where reliable observation data is not available.

Mohsen Pourreza Bilondi et al., (2013) made a study to calibrate and validate the rainfall-runoff SWAT model in Qezel Ozan basin in Iran. Three different uncertainty approaches (Differential Evolution Adaptive Metropolis DREAM, Methods of Particle Swarm Optimization. PSO, and Sequential Uncertainty Fitting SUFI2) were applied to calibrate and validate the rainfall-runoff model.The study concludes that the calibration and validation results obtained by these three methods were close enough to each other, the only difference was in their number of runs.

Vikash Shivhare et al., (2014) Implemented the SWAT model in Tapi sub-basin (Burhanpur watershed, India) to evaluate surface runoff. The SWAT model with daily meteorological input data was run for a time period of four years (1992 to 1997), and the output result was examined at a monthly time step. In this study, the performance of the model was tested by checking the similarity between observed and simulated runoff. The results of this study showed that the model calibrated the Tapi sub-basin with a satisfactory correlation between simulated and observed runoff. The coefficient of determination at the basin outlet for four years of record (1992-93 to 1995-96) was found 0.82, 0.68, 0.92, 0.69 respectively.

The study, conducted by Tesfa Worku et al.(2016), studied the effect of land use /land cover change on runoff and sediment in Beressa watershed by applying the SWAT model. Available data from 1980-1999 and 2000-2014 were calibrated and validated respectively through SWAT-CUP software. The Land use/Land cover analysis of this study showed that between 1984 and 2015 farmland and residential areas increased, though barren, pasturelands, and forest areas decreased, because of these situations runoff and sediment yield were increased by approximately 4.51 to 6% and 75.4 to 137.5% between 2010 and 2014 correspondingly. Finally, the authors of this research concluded that change in Land use/ Land cover (LU/LC) had an important impact on runoff and sediment yield.

Another study utilized the SWAT model into the agriculture river basin (Berkeri Shah River basin, Madhya Pradesh, India). Accessible 12 years of monthly and daily hydrological data (1995-2008) with one year of the warm-up period were provided to the model. The entire basin was divided into 11 main sub-basins. SWAT-CUP with the SUPI-2 algorithm was used to calibrate and validate monthly and daily streamflow using the primary objective function Nash Sutcliff Efficiency (NSE). The result of that study shows good agreements between measured and simulated streamflow, with the values of Nash Sutcliff Efficiency (NSE) of 0.724, 0.87 and 0.765, 0.88 for daily and monthly calibration and validation respectively. The study concluded that the accuracy of the SWAT model is highly dependent on high resolution gridded precipitation data or more accurate measured meteorological data (Shanbor Kurbah and Manoj Jain, 2017).

Soil and Water Assessment (SWAT) Tool was once again used in Madhya Pradesh city, India in order to model the response of hydrological parameters on urban runoff. By applying the regionalization method, Hydrological Model parameters of the gauged watershed (Mandlshwar) were transferred to estimate runoff in the target area. A SWAT-

CUP with SUFI-2 Algorithm was used to calibrate and validated accessible simulated and transferred observed data for a time period of 16 years (1979 to 2013). Discharge data transferability options were explored to calculate ungauged basin runoff. The study reported that the SWAT model is an important tool for determining water balance and applying basic management of water resources to urban catchments to predict and determine water availability, as urban areas are growing significantly (Afera Halefom et al., 2017).

Another study (Umit Duru et al., 2017) applied the SWAT model in Ankara River Basin to predict streamflow and sediment yield, and to create a soil erosion map of the required study area. Accessible 13 years of streamflow data both on a daily and monthly basis and 13 years of sediment data on a monthly basis were used for the calibration and validation purposes. The SWAT model performance was tested with relevant statistical measures. The values of Nash Sutcliffe, Relative Error, and coefficient of determination were checked for streamflow and sediment yield during calibration (1989 to 1996) and validation (1982 to 1984) periods. The values of the statistical parameters (Nash Sutcliffe, Relative Error, and coefficient of determination) were found to be 0.61, -0.55, and 0.78 for daily streamflow calibration and 0.79, -0.58, and 0.89 for monthly streamflow calibration. For sediment yield during the calibration period, it was found to be 0.81, -1.55, and 0.93. The results of this study stated that an important part of the urban and extremely agriculture area next to the stream network is more susceptible to soil erosion. Finally, the researchers of this study concluded that the SWAT model is a useful tool for simulating sediment yield and streamflow and that it can be used to decide water resources planning and management practices in a catchment with similar characteristics.

Rohtash et al., (2018), conducted a study using SWAT to analysis the rainfall-runoff modeling processes of the Chaliyr River Basin at Kuniyil, India, covered an area of 2013.4km^2. The entire watershed was divided into 15 sub-basins, and 103 hydrological response units were created through watershed delineation. A trend analysis of rainfall at four different stations was conducted, which indicated that the tendency was not statistically significant over the period 1991 – 2011. The Auto-calibration tool (SWAT-CUP) was used to calibrate and validate daily four years of data from 2003 to 2007, and from 2008 to 2011 respectively. The result of that study indicated a good correlation between observed and simulated daily flows, with the values of Nash-Sutcliffe Efficiency (NSE) 0.75, 0.73, and coefficient of determination (R^2) 0.77, 0.77 for both calibration and validation respectively.

Two different models Artificial Neural Network (ANN), and SWAT model, were used for estimating daily streamflow in two watersheds located in Peninsular Spain with contrasting climatic conditions; Atlantic and Mediterranean climates. The results obtained by these models were compared to each other in order to evaluate the capabilities of the models. The results of the study show that SWAT has a better performance in estimating very low values of streamflow, whereas ANN estimated very high values with greater precision in all cases studied. Generally, the simulated results by both models were good in the case of humid climate conditions. The results of this study suggested that the option between choosing SWAT or ANN has a direct effect on the accuracy of the simulated flow and it is still important to develop evaluation models with theoretical ideas (Patricia Jimeno-Sáez et al., 2018).

Agarwal Ashish et al., (2019) conducted a study in an ungauged watershed Rupen located in Gujrat, India, to evaluate the rainfall-runoff tendencies. Remote sensing data and GIS together with the SWAT model were applied to create a proper rainfall-runoff model of the study area. The model was run for a time period of 17 years including 14 years of warm-up period, and for the relevant rainfall, the runoff of each sub-basin was measured on a monthly and annual basis. From the similarities, which were checked between rainfall and discharge, and between rainfall and runoff can be observed that the model calibrates the watershed in a good manner. The coefficients of determination for rainfall-discharge and rainfall-surface runoff were found to be 0.871 and 0.949 respectively. Finally, the study concluded that the SWAT model is a useful tool to evaluate discharge and runoff and other hydrological components in the ungauged river basin of semi-arid regions.

2.6 Recent Studies in Kabul River Basin using SWAT model

Mohammad Tayib Bromand, (2015) applied the SWAT model with local and global meteorological data to estimate water availability and sectoral water demand of the Kabul River Basin in Afghanistan. Since the local data contained missing data, the Normal ratio Method was applied to fill the gaps. Available local climate data and gridded climate data from Tropical Rainfall Measuring Mission (TRMM) were compared to each other. The output results of runoff from the TRMM gridded weather data were calibrated on a monthly basis from 2008 to 2012 in three different hydrological stations (Dakah, Nawabad, and Shukhi stations). The whole basin was divided into 23 sub-basins with a number of 827 hydrological response units (HRUs). 14 sensitive parameters were calibrated and found that TIMP (Snow pack temperature lag factor), SMTMP (Snow melt base temperature), GW_DELAY (Groundwater delay), and CN (SCS runoff curve number II) were the most sensitive parameters to the runoff. This study claims that TRMM weather data provides better runoff results and that the SWAT model can be applied with gridded data if sufficient local data are not available. Both the above and the present study cover the whole Kabul River Basin. The main difference is that the above study applied gridded data from 12 different TRMM meteorological stations. Since the KRB covers a large area it needs to estimate runoff in more stations, where in this study only calibration on a monthly base was performed in three stations, not validation. SWAT manual calibration helper was used to calibrate the model outputs. Where in the present study instead of global data, local weather data from 18 different stations are used, and the SWAT model runoff output is calibrated and validated in seven stations by using SWAT-CUP software both on a monthly and daily time scale. Basin is divided into 48 sub-basins with 770 hydrological response units (HRUs). Instead of 14 sensitive parameters, the present study calibrates 27 sensitive parameters that have a strong effect on runoff and found that GWQMN.gw (Treshold depth of water in the shallow aquifer required for return flow to occur), SMTMP.bsn (Snow melt base temperature), CN2.mgt (SCS runoff curve number II), PLAPS.sub (Precipitation lapse rate), and HRU_SLP.hru (Average slope steepness) are the most sensitive parameters.

Another study conducted by (Hafizullah Rasoul et al., 2015) applied the Snowmelt Runoff Model (SRM) to estimate runoff in the upper part of Kabul River Basin (Paghman sub-basin). The model was calibrated in 2009 and validated in 2011. The estimated annual average discharges for the year 2009 during the calibration and for the year 2011 during the validation were 5.6 m^3/sec and 1.31m^3/sec respectively which indicates a good agreement between measured and simulated discharge with the values of R^2, 0.904, and 0.903 for calibration and validation respectively. The result of that study shows that changes in temperature and rainfall have a significant influence on the runoff, whenever the temperature and precipitation are increasing the runoff will increase as well. According to them, the SRM model can be applied in the snow-fed sub-basin and mountain basins. A single output value of mean yearly discharge for a specific year is presented and does not consider monthly or daily series output values of discharge, also they ignored soil and land cover data that have a strong effect on runoff. The present study provides series of runoff data based on a monthly and daily time scale from 2010 to 2017 for the defied hydrological stations (Pul-i-Ashawa, Pul-i-Behsod, Pul-i-Qarghayi, Shokhi, Pul-i-Surkh, Tang-i-Sayedan, Chaghasarai) located in the KRB.

Tooryalay Ayoubi and Dongshik Kang, (2016) performed a study in the Panjshir sub-basin located in Kabul River Basin, Afghanistan. The researchers of that study applied the SWAT model with two types of local land cover data (1993 and 2010) to investigate the impact of land-use changes on surface runoff. SWAT-CUP software was used to calibrate the daily data from 2010 to 2012 and to validate the data from 2012 to 2013 in a single upstream station (Shukhi). The result shows that urban, rangelands, forests, and orchard increased from 0.7% to 0.96 %, 70.56% to 75.55%, 0.81% to 1.51%, and 1.3% to 2.56% respectively, while surface runoff decreased by 10.24% to 7.2%. According to them, urbanization, barren land growth, deforestation, and snowmelt are the largest contributor to surface runoff, and that the SWAT model can be used to evaluate the impact of land-use changes on surface runoff. Only sub-basin of the KRB is discussed in above study, and calculated short-term daily runoff of a single station under two different land cover data. While the present study, covers the whole Kabul River Basin and estimates runoff under single global land cover data at seven different stations for a long period of time.

Another study conducted by Tooryalay Ayoubi and Kang Dongshik (2016) utilized the SWAT model in Ghurband and Panjshir sub-basins located in the Kabul River Basin with local and global weather data to simulate streamflow and to estimate water balance in the Panjshir sub-basin for freshwaters and irrigations. SWAT-CUP was used to calibrate available data from 2010 to 2012 and to validate one year of data from 2012 to 2013 on a monthly scale in three different hydrological stations (Omerz, Pul Ashwa, and Shukhi). The local land cover data for 2010 and global soil data were used in the model. The observed and simulated results were in good agreement with the values of R^2 (0.82, 0.77, and 0.90) for calibration and the values of R^2 for validation were found 0.85, 0.91, and 0.93 respectively for Omerz, Pul Ashwa, and Shukhi stations. According to them, the SWAT model is a potential monitoring tool for watersheds in the mountainous area. In above study, mixed weather data from global and local stations were used, the model was calibrated and validated with limited data only for some stations located in the upstream part of the basin and does not provide information about the downstream part of the basin. While in the present study, time series of observed local meteorological and hydrological data is used. In addition, the present study covers both upstream and downstream stations located in the KRB and calibrates the results for seven different hydrological stations both on monthly and daily basis.

The study conducted by (Taha Aawar and Deepak Khare, 2020) implemented the SWAT model to the sub-basin of the Kabul River Basin (Kabul sub-basin) in Afghanistan in order to predict future streamflow and climate change impact on runoff. Available monthly runoff data for a time period of 7 years (2003 to 2010) were used for calibration and from 2010 to 2018 were used for validation processes. Three different statistical measures coefficient of determination (R^2), Nash Sutcliffe Efficiency (NSE), and present bias parameter (PBIAS) were used to check the model performance. The result of that study indicates that streamflow can be significantly affected by changes in climate variability, soil type, and land use/land cover. A small part of the Kabul River Basin is covered, runoff is estimated only for one station (Istalif station), and was calibrated and validated on a monthly basis. While in the present study, three stations (Pul-i-Qarghayi, Pul-i-Surkh, and Tang-i-Sayedan) located in the same area are used. Instead of monthly calibration and validation, stations are calibrated and validated both on daily and monthly basis.

The studies discussed above have been conducted using the SWAT model for estimation of runoff and for analyzing the effect of land cover changes on surface runoff. In general, the above studies applied the models with a short period of data or with gridded weather data in some sub-basins of the Kabul River Basin. Mostly, mentioned studies calibrate or validate runoff in just one, two, or three stations on a monthly or daily basis, while there are more than 31 meteorological and hydrological stations in Kabul River Basin. While in this study, instead of gridded weather data, long term local weather data is used and instead of one particular sub-basin, the whole Kabul River Basin is studied. The other main difference of this study with above studies is that 18 main local metrological stations data is used and the output runoff results of the SWAT model is calibrated and validated for a long period of time (2010 to 2017) in seven different hydrological stations both on monthly and daily time scale. Mostly, in the present study, runoff data are calibrated for the stations that are located both in the upstream and downstream parts of the KRB in the main channel.

The current study focus on the Rainfall-Runoff modeling of Kabul River Basin using the SWAT model. The main purposes of the present study are (1) to determine the most sensitive parameters that affect the catchment flow, (2) to estimate monthly and daily flows of the basin from the available meteorological station's data, (3) to calibrate and validate the simulated and observed flow data for different hydrological stations located in Kabul River Basin, in order to check the performance of the SWAT model, and (4) to determine the total amount of surface runoff and water yield in Kabul River Basin. In order to prevent futures floods or hydrological events in the Kabul River Basin, it is important to have enough information about the areas that are prone to heavy rainfall and flooding. Therefore, the results of the present study could be used to control floods or some other hydrological disasters in the Kabul River Basin. Hence, the results of this study will contribute to predict flow and can be used to make decisions for proper planning, designing, and managing water resources in the Kabul River Basin in the future.

CHAPTER 3

DESCRIPTION OF THE STUDY AREA

3.1 Location

Kabul River Basin is a cross-border watershed between Afghanistan and Pakistan, where the eastern part of Afghanistan is covered by Kabul River Basin and covers the Chatral Valleys in Pakistan. The Kabul river basin located between latitudes 33 ˚ N and 37 ˚ N, and longitudes 67 ˚ E and 74 ˚ E as presented in Figure 3.1, and starts from the central upland at an average elevation of 6000 m above mean sea level and extends to the eastern valley at an average elevation of 400 m above mean sea level. The Kabul river basin covers approximately 12 percent of total Afghanistan's area and the drainage area of the basin is around 72000km^2. It is the fastest-growing population area which represents 35% of Afghanistan population (World Bank, 2010). The basin is divided into 7 sub-basins (Alingar, Kunar, Kabul, Shamal, Gomal, Ghorband Wa Panjsher, and Chak Wa Logar Rod) as shown in Figure 3.2 and 13 provinces of the country are located in Kabul River basin including Kabul as well. The Kabul river basin contains three distinct regions, which are Logar Midan region including three river branches (Maidan, Paghman, and Qargh rivers), Panjshir Ghorband region including three river branches (Ghorband, Salang and Shatul rivers), and Lower Kabul region including two river branches (Panjshir and Maidan rivers). The Kabul river basin provides water to around 10 million people for their critical daily needs, as well as for agricultural and power generation purposes, which are important for the development of the country. This basin has strong potential that can be used for future hydropower generation, where some hydropower stations have been partially developed along the river, such as Jabul Saraj Dam which was constructed in 1918 by the American company, Surobi Dam constructed by a German company in 1953, Mahipar Dam built by a German company in 1966, Naghlu Dam constructed by Afghan and Soviet in 1967, and Darunta hydropower station constructed in 1967 by USSR and China (Ahmad Shukran Sahaar, 2013).

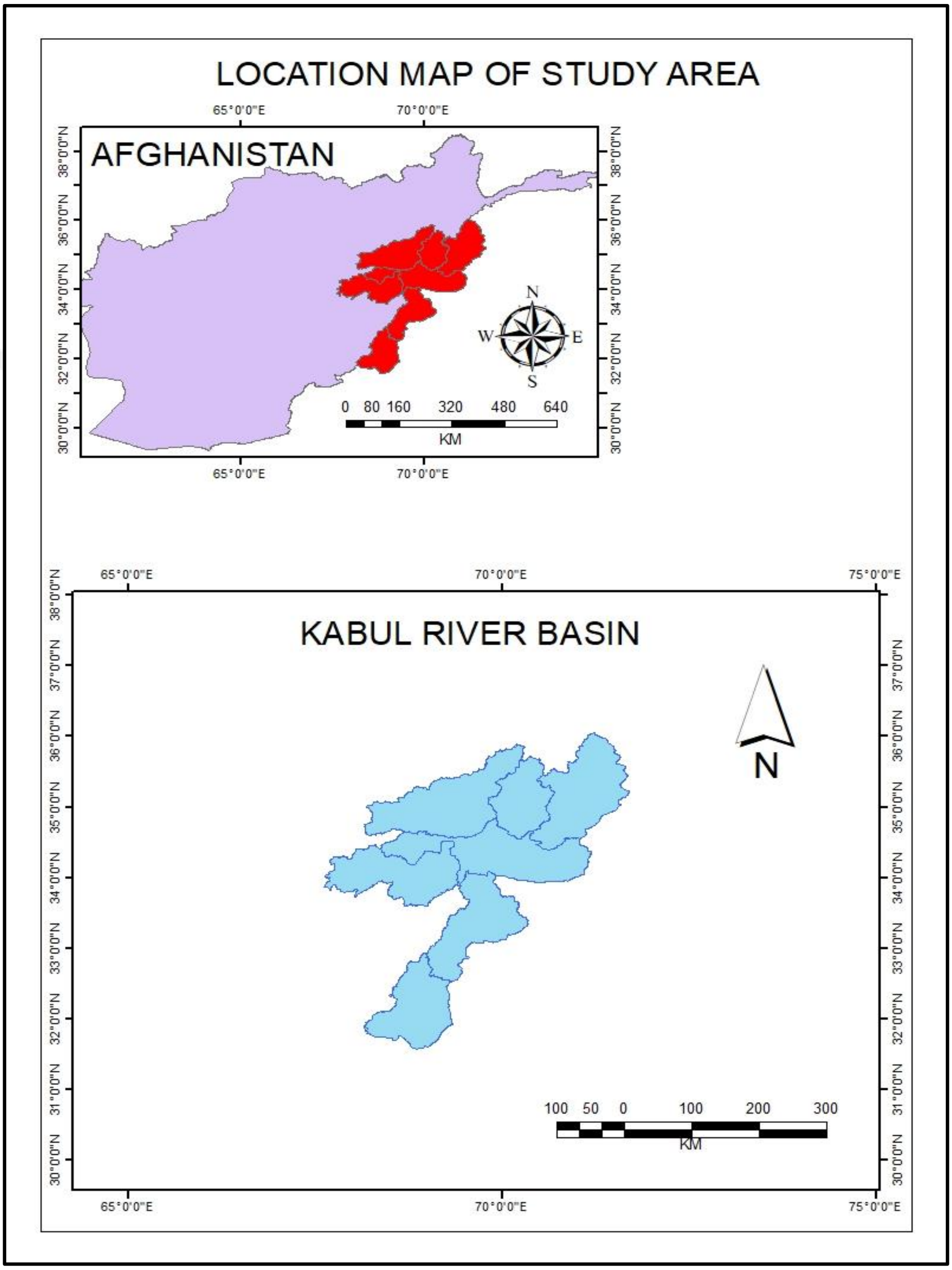

Figure 3. 1 Location Map of The Kabul River Basin

(Source: Ministry of Energy and Water)

3.2 Sub-Basins of Kabul Watershed

Kabul River basin is divided into seven sub-basins which is mentioned in the previous section, here some brief information is presented about these seven sub-basins.

1) Kabul Sub-basin: It is the largest sub-basin of the Kabul watershed. The elevation of the Kabul sub-basin is in the range of 378m downstream to 4719m upstream above mean sea level and the drainage area of the Kabul sub-basin is around 12997km^2. This sub-basin contains a large number of rivers and some small tributaries, most of which flow towards Pakistan joining with Indus River. Due to the enormous amount of water in the Kabul sub-basin, the government plans to build extra dams and reservoirs for hydropower generation, so far three dams (Naghlu, Sarobi, and Darunta) and some reservoirs are constructed along the basin. The average yearly flow of the Kabul sub-basin is recorded 6,000 million cubic meters and 19,900 million cubic meters at Durunta and Dakah stations respectively.

2) Chak Wa Logar Rod sub-basin: It is located in the south of the Kabul city, with an elevation in the range of 1777m downstream to 4283m upstream above mean sea level. It accounts for nearly 75% of the Logar-Kabul drainage area which is around 9968km^2. The most agricultural areas in Chak Wa Logar Rod sub-basin is located along the Logar River. The mean yearly flow in Chak Wa Logar Rod sub-basin is 230 million cubic meters and 300 million cubic meters recorded in Kajab and Sangi Naweshta stations respectively.

3) Ghorband Wa Panjsher sub-basin: It is located to the north of the Kabul sub-basin with elevation in the range of 1021m downstream to 5430m upstream above mean sea level and consists of the Ghorband River, which flows through the Panjsher River. The drainage area of this sub-basin is approximately 12964km^2 and the average yearly recorded flow for the Ghorband Wa Panjsher sub-basin is around 730 million cubic meters.

4) Alingar Sub-basin: It is located in the north-east of the Kabul sub-basin. This sub-basin contains two rivers (Alingar and Alishang rivers) that merge near the Lagman city and creates the Laghman river, which is one of the main sources of fresh water. The elevation of the Alingar sub-basin is in the range of 641m downstream to 5420m upstream above mean sea level. The drainage area of this basin is 6239km^2 and the average yearly recorded flow is 1850 million cubic meters.

5) Kunar Sub-basin: It is located to the east of the Alingar sub-basin. The main source of this basin is the Kunar River, which originates from the Karakoram mountains located in the south of the Wakhan corridor in Pakistan providing a large amount of water during the summer. The elevation of the Kunar sub-basin is in the range of 501m downstream to 6077m upstream above mean sea level, with a drainage area of 11665km^2 and the average yearly flow in this sub-basin is 12,130 million cubic meters and 14,830 million cubic meters recorded in Asmar and Pul e Kama stations respectively.

6) Shamal and Gomal Sub-basins: Both Shamal and Gomal sub-basins are located in the Southwest of the Kabul sub-basin. These sub-basins contain small rives that directly flows toward Pakistan, joining with Indus River. The drainage area of the Shamal and Gomal sub-basin are 9014km^2 and 9856km^2 respectively.

3.3 Water Resources of Kabul River Basin

KRB is the network of all Afghanistan rivers (FAO and Ministry of Energy and Water, 2015) , which join with Indus River. Since Indus River flows into Indian Ocean, Kabul River Basin is the only basin in Afghanistan that is directly connected to the Indian Ocean. The main water sources of the basin are the Kotali Shibar and the Paghamn mountains located in the west of the basin and supply water to the north of the Kunar valley. The Spingar Mountain is the other source of water of the basin, which is located in the south of the basin and provides a large amount of water to the southern part of the Nangarhar province located in the basin. Some valleys such as Panjsher and Salang located in the north of the basin provides some portion of water to the Kabul river basin. The eastern part of the basin contains a large number of mountains covered by snow and glaciers, the rivers which are located in this region preserve water to flow through the summer months. The total amount of water in the Kabul River Basin is around 43 billion cubic meters.

In general, the major source of water of the Kabul River Basin is the northern and northeastern regions, where there are numerous snow-covered mountains in the winter seasons, and the melting of snow in the summer periods provides a large amount of runoff in the basin. Due to the increases and decreases of runoff, water supply differs from year to year. Generally, more than 72 % of the runoff takes place between May and September, and 40% between October and April.

Also, the trans-basin division carries a large amount of water from the Pakistan's Chateral Valleys to the Kabul River basin. The water demand generally increases during the months of July and Agust due to the Agriculture sector.

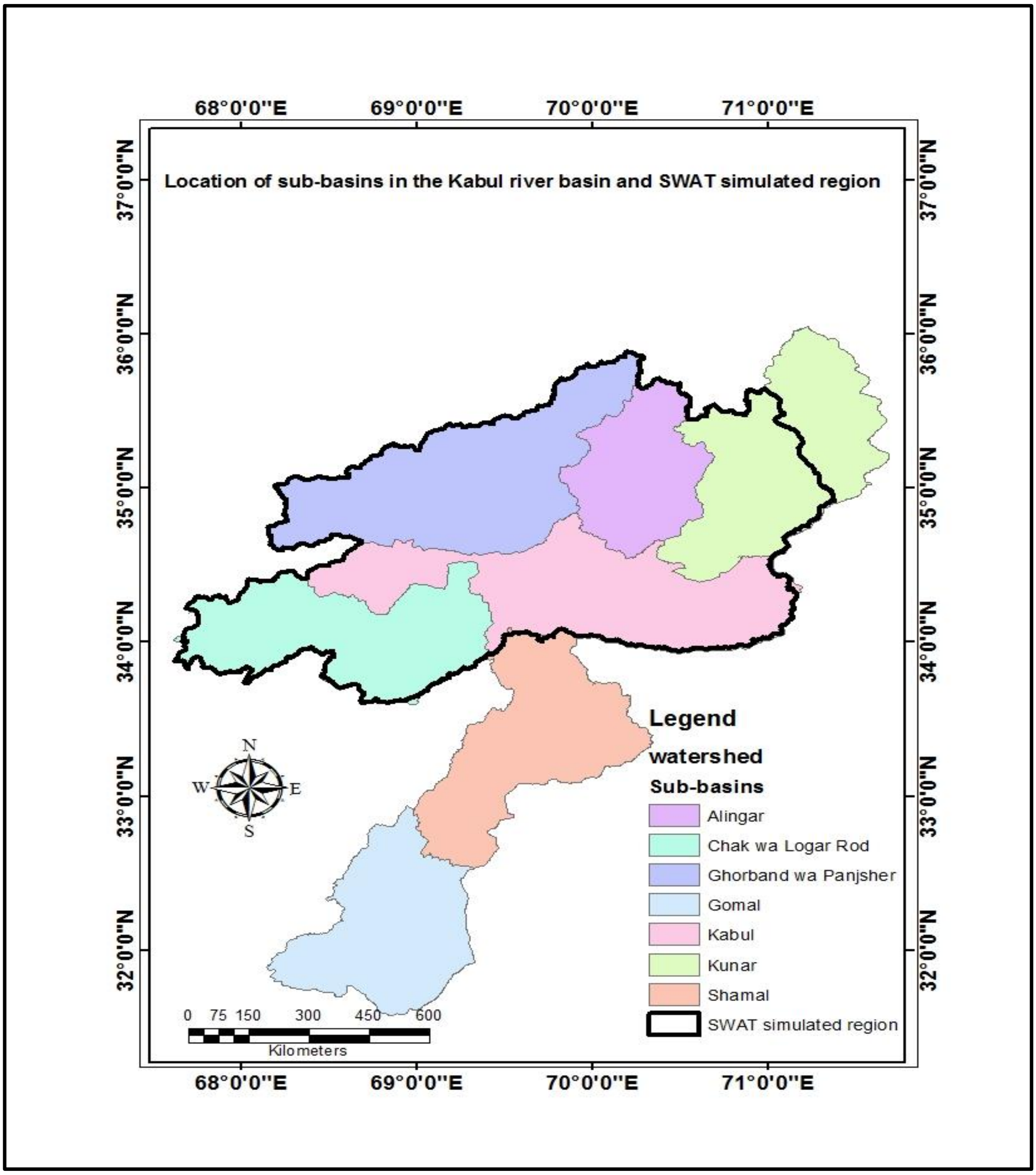

Figure 3. 2 Location of sub-basins in the Kabul watershed

The Kabul river basin contain four aquifers (Torge Tünnermeier and Georg Houben, 2003), where two of them are located in the Logar Rod sub-basin and the other two aquifers are situated in the Paghman-Darulaman basin, extending along the route of the Paghman River and upstream of the Kabul River. The main charging sources for this aquifer are irrigation, and surface water infiltration from rivers and canals. These aquifers are a major domestic water source and are refilled for irrigation purposes.

3.4 Climate

The Kabul River Basin located under semi-arid and continental type climate conditions with cold winters and hot summers, however, there are many distinct regional differences due to the attendance of numerous mountains and hills in the basin. There is significant heterogeneity between the upper and lower part of the Kabul river basin in terms of altitude, rainfall, and temperature differences so the climatic conditions are various from sub-basin to sub-basin. The average yearly rainfall in the Kabul River Basin was estimated 530mm with a clear concentration of rainfall during the winter periods from December to April see Figure 3.3, and the average yearly temperature was recorded as 9C^{o}. The maximum temperature was recorded in the Nangarhar area, located in the downstream part of the Kabul River Basin around 48C^{o} during the summer months, at the same time minimum temperature in the eastern part of the basin (Chatral valleys) was recorded as -28C^{o}. In 2013 the average minimum yearly temperature in the upstream part of the basin was recorded as 6.4C^{o} and average maximum temperature was recorded to be 20C^{o}, at the same time in the downstream part of the basin (Nangarhar). The average minimum and maximum recorded temperatures were 17C^{o} and 28C^{o} respectively with a total average yearly rainfall of 327mm (Fazlullah Akhtar, 2017).

3.5 Water Uses in the Kabul River Basin

The Kabul Basin uses around 14 percent of Afghanistan's total water use (FAO and Ministry of Energy and Water, 2015). The uses of water in the Kabul river basin have been divided into three categories; controlled or managed water use, beneficial water use, and non-beneficial water use. The controlled water use is classified into three groups as irrigation, domestic and livestock water uses. Most of the amount of controlled water has been used for the purpose of Irrigation, which occupies about 7,100 million cubic meters. In addition to controlled water use, the lands that are used for rangeland, account for the largest water usage, accounting for nearly 41 percent of the total water use in the basin.

The estimated breakdown of various uses and the ratio to the total water consumption are shown in Table 3.1.

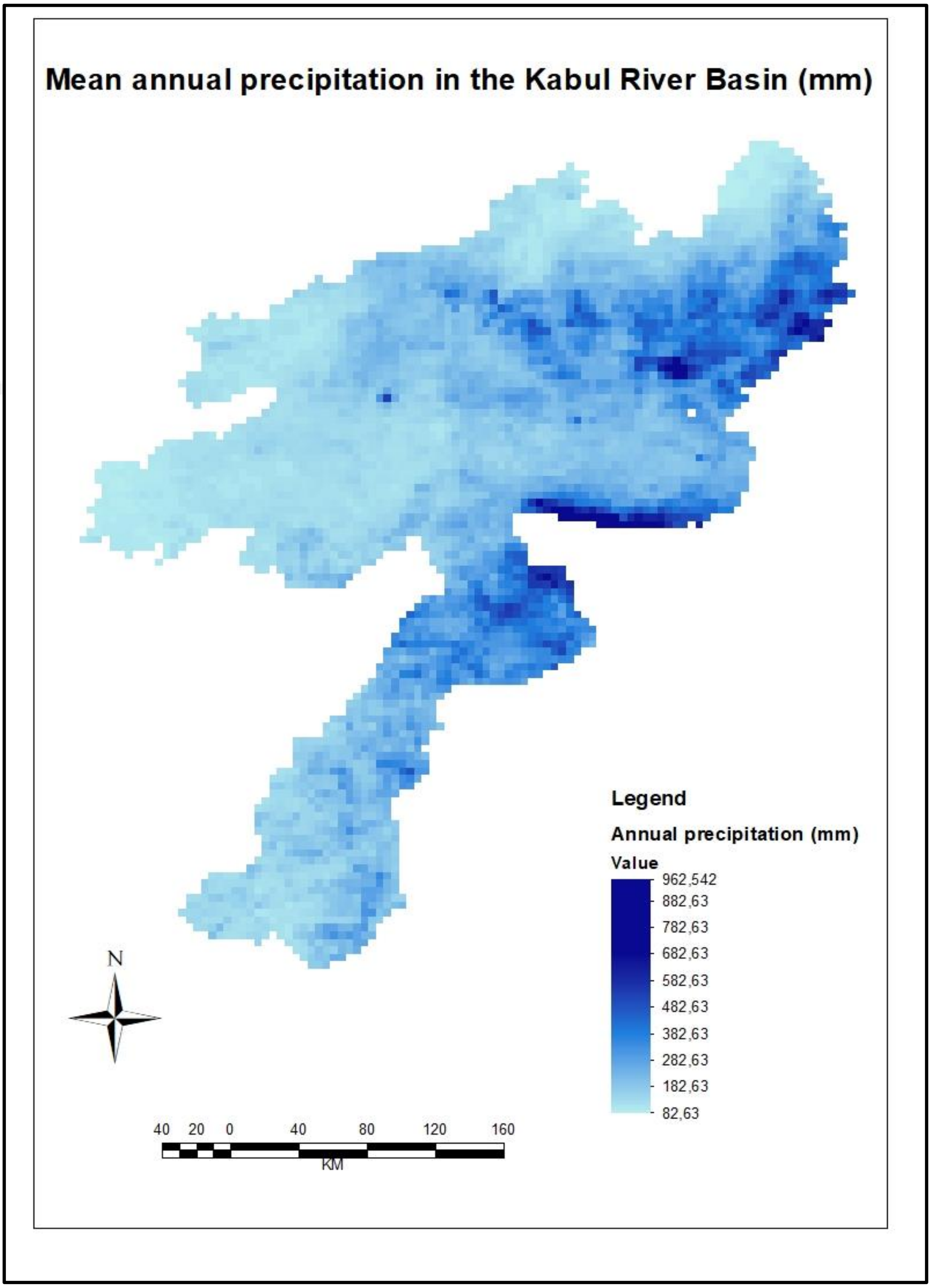

Figure 3. 3 Mean Annual precipitation in the Kabul River Basin from 2010-2017

(Source: TRMM)

Table 3. 1 Uses of water in Kabul River Basin (Source: FAO And Ministry of Energy and Water)

Water Use Type	Use sub-Type	Use Purpose	Mm^3	Percent (%)
Controlled Water Use	Irrigation	Irrigated Crops	6,442	24.3
		Irrigated Fruits	468	1.8
		Vine-Yards	174	0.7
	Domestic use	Urban Population	137	0.5
		Rural Population	60	0.2
	Livestock	Cattle	15	0.1
		Horses/donkeys	3	0.00
		Sheep/Got	38	0.1
Beneficial Water Use	Utilized Land Use	Rain-fed Crops	64	0.2
		Forest and Shrubs	4,014	15.1
		Rangeland	10,853	40.9
Non Beneficial Water Use	Unutilized Land Use	Barren Land	2,157	8.1
		Sand cover	27	0.1
		Built Up Area	219	0.8
	Losses from water bodies	Perennial waterbodies	310	1.2
		Temporary waterbodies	505	1.9
		Snow cover	1,026	3.9

CHAPTER 4

MATERIALS AND DATASET

4.1 Digital Elevation Model (DEM)

The Digital Elevation Model is an essential part of the Rainfall-Runoff SWAT modeling cycle. Incomplete and defective DEM files cannot completely represent a region. Hence, users of the SWAT model should carefully select the DEM file and select the appropriate DEM file that contains all the features that the region requires. The Topography of the present study area Kabul River Basin was defined by DEM, which describes the elevation of all points and the area between different points at a specific resolution. The DEM file with a high resolution and with a cell size of 30x30m has been downloaded from the DIVA-GIS website (https:/www.diva-gis.org/gdata) for the entire country territory. The downloaded DEM file contained a number of gaps that were filled in by ArcGIS Spatial analysis tools to prevent the error in the further analysis.

The DIVA-GIS website provides more raster and shapefiles datasets such as inland water, highways, railroads, elevation, land cover, population, and Gazetteer and can be downloaded free of charge for any region. The SWAT model work on the projected coordinate system, in the case, if the DEM file is in the Geographic coordinate system should be converted to the projected coordinate system requires by model, otherwise, an error will occur in the processes of watershed delineation.

The Digital Elevation Model (DEM) file of the country and the specific shapefile of the Kabul River Basin were loaded into ArcGIS 10.3, Spatial Analysis tools, and Extract by Mask tool were used in order to extract DEM file of the relevant study area (Kabul River Basin). The extracted DEM file of the basin was projected in WGS-1984 / UTM zone 42 projected coordinate system using ArcGIS 10.3. The projected DEM was used in the SWAT model for the purpose of watershed delineation, drainage area, flow direction, flow accumulation, stream generation along the basin, rivers, subbasin parameters, etc.

The topography of the Kabul River Basin represented by the Digital Elevation Model (DEM) ranges from 387m to 5718m above sea level, with an average elevation of 2480m, see Figure 4.1. From Figure 4.1, it can be seen that the northern, northwestern, and some parts of the northeastern regions of the study area have high elevation ranges, while the eastern regions have a low elevation range.

Generally, the DEM file can be used for different issues, and that it can be used to represent the characteristics of different basins and sub-basins for instance altitude, slope length and steepness, and relief ratio of streams.

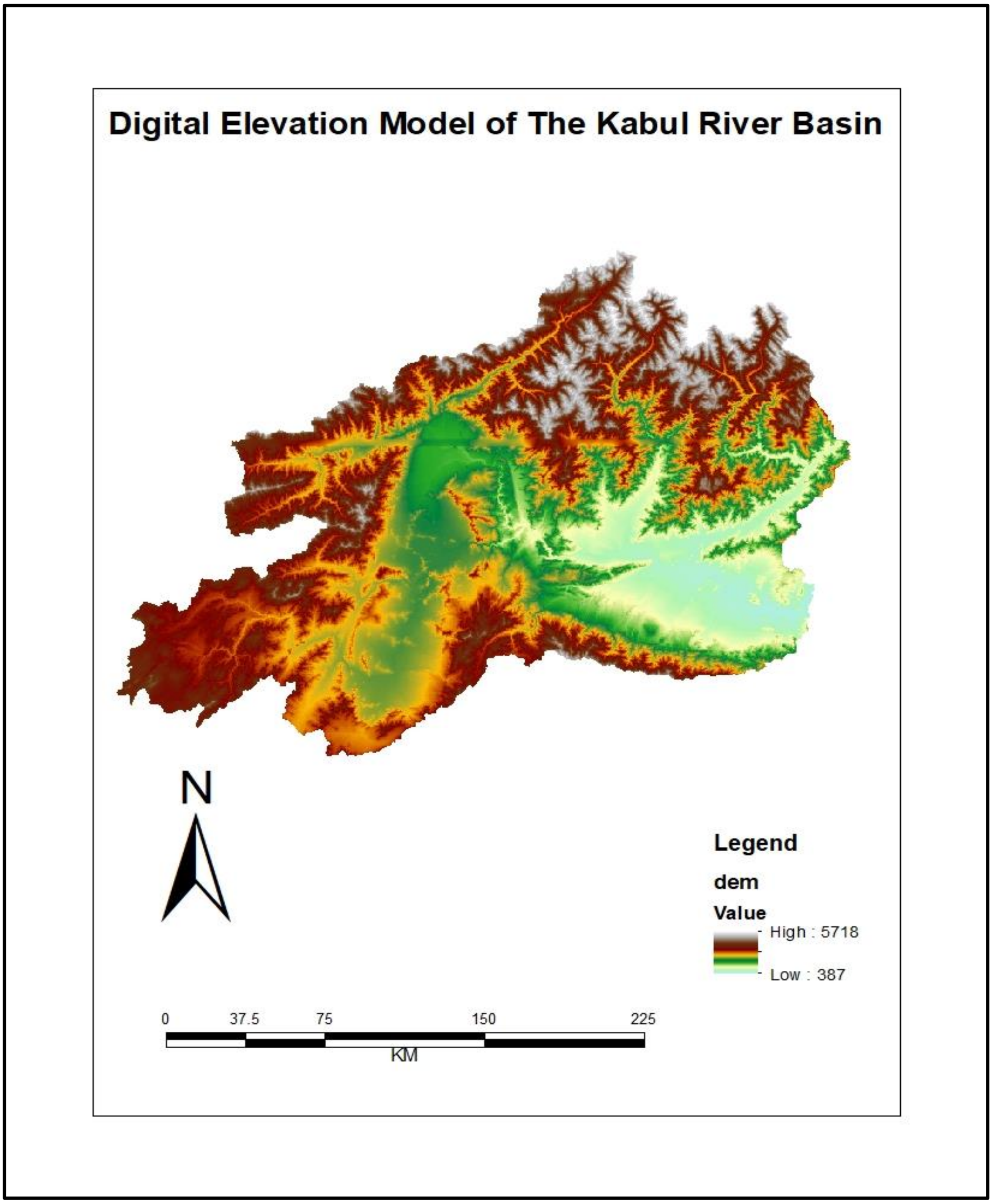

Figure 4. 1 Digital Elevation Model of the Kabul River Basin

(Source : DIVA_GIS)

4.2 Land use Land cover (LULC) Classification Map of the Kabul River Basin

Land use Land cover (LULC) classification map is an integral part of SWAT rainfall-runoff modeling and it is a critical factor influencing surface runoff within the watershed. Land use Land cover maps can also be applied to classify vegetation types that affect local hydrological processes. “The first Land cover map of Afghanistan was published in 1972 by Afghanistan Geodesy and Cartography Head Office” (Ahmad Shukran Sahaar, 2013). Nowadays most of the websites provide Global Land Use Land Cover (LULC) database that can be accessed free of charge, such as Global Land Cover Facilities (GLCF), Food and Agriculture Organization of the United Nations (UN-FAO), USGS Land Cover Institute (LCI), etc. For an accurate rainfall-runoff SWAT model, the users need to define an accurate land use land cover data.

In this study, a digital Map of the Asia Land Cover in a GeoTIFF format provided by the USGS Land Cover Institute (LCI) was used to derive land cover classification map of the Kabul River Basin. The digital land cover map is 43200x86400 pixels at a scale of 0.5 km with sixteen land cover classes as shown in Table 4.1.

The available land cover database from 2001 to 2010 for the Asian countries was downloaded from the USGS Land Cover Institute (LCI), (https://archive.usgs.gov/archive/sites/landcover.usgs.gov/global_climatology.html) web site.

The digital land cover map of Asia and shapefile of the study area (Kabul River Basin) were loaded into ArcGIS 10.3, Spatial Analysis tools and Extract by Mask tool were used in order to extract the land cover database of the study area from the digital Asian land cover map. The extracted land cover database of the basin was projected based on WGS-1984 / UTM zone 42 projected coordinate system using ArcGIS 10.3 and the land cover types were reclassified according to the SWAT format.

4.3 Soil Classification Map of the Kabul River Basin

The SWAT model database requires different soil types, along with their properties such as moisture content, soil texture, conductivity, and black density for different layers of each soil type. In this study, a digital soil map of the world, in the shapefile format was downloaded from Food and Agriculture Organization Of the United Nations (FAO) GeoNetwork(http://www.fao.org/geonetwork/srv/en/metadata.show%3Fid=14116) web site at 1:5.000.000 scale, which contains 28 major soil grouping, subdivided into the second level of 153 soil units (FAO, 1997).

Table 4. 1 Global USGS Land Cover Classification

(Source :USGS)

CLASSES	NAME
0	Water
1	Evergreen Needle leaf Forest
2	Evergreen Broadleaf Forest
3	Deciduous Needle leaf Forest
4	Deciduous Broadleaf Forest
5	Mixed Forests
6	Closed Shrublands
7	Open Shrublands
8	Woody Savannas
9	Savannas
10	Grasslands
11	Permanent Wetland
12	Croplands
13	Urban and Built-Up
14	Cropland/Natural Vegetation Mosaic
15	Snow and Ice
16	Barren or Sparsely Vegetated

The required soil data of the study area (Kabul River Basin) was extracted from the World soil map, through using ArcGIS spatial Analysis tools, and it was projected based on WGS-1984 / UTM zone 42 projected coordinate system. The SWAT model is working on four Soil Hydrologic Group (A, B, C, and D), where A group soil has high infiltration rate, B group soil have moderate infiltration rate, C group soil has slow infiltration rate, and D group soil has very slow infiltration rate.

4.4 Meteorological and Hydrological Data

SWAT model needs long year meteorological data for rainfall-runoff simulation, based on a daily or sub-daily scale. A maximum of 150 years of meteorological data on a daily base, can be applied in the SWAT model for hydrological simulation processes (M. Winchell et al., 2013).

The main problem with this study was to find the correct Meteorological and Hydrological data of the Kabul River basin to obtain accurate SWAT simulation results. The meteorological data provided by the Ministry of Energy and Water (MoEW) from 1979 to 2009 is full of errors, and there are gaps in records due to instability and civil wars. In 2006, the Ministry of Energy and Water set up 31 weather stations along the Kabul River Basin with financial support from the World Bank, but most of them have technical problems that do not accurately record meteorological data. From the total weather stations located in the Kabul River Basin, only eighteen stations in the basin recorded meteorological data such as daily and monthly precipitation, maximum and minimum temperatures from 2009 to 2018.

From the DEM file, it can be observed that most of the regions in the basin are located above 2480m mean sea level, where there are no weather stations at the high elevation of 3000 meters above sea level in the basin.

In this study, eighteen weather stations were selected for the study area, and other stations with incomplete meteorological data were ignored. The meteorological data for the observatory stations were obtained from the Ministry of Energy and Water (MoEW). Table 4.2 and Table 4.4 represents the name, location, elevation, Drainage Area, beginning and ending time of meteorological data (precipitation, maximum and minimum temperature) for each selected weather station in the study area. Other meteorological data such as wind speed, solar radiation, and relative humidity were not available.

Available Hydrological data for 31 different stations were obtained from the Ministry of Energy and Water (MoEW). This data also contains gaps and most of the data were not available for a long time of period. Due to insufficient Hydrological data, only seven hydrological stations data shown in Table 4.3 were considered in this study for the processes of calibration and validation. As shown in Figure 4.2, all of the selected weather stations are located in the plain area of the basin, below the mean sea level of 2480m. Based on the World Meteorological Organization (WMO) standard, at less one weather station, should be placed in the range of 100km^2 to 250km^2 for the flat region (Goyal, 2016), where, in this study without Bagh-i-Omomi, Qala-i-Malek, and Keraman stations which are in the range of the WMO standard, other fifteen stations are outside of the range that may do not record the meteorological and hydrological data correctly.

Table 4. 2 Weather stations in the Kabul river basin

Station	Elevation (m)	Latitude	Longitude	Drainage Area (km^2)
Pul-i-Kama	558	34.46870556	70.55703056	26005
Naghlo	998	34.63726389	69.71703611	26046
Pul-i-Qarghayi	643	34.54697778	70.24248889	6155
Bagh-i-Omomi	1587	35.14879722	69.28754167	205
Tang-i-Gulbahar	1625	35.14879722	69.28868333	3565
Bagh-i-Lala	1698	35.15176111	69.22051111	485
Pul-i-Ashawa	1624	35.08880000	69.14188611	4020
Qala-i-Malek	2211	34.57745833	69.97010278	69
Asmar	832	34.91500833	71.20171667	19960
Chaghasarai	847	34.90926944	71.12883611	3855
Dakah	419	34.23070556	71.03855	67370
Doabi	2059	35.34829722	69.61877222	789
Keraman	2232	35.28355278	69.65692778	110
Khawak	2405	35.56481111	69.89494167	369
Omarz	2042	35.375825	69.64085278	2240
Nawabad	796	34.81969167	71.12031944	23960
Payin-i-Qargha	1970	34.55253889	69.03574444	1970
Pul-i-Surkh	2216	34.36684167	68.76965278	1305

Table 4. 3 Summary of the available Hydrological data

Hydrological Stations	Latitude	Longitude	Hydrological data period
Pul-i-Behsod	34.442347	70.459831	2009-2017
Pul-i-Ashawa	35.08880000	69.14188611	2009-2017
Pul -i- Qarghayi	34.54697778	70.24248889	2009-2017
Shokhi	34.93616667	69.48439444	2009-2017
Pul-i-Surkh	34.36684167	68.76965278	2009-2017
Tang-i-Sayedan	34.408975	69.10441111	2009-2017
Chaghasarai	34.90926944	71.12883611	2009-2017

Table 4. 4 Summary of the available Meteorological data

Station	Meteorological data period				
	Rainfall	Relative humidity	Solar radiation	Wind speed	Temperature
Pul-i-Kama	2009-2018	not available	not available	not available	2009-2018
Naghlo	2009-2018	not available	not available	not available	2009-2018
Pul-i-Qarghayi	2009-2018	not available	not available	not available	2009-2018
Bagh-i-Omomi	2009-2018	not available	not available	not available	2009-2018
Tang-i-Gulbahar	2009-2018	not available	not available	not available	2009-2018
Bagh-i-Lala	2009-2018	not available	not available	not available	2009-2018
Pul-i-Ashawa	2009-2018	not available	2009-2018	2009-2018	2009-2018
Qala-i-Malek	2009-2018	not available	2009-2018	2009-2018	2009-2018
Asmar	2009-2018	not available	not available	not available	2009-2018
Chaghasarai	2009-2018	not available	not available	not available	2009-2018
Dakah	2009-2018	not available	not available	not available	2009-2018
Doabi	2009-2018	not available	not available	not available	2009-2018
Keraman	2009-2018	not available	not available	not available	2009-2018
Khawak	2009-2018	not available	not available	not available	2009-2018
Omarz	2009-2018	not available	not available	not available	2009-2018
Nawabad	2009-2018	not available	not available	not available	2009-2018
Payin-i-Qargha	2009-2018	not available	not available	not available	2009-2018
Pul-i-Surkh	2009-2018	not available	not available	not available	2009-2018

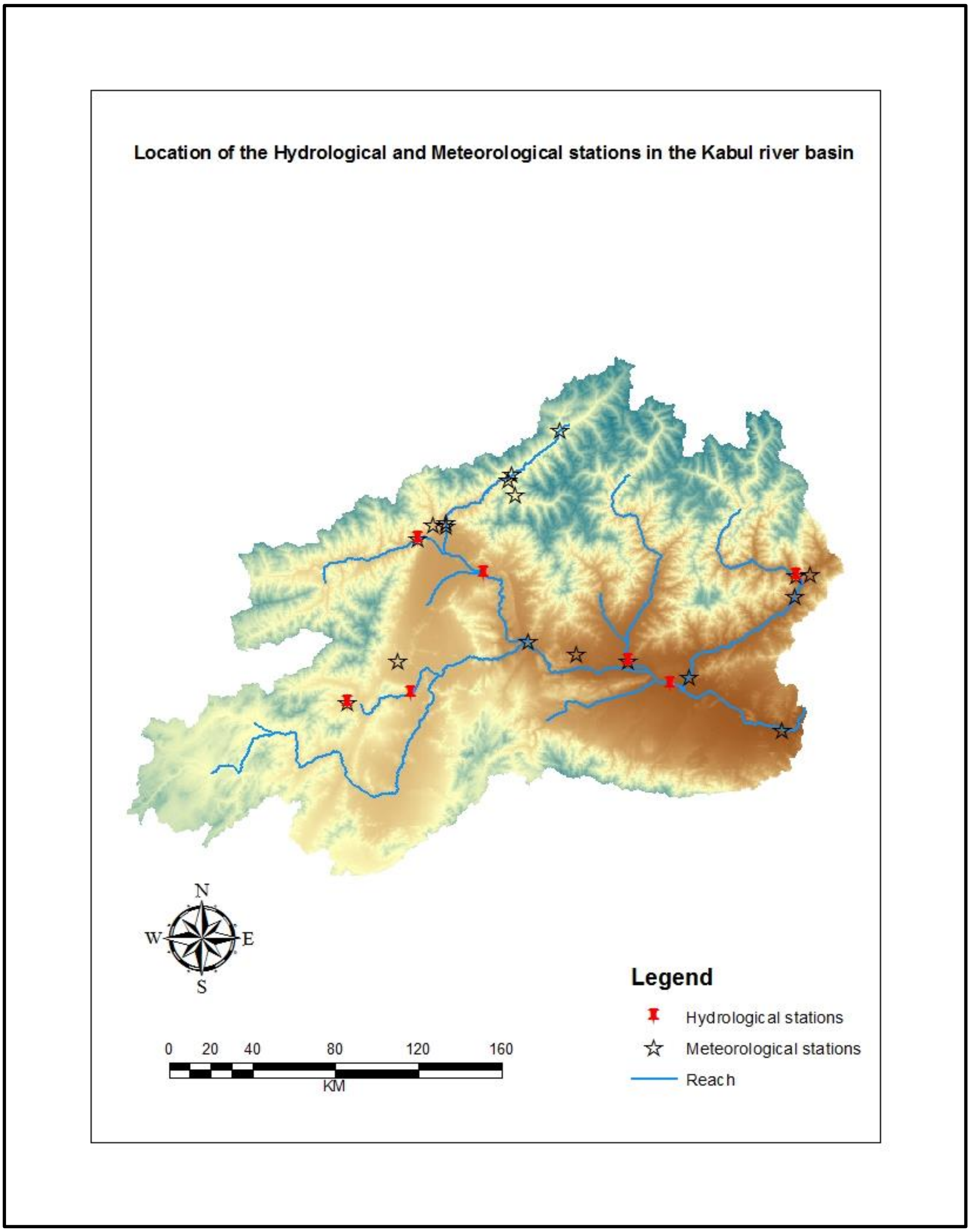

Figure 4. 2 Meteorological and Hydrological Stations in the Kabul River Basin

CHAPTER 5

SOIL AND WATER ASSESSMENT TOOL (SWAT) MODEL

This chapter covers the theoretical background of SWAT model for different hydrological modeling. This chapter provides a brief introduction of the SWAT model components and the mathematical relationships utilized for the simulation of various hydrological processes.

5.1 SWAT Model Description

SWAT model is a long term, a continuous, physically-based model of a river basin, that works on a daily or sub-daily time phase. The SWAT model was established for the U.S. Department of Agriculture and Agriculture Research Service (USDA-ARS) by Dr. Jeff Arnold. This model has been widely used to model watershed hydrology. It was designed for the purposes, of the prediction of water, sediment, and pesticide yields during a long period of time in massive and complicated catchments with varying land use land cover and soil conditions. It could be used to determine the effect of land activities on the water, and sediment yield, etc.

SWAT requires specific data such as climate, landscape soil, flora, and land management activities happening in the watershed. These parameters are important inputs for the hydrological and water quality simulation of a basin in the SWAT model. By using the input data as presented in Chapter 4, SWAT will directly model the physical process related to water and sediment movement and recycling of nutrients, etc.

SWAT split the whole catchment into a number of sub-catchments, then each sub-catchment is divided into a number of hydrologic response units (HRUs). The HRU represents a homogeneous grouping of soil, land use, slope and topography of the sub-basin. The user can select to have each HRU combination in the model or may choose to specify a minimum field threshold to limit the number of hydrological response units to be modeled. The combination of similar hydrological response units (HRUs) in the sub-basin is considered as a lumped area in the SWAT.

Generally, the components of the SWAT model are classified under sub-watershed, and routing some parts of these components are briefly described below with the mathematical equations in which the model is working.

5.2 Sub-Basin Components

The key components of sub-basin are as follows:

5.2.1 Hydrologic Cycle

The simulation of the hydrological cycle of a basin contains water and land phases. The water balance equation is the key that can be used for simulation of the land phase. The model calculation is carried out based on the water balance method individually for each HRU.

As the model provides a continuous water cycle the division of the catchment helps the modeller to consider variations in evapotranspiration for different soils and crops. Therefore runoff of each HRU is estimated individually and redirected to get the overall runoff of the basin (S.L.Neitsch et al., 2005). This makes the water balance much more accurate and provides a much better physical explanation.

As mentioned earlier the SWAT model utilizes the water balance method for the hydrologic simulation of the land phase. Therefore, the formula of the water balance applied in the SWAT can be described as follows.

$$SW_t = SW_0 + \sum_{i=1}^{t} \left(R_d - Q_s - E_a - W_{seep} - Q_g \right) \qquad (5.1)$$

Where;

SW_t final soil water content (mmH_2O),

SW_0 shows the initial water content of soil (mmH_2O),

R_d represent the rainfall (mmH_2O),

Q_s is the quantity of runoff (mmH_2O),

E_a is the quantity of evapotranspiration (mmH2O),

W_{seep} is the amount of water from the soil profile (mmH_2O) reaching the vadose region, and

Q_g is the quantity of flow return (mmH_2O).

Climate factors like precipitation, humidity, temperatures, solar radiation, and wind speed, afford the energy and moisture inputs needed to drive the hydrological cycle. Such factors can be obtained from the station recorded data, or modeled by the weather generator. Figure 5.1 represents the water balancing system of the SWAT model, that simulate the hydrology of the basin.

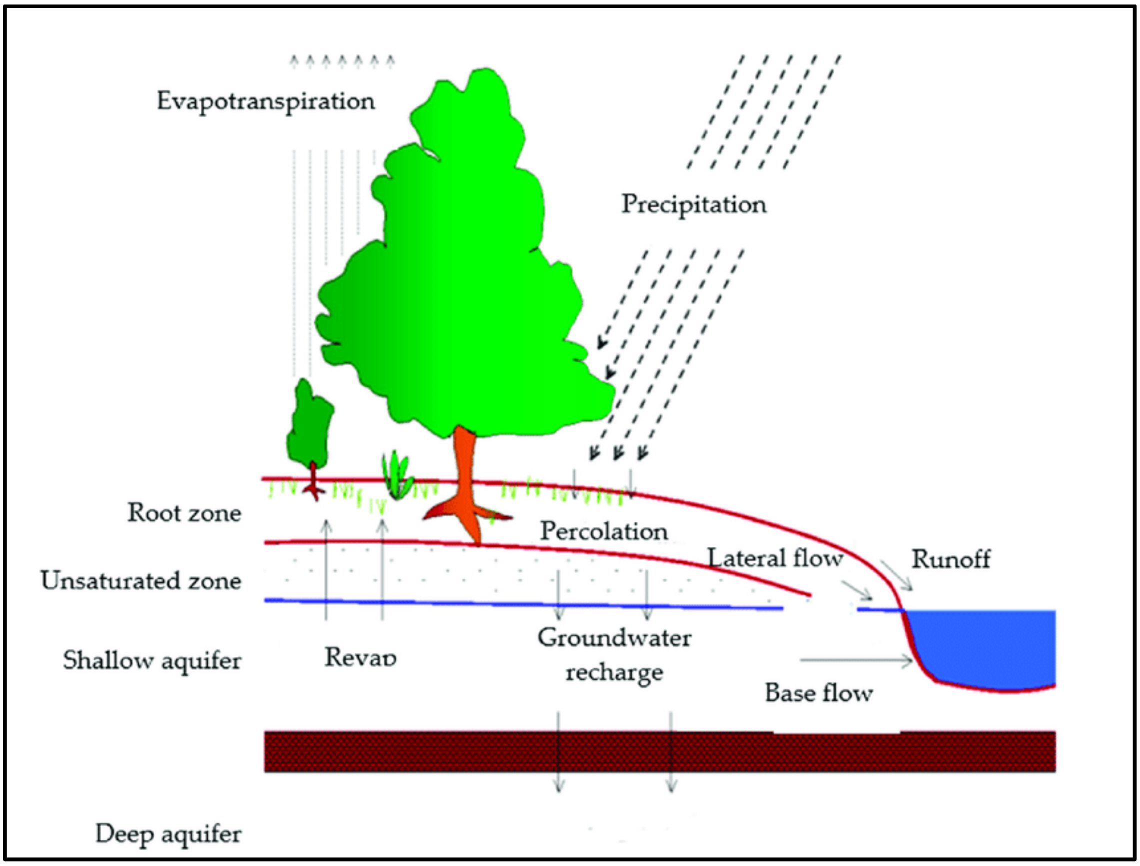

Figure 5. 1 Water balance system of the SWAT model

(Source: S.L.Neitsch et al, 2005)

5.2.1.1 Runoff

The surface runoff component of the SWAT model uses two different methods for calculations of volume, and peak runoff rates. Either the soil conservation service (SCS) curve number or Green and Ampt infiltration method can be used in the SWAT to evaluate runoff volume, but mostly the researcher prefers to use the SCS methods due to its simplicity and accuracy.

In the SCS method, the curve number changes nonlinearly depending on the moisture content of the soil. The number of curves decreases as the soil reaches the wilting point, and the number of curves increases to near 100 as the soil approaches saturation. The SWAT model uses the following equations, in order to simulate surface runoff and peak runoff rates.

$$Q = \frac{(R - I)^2}{(R - I + S)} \tag{5.2}$$

$$q_p = \frac{C * i * A}{3.6} \tag{5.3}$$

Where;

Q is runoff volume in mm,

R is the precipitation depth in mm,

I is initial abstraction in mm,

S is the retention parameter in mm,

q_p is the peak runoff rate in (m^3/sec)

C is the runoff coefficient,

A is the area of the basin in km^2, and i represent the intensity of precipitation in mm.

For simplicity in the real application, the retention parameter (S) is defined by the dimensionless parameter CN (curve number). Therefore, the relationship between retention parameter (S) and curve number can be expressed as

$$S = 25.4\left(\frac{100}{CN} - 10\right) \tag{5.4}$$

Where, the CN represents the curve number.

Generally, the initial abstraction (I) in the calculation is approximated to be equal to 0.2S. In this case, the general equation of the surface runoff volume can be stated as

$$Q = \frac{(R - 0.2S)^2}{(R + 0.8S)} \tag{5.5}$$

The surface runoff only takes place when precipitation depth (R) is greater than initial abstraction (I), (R>I). In the SWAT model, the antecedent moisture conditions (AMC) are described based on the Curve Numbers Antecedent moisture conditions. This is made based on the soil moisture content that the model calculates to evaluate CN. The AMC is defined as the amount of moisture, initially present in the soil at the start of the rainfall-runoff occasion. The SCS method classifies the antecedent moisture conditions into three groups as AMC-1, AMC-2, AMC-3, where the AMC-1 represent dry, AMC-2 represent average, and AMC-2 represent wet moisture conditions.

The SWAT model use equations (5.6) and (5.7), in order to calculate CN for moisture conditions 1 and 3.

$$CN_1 = CN_2 - \frac{2000 - 20CN_2}{100 - CN_2 + \exp[2.533 - 0.0636(100 - CN_2)]} \tag{5.6}$$

$$CN_3 = CN_2 * \exp[0.00673(100 - CN_2)] \tag{5.7}$$

Where;

CN1, CN2, and CN3 represent the curve numbers of the moisture conditions AMC-1, AMC-2, and AMC-3 respectively.

The Green and Ampt equation was established to predict infiltration and always assumes excess water on the surface. The equation considers that the soil profile is uniform and that the antecedent moisture is evenly distributed within the profile. This method estimate infiltration based on sub-daily precipitation data. The equation of Green & Ampt in the SWAT model can be expressed as follows.

$$f_{in} = K_e \left(1 + \frac{\omega_w * \Delta\theta_v}{F_{in}}\right) \tag{5.8}$$

Where;

f_{in} represents the infiltration rate (mm/hr),

Ke represents the hydraulic conductivity (mm/hr),

ω_w represents the wetting front matric potential (mm),

$\Delta\theta_v$ represents changes in volumetric moisture content (mm/mm), and

F_{in} represents the total infiltration (mmH_2O)

In a case where the rate of infiltration is greater than the intensity of precipitation, all precipitation will infiltrate over a period of time, and the equation (5.9) can be used to measure the cumulative infiltration over that period.

$$F_{in,t} = F_{in,t-1} + R \tag{5.9}$$

Where, $F_{in,t}$ and $F_{in,t-1}$ represents the total infiltration for a given time step and previous time step respectively, and R shows the amount of precipitation.

By replacing the f_{in} to dF_{in}/dt, equation (5.8) can be expressed in the following way, in which the SWAT model solves equation (5.10) iteratively for $F_{in,t}$.

$$F_{in,t} = F_{in,t-1} + K_e * \Delta t + \omega_w * \Delta\theta_v * \ln\left(\frac{F_{in,t} + \omega_w * \Delta\theta_v}{F_{in,t-1} + \omega_w * \Delta\theta_v}\right) \tag{5.10}$$

5.2.1.2 Lateral Flow

Lateral flow is important in regions where the soil of the surface layers has high hydraulic conductivity or in areas where the soil has an impervious or semipermeable surface at a shallow depth. In such cases, the precipitation will infiltrate vertically until reaches to the impervious surface. After reaching the impervious layers, the water then accumulates above the impervious surface and creates a saturation region of water. The key water source for lateral subsurface flow is this saturated area. The SWAT model applies the kinematic storage model developed by Sloan in 1983 for lateral flow simulation. The kinematic wave approximation of lateral flow considers that the lines of flow in the accumulated infiltrated water above the impervious area are equivalent to the impervious boundary. The SWAT model applies the following equation for calculation of the amount of lateral flow.

$$Q_l = 0.024 * \left(\frac{2 * SW * K * Sl}{\emptyset * L}\right) \tag{5.11}$$

Where, SW shows the storage volume of water in the saturated region (mm), K is hydraulic conductivity, S_l represent the hill slope, ∅ is the soil porosity, L indicates the hillslope length (m), and Ql is the lateral subsurface flow (mm/day).

In a large sub-basin with a concentration time exceeding one day, only a part of the lateral flow can enter the channel on the day it is produced. SWAT has a built-in lateral flow storage function to lag some of the lateral flow releases to the main channel. When lateral flow calculation is completed, the SWAT model measures the amount of lateral flow released into the channel by applying the following equation.

$$Q_l = \left(Q'_l + Q_{l,i-1}\right) * \left(1 - \exp\left[-\frac{1}{T}\right]\right) \tag{5.12}$$

Where Q_l is the amount of released lateral flow, Q'_l is the amount of lateral flow generated on a given day (mm) in the sub basin, $Q_{l,i-1}$ is the amount of lateral flow from the previous day (mm), and T represents the travel time of lateral flow (days).

5.2.1.3 Ground Water

The saturated zone of groundwater contains two types of regions (S.L.Neitsch et al., 2005); regions with high conductivity and regions with low conductivity. The regions which have high conductivity contains coarse-grained particles together with a large number of Macro pores, which allow the water to move easily. The region with low conductivity consists of fine particles with a high proportion of mesopores and micropores that limit the speed of water movement.

The groundwater is divided into shallow and deep systems of aquifers in the SWAT model. The model simulates both aquifer systems for each sub-basin. Water flows to the main sub-basin channel in the shallow unconfined aquifer system , wherein the deep confined aquifer system, water contributes to streamflow outside of the catchment. The SWAT model uses the following water balance equations for shallow and deep aquifers.

$$q_{sh} = q_{sh,i-1} + w - Q_g - w_r - w_p \tag{5.13}$$

$$q_d = q_{d,i-1} + w_d - w_{pd} \tag{5.14}$$

Where, q_{sh} and $q_{sh,i-1}$ represents the volume of storage water in the shallow aquifer at the present and preceding day respectively (mm), W is the refill amount of water which reaches the shallow aquifer (mm), Q_g is base flow (mm), W_r represents the volume of water which moves to the soil zone (mm), W_p is the volume of water, pumped from the aquifer (mm), q_d shows the volume of water that is deposited in the deep aquifer (mm), $q_{d,i-1}$ is the volume of water that is deposited in the deep aquifer in the previous day (mm), W_d is the amount of water which infiltrate from shallow aquifer into deep aquifer (mm), and W_{pd} represents the volume of water pumped from deep aquifer (mm).

5.2.2 Weather

SWAT model uses daily or sub-daily weather data for example, temperature, wind speed, solar radiation, rainfall, and humidity. During the application of the model, the users can choose to create monthly average data files for each weather parameter (rainfall, temperatures, etc.) for a series number of years, or they can directly select the weather data provided by the model. SWAT provides the WXGEN climate generator model for filling the gaps in the recorded station data or for creating a new climate data.

The incidence of precipitation on a particular day has a significant influence on the climate parameters of the day. The WXGEN climate generator independently makes rainfall data for a defining day. Once rainfall data is finished, the climate generator will use these rainfall data to generate temperature, solar radiation, and humidity data for the specific day. Finally, the WXGEN climate generator will generate wind speed data independently for SWAT model.

The SWAT model applies the first-order Markov chain model to determine the wet and dry conditions of the day. The model uses the skewed distribution or exponential distribution to simulate rainfall under wet day conditions. The following skewed distribution equation in the SWAT model can be used to calculate the amount of rainfall on a wet day.

$$P = \mu + 2 * \sigma * \left(\frac{\left(\left[\left(S - \frac{g}{6} \right) * \left(\frac{g}{6} + 1 \right) \right]^3 - 1 \right)}{g} \right) \tag{5.15}$$

where; p is the amount of precipitation (mm), μ is the average daily precipitation (mm) , σ is the standard deviation of daily rainfall (mm), S is the normal standard deviation, and g represents the factor of skew for daily rainfall.

The exponential distribution needs less inputs, and it is most commonly used in the case when the basin has limited data of precipitation. SWAT model provides the following equation of exponential distribution to calculate the amount of daily precipitation.

$$P = \mu * (-\ln(rd))^{r} \quad (5.16)$$

where; r_d represents a random number in the interval from 0 to 1, and r represents an exponent and it must be in the interval from 1 to 2.

The temperature model needs monthly or daily based average maximum and minimum temperatures data, and standard deviation of the maximum and minimum temperatures as input. The SWAT model applies the following equations for calculation of maximum and minimum temperature, and solar radiation.

$$T_{max} = \mu_{max} + X_i(1) * \sigma_{max} \quad (5.17)$$

$$T_{min} = \mu_{min} + X_i(2) * \sigma_{min} \quad (5.18)$$

$$H_d = \mu_{rad} + X_i(3) * \sigma_{rad} \quad (5.19)$$

where; T_{max} and T_{min} represents the maximum and minimum temperatures of the day respectively (C^0), μ_{max} and μ_{min} represents the maximum and minimum average daily temperature respectively (C^0), X_i (1) and X_i (2) represents the residual of maximum and minimum temperature respectively, σ_{max} and σ_{min} represents the standard deviation of maximum and minimum temperatures respectively (C^0), H_d represents the solar radiation of the day (MJ m^{-2}), μ_{rad} represents the mean solar radiation (MJ m^{-2}), X_i(3) represents the residual of solar radiation, and σ_{rad} represents the standard deviation of daily solar radiation (MJ m^{-2}).

The SWAT model requires relative humidity, in the case when the Penman-Monteith equation is applied for calculation of evapotranspiration. The model uses a triangular distribution method in order to calculate daily mean relative humidity from monthly relative humidity data. The triangular distribution method in the SWAT model takes four inputs into account to generate daily relative humidity for further calculation. Thus the inputs are defined as average monthly relative humidity, a random number in the interval from 0 to 1, and maximum and minimum relative humidity permitted per month. The upper limit of the triangular distribution, which represents the maximum relative humidity can be calculated from monthly average relative humidity data by applying the following equation.

$$R_u = R_{mh} + (1 - R_{mh}) * \exp(R_{mh} - 1) \quad (5.20)$$

where; R_u is the upper limit or maximum relative humidity, it can be created for a given day in the month, and R_{mh} represents the mean relative humidity of the month.

The lower limit of the triangular distribution represents the minimum relative humidity; SWAT model applies the following equation to calculate minimum relative humidity from monthly average relative humidity data.

$$R_L = R_{mh} * (1 - \exp(-R_{mh}) \quad (5.21)$$

where; R_L is the lower limit or minimum relative humidity, it can be created for a given day in the month.

Wind speed also has a role in the SWAT hydrological modeling, so it is required to be considered during the model application. SWAT model applies the following modified exponential equation to generate average daily wind speed.

$$W_d = W_m * (-\ln(rd))^{0.3} \quad (5.22)$$

where; W_d represents daily wind speed (m/sec), W_m represents the mean wind speed of the month (m/sec), and rd is a random number in the interval from 0 to 1.

CHAPTER 6

SOIL AND WATER ASSESSMENT TOOL (SWAT) MODEL SETUP

This chapter covers SWAT model set-up step by step. For a better simulation of the model, it is important to prepare the input data properly and it must be in the format of SWAT database which is recognized by the model. The inputs data for rainfall-runoff simulation are discussed in Chapter Four .These data sets are employed into the model for rainfall-runoff simulation processes in Kabul River Basin, also the format of inputs files are discussed in that chapter.

6.1 SWAT model Installation Requirements and Database

Before installing and running SWAT model, the user needs to be aware of some model requirements for installing and running processes, otherwise, an error would occur while applying the model. These model requirements are defined as follows:

1) SWAT's minimum hardware requirements are a personal computer, with a recent processor, running at 2 GHz or higher. A hard drive with at least 500 MB of free memory and access to at least 2 GB of RAM is required, but a 2 GB hard drive is suggested.
2) To run the SWAT model, ArcGIS 10 or 10.1 versions, Windows operating system XP or Windows 7 or the most recent one, Microsoft Net Framework 3.5, and ArcGIS spatial analyst extension must be installed in the computer.

After proper installation of the SWAT2012 model or any other version, the user needs to check the SWAT database, SwatCheck, ArcSWAT help materials, and ArcMap layer files, it can be found in the folder where the SWAT software is installed. The SWAT database is the main source of the model, which contains different land cover classes, soil classes, urban classes, etc. The SWAT2012 database is created based on the United States Geological Survey (USGS) data sets, so if the user data are different from USGS data then the user needs to edit the SWAT2012.mdb data set file or the user may import data for a specific selected part such as soil, land cover, etc. into the SWAT database from some other sources, such as Map window. In this study, the resent available ArcSWAT2012 model is used for the rainfall-runoff simulation. The model setup processes are presented below step by step.

6.2 Watershed Delineation

Digital Elevation Model (DEM), Land use Land cover data, and soil data are prepared as presented in Chapter 4. The first option is to save or open the SWAT project in the graphic user interface (GUI) of ArcGIS. From the ArcGIS toolbars menu, the SWAT menu bar must be selected otherwise the SWAT menu bar or options does not appear in the interface of ArcGIS as shown in Figure 6.1. The user starts with the first menu option from the left-hand side ‘SWAT project Setup’. The SWAT project setup provides information about the project name and the place where the SWAT project is saved. In most cases, it is recommended that the project should be saved in the folder where the SWAT model is installed.

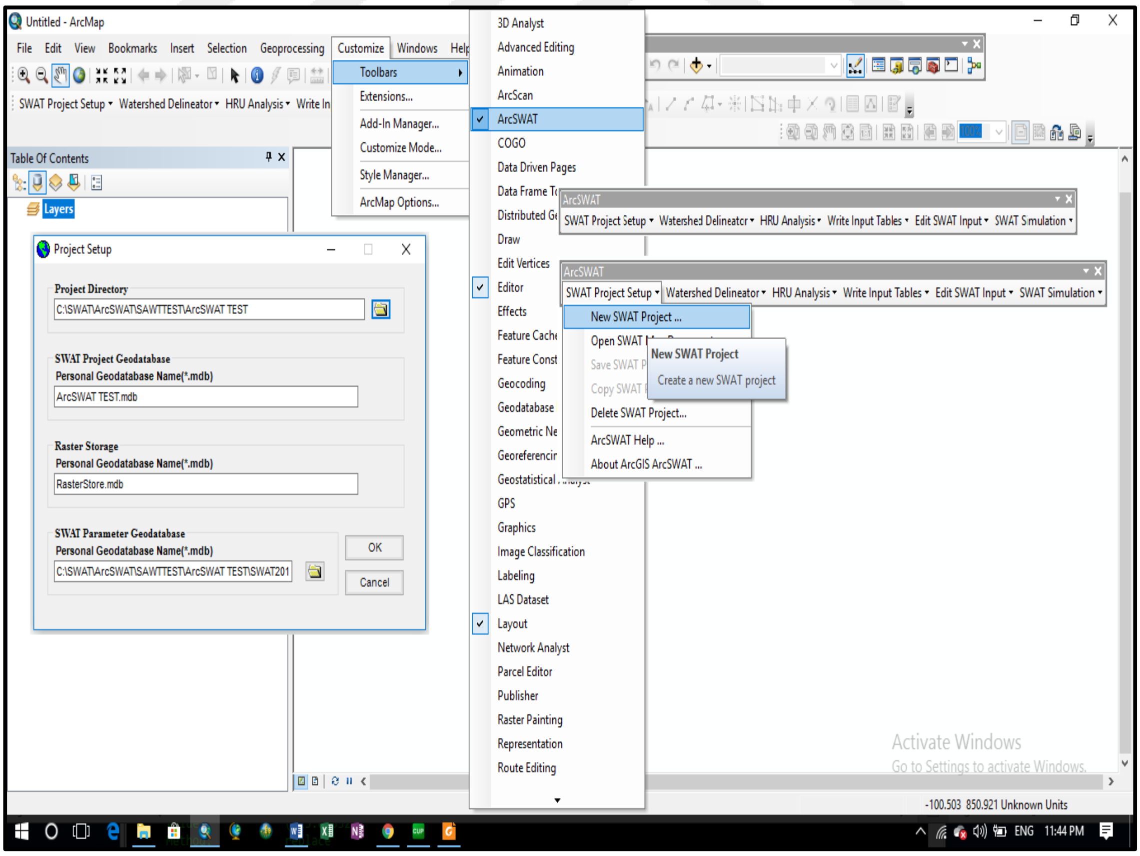

Figure 6. 1 SWAT Toolbar and project setup menu

The next menu from the left side in the SWAT menu bar is the Watershed Delineation sub-menu as shown in Figure 6.1. The Watershed Delineation performs advanced GIS functions to help the users to divide the basin into several hydrologically related sub-basins for use in basin modeling with SWAT. In the Watershed Delineation sub-menu, the first option is the Digital Elevation Model (DEM) setup as shown in Figure 6.2. In this section, projected DEM file of the study area (Kabul River Basin) in the ESRI grid format is loaded. The “Mask” and “Burn in” are optional inputs, where the Mask can be used in the case when the DEM size is so large, then by using Analysis Tools in ArcGIS specific part from the DEM file can be masked and the SWAT model then only considers the part of the DEM file covered by the mask. The Burn-In option can be used in the case when the DEM file does not provide sufficient information to enable the application to predict the position of the stream network accurately. Polyline shapefile with different stream network locations need to be created by the user in ArcGIS. By importing this shapefile, the “burn-in” option defines the location of the streams in the DEM file.

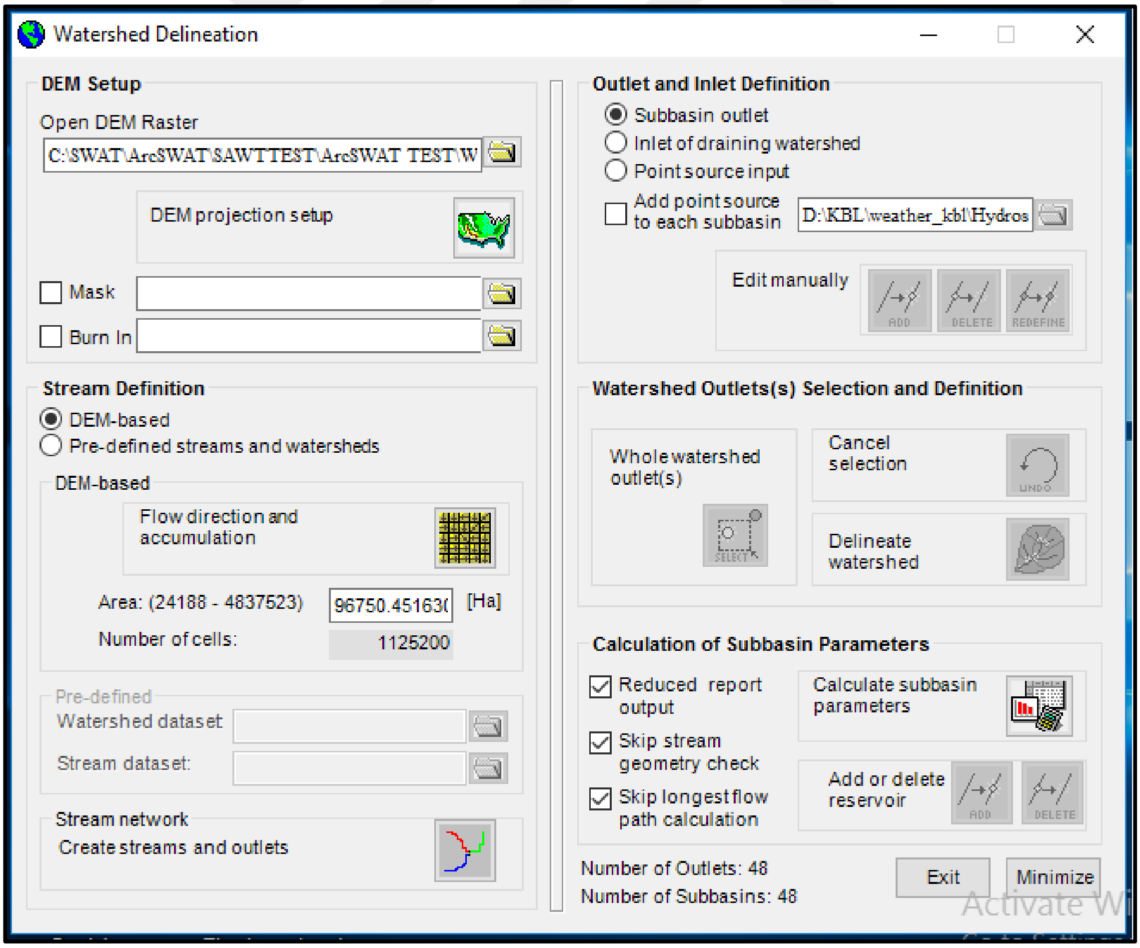

Figure 6. 2 Watershed Delineation Menu

After defining the DEM, flow direction and accumulation option is used to pre-process the DEM by filling sinks and computing the flow direction and flow accumulation grids. When accurate streams data are available, the user can load the data by selecting a stream data set from the pre-defined watershed option. If streams data are not available, the user can select the create streams and outlets option to create streams network directly from the loaded DEM file. In this study, streams are created from the DEM file by using the create streams and outlets option.

To properly delineate a watershed, outlets and inlets must be defined perfectly within the basin. Based on the inlets and outlets, the SWAT model divides the basin into sub-basins and each outlet represents the properties of the corresponding sub-basin. Outlets are the main part of the watershed delineation and are defined as the points in the basin or sub-basin where streamflow exits the basin or sub-basin area. Inlets and outlets can be added to the stream network either by loading a predefined table created by the user or by clicking and defining them manually from the stream network map. To define the locations of outlets in the stream map, attention must be taken to select the locations closest to the available monitoring stations, which is useful for comparison of model predicted discharge with observed discharge.

It is necessary to select a suitable outlet before delineating a watershed, at least one outlet must be selected to delineate the watershed. In the present study, 18 outlets are defined in the main channel of basin, by choosing one appropriate outlet, the basin is delineated and it is divided into 48 sub-basins and geomorphic characteristics of the sub basins and reaches are calculated by clicking the "Calculate Sub-basin parameters", also this option can be used to define the location of reservoirs in the basin.

Once all parameters have been successfully calculated, a new item called Topographic Report is available from the Watershed Reports. This report includes a statistical overview and distribution of individual land surface elevations in the basin and all sub-basins. The last option in the watershed delineation menu is to add or delete reservoirs that provide one convenient way to reflect the amount of water in the model. In the current study, the reservoirs are not included in the analysis due to insufficient reservoir data.

6.3 Hydrological Response Unit (HRU) Analysis

Hydrological models such as SWAT need several data classes of land use and soil and the model calculates the area and hydrological parameters of each land-soil category in each sub-basin. The HRU analysis menu on the ArcSWAT toolbars is defined as the second important sub-menu of the SWAT model consisting of land use, soil, and slope layers. The HRU analysis tools enable users to upload land use and soil data into the project, to evaluate slope characteristics, and to determine combinations and distributions of land use / soil / slope category for the delineated basin and each sub-basin respectively. Land use and soil datasets must be in an ESRI grid or shapefile that has the same coordinate system as the DEM. The SWAT model converts the ESRI grid and shapefile of the land use and soil datasets into the raster format for the overlay process. The first option in the HRU Analysis sub-menu is the Land use/Soils/Slope definition as shown in Figure 6.3. By clicking the Land use/Soils/Slope definition, the pop-up window as shown in Figure 6.3 opens.

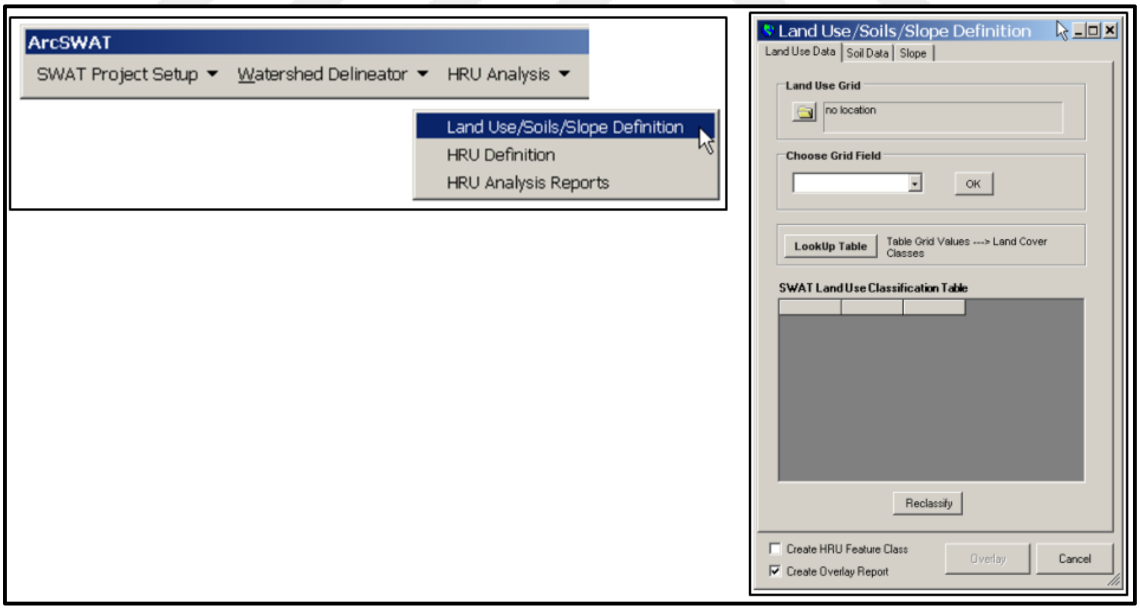

Figure 6. 3 Menu for HRU Analysis (Source: M.Winchell et al, 2013)

After loading and linking a land use and soil dataset, the user has options to define the land use and soil classes directly from the SWAT user's soil, urban, and crop database.

These soil and land use datasets can be added manually by double-clicking the LanduseSwat and Name column, as shown in Figure 6.4 and Figure 6.5.

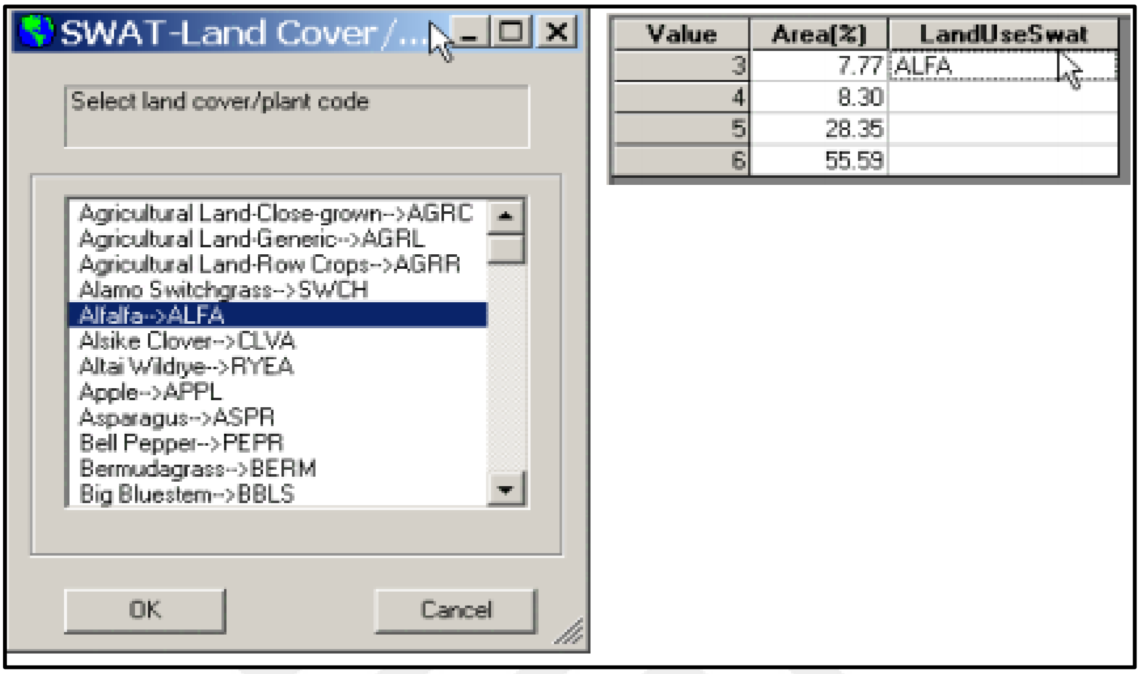

Figure 6. 4 Adding Land use Classes manually from the SWAT crop or urban database (Source: M.Winchell et al, 2013)

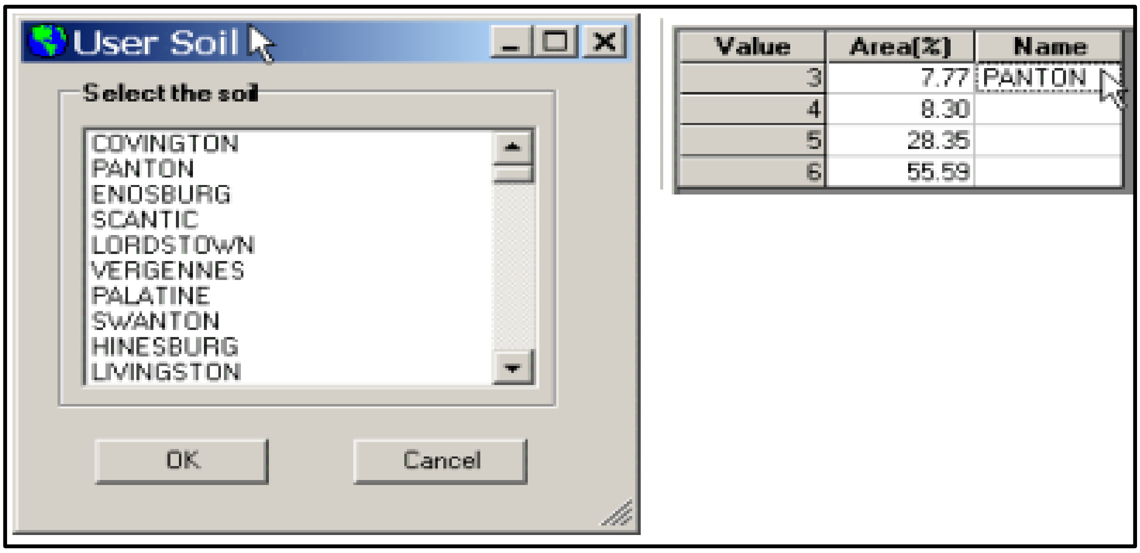

Figure 6. 5 Adding Soil Classes manually from the SWAT user soil database

(Source: M.Winchell et al, 2013)

In the case, when the user data is from elsewhere than the United States, then the user can not directly use the SWAT soil or land use database as mentioned before. The SWAT model database is created based on the United States Geological Survey (USGS) data sets and the SWAT database only contains the data for the United States. In these situations, the user needs to define each soil and land use class separately and prepare a look-up table for both soil and land use classes. In this study, look-up tables in the Text format are prepared based on the soil and land use classes of the basin. The lookUp Table option shown in Figure 6.3 is used to load the created look-up tables. The look-up table and the attribute table of the loaded ESRI grid or shapefile must contain the same soil and land use classes, otherwise errors occur during the reclassify processes. SWAT recognizes two types of lookup table formats, dBase table format and ASCII (.txt) table format. For the current study, the look-up table of soil and land use are prepared in the ASCII (.txt) format for SWAT as shown in Figure 6.6.

ArcSWAT's HRU analysis includes the segmentation of HRUs by slope classes as well as land use and soil. This is especially important when the basin or sub-basins contains an extensive range of slopes. In SWAT, the user needs to generate a slope classification based on the loaded DEM file used during watershed delineation. For defining a slope, the user can choose to use a single slope across the whole basin or multiple slopes to divide the basin or sub-basin into specified elevation zones. In this study, multiple slopes with four classes as shown in Figure 6.7 is defined. Once all required data (land use, soil, and slope classes) in the HRU Analysis menu are defined and reclassified successfully, the overlay button at the bottom of the HRU Analysis menu shown in Figure 6.3 becomes active. In this study, land use and soil grid data are overlaid successfully with an overlaid percentage of 99.98 % and it pointed out that the uploaded data is correct.

After the overlaying process is done, the HRU analysis reports command becomes active, by clicking this command the user can see two types of reports (Land use-soils-slope distribution and Final HRU distribution reports) created during the HRU definition processes. The Land use-soils-slope distribution report describes the distribution of land use, soil and slope groups in the basin and all sub-basin in details, and provides information about the watershed and sub-basin area covered by these three parameters.

The final HRU distribution report represents the total number of the HRUs of the whole basin and also provides a detailed description of the proportion of area occupies by each HRU in a basin or each sub-basin. In this study, the number of HRUs for the whole basin is 770.

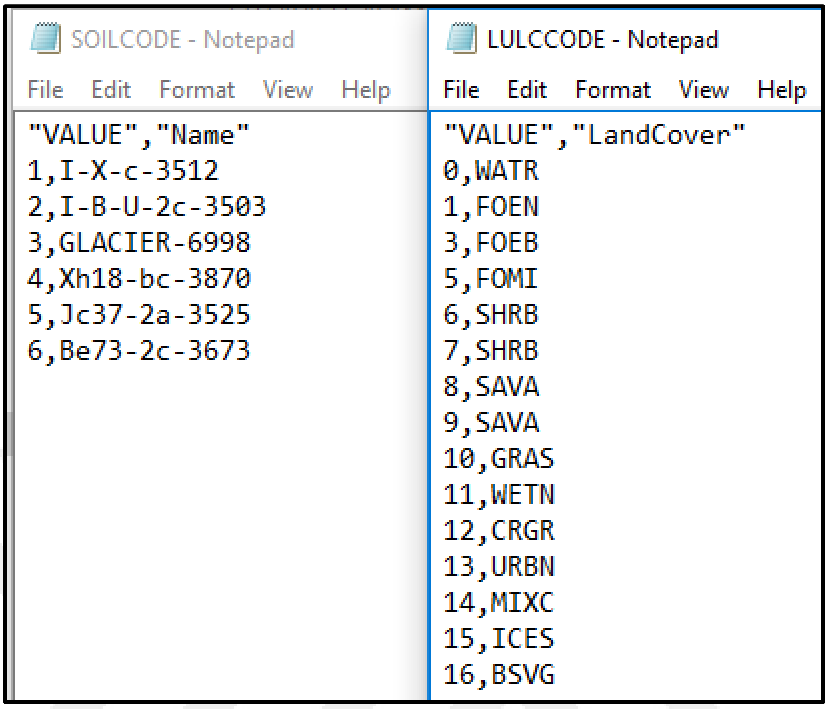

Figure 6. 6 Land use and Soil Look-up Table format of the Study area

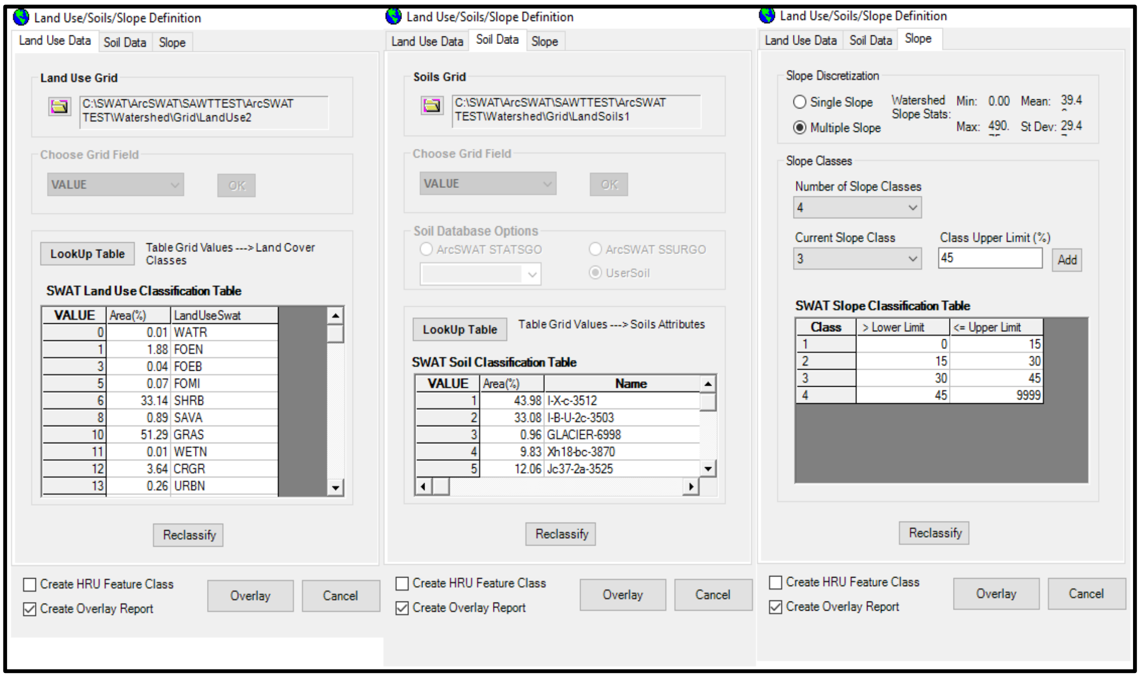

Figure 6. 7 Multiple Slope classes of the Study area

6.4 Write Input Tables

Once the HRUs distribution is defined successfully, the next step is to upload the meteorological station's data using the weather station command from the Write Input Tables menu item on the SWAT toolbar shown in Figure 6.8. The first option in the weather menu is 'Weather Generator Data', for this study the WEGN-user weather database is selected. The other weather database such as WEGN-US-FirstOrder, WGEN_US_COOP_1960_1990,WGEN_US_COOP_1960_2010, WGEN_US_COOP_1970_2000, andWGEN_US_COOP_1980_2010 only provide WGEN statistics for the climate stations located around the United State. These weather databases cannot be applied in the case when the user applies the model with different weather data rather than United State's. Different techniques have been applied to create the WGEN database for the SWAT model. In the present study, the Swat Weather Database Tool is applied to create appropriate WGEN statistics of several weather stations located within the basin.

The location of weather stations with their data is prepared in the text file and must be in the format defined in the SWAT user manual with the same naming convention. Both the station location text file and the data text file of each station must be in the same folder, whereby uploading the station's location the model links each station to their data in the folder and the data is loaded by the model for further calculation.

In this study, daily meteorological data (rainfall, maximum and minimum temperature) as mentioned in Chapter 4 are set-up. Other meteorological data such as relative humidity, solar radiation, and wind speed are simulated by SWAT model. These meteorological data are prepared in the text file as shown in Figure 6.9. Figure 6.9 represents the meteorological data of the Bagh-i-Lala station. If the same stations are using for all weather data, like in this study, then the user needs to rename the station's locations in the manner such that each station is linked to their weather data. For example, in this study, the pBagh-i-Lala and tBagh-i-Lala represent the precipitation and temperature of the Bagh-i-Lala stations, respectively. The name of the station in the loaded text file must be the same with the data containing the text file as shown in Figure 6.10. After the weather station is successfully loaded, the next step is to create a database file containing the information needed to create a default entry for SWAT. By using the Write All command from the Write Input Table menu shown in Figure 6.8, all input files in the defined folder are read and all remaining data files needed for the SWAT model are created.

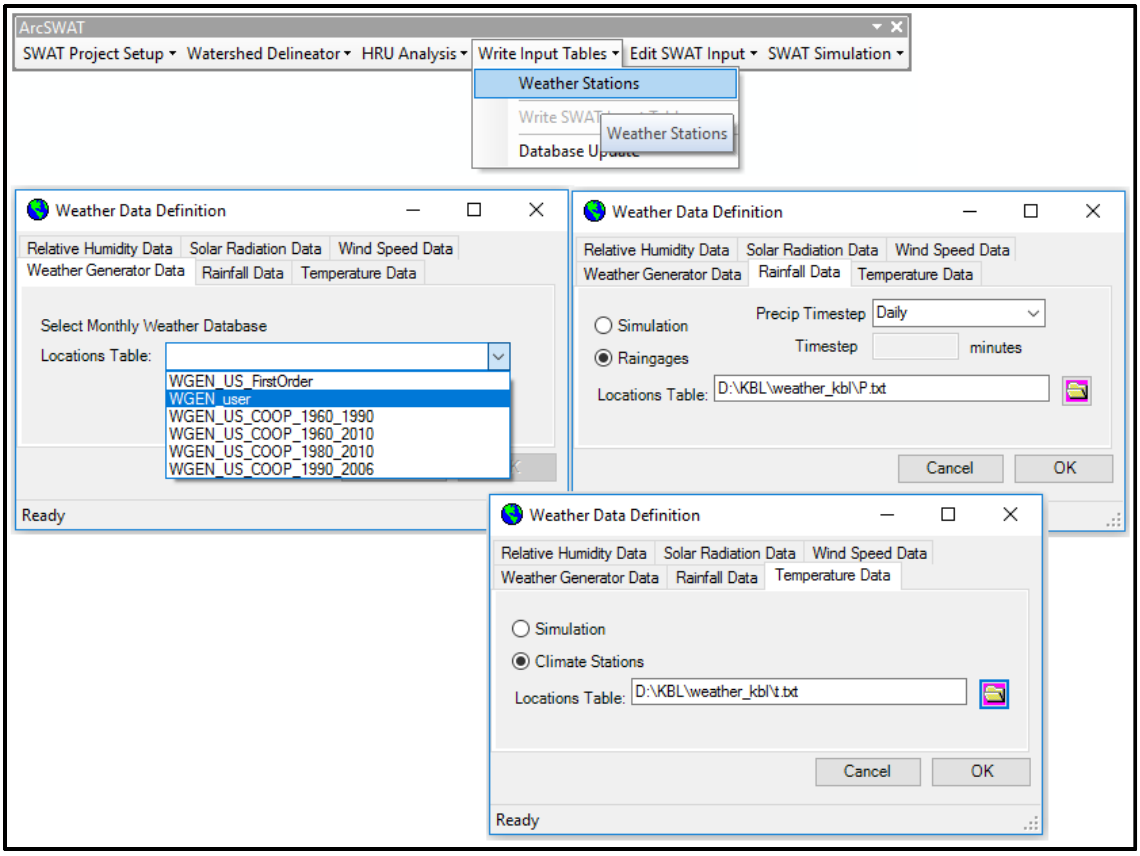

Figure 6. 8 Write Input Tables Menu

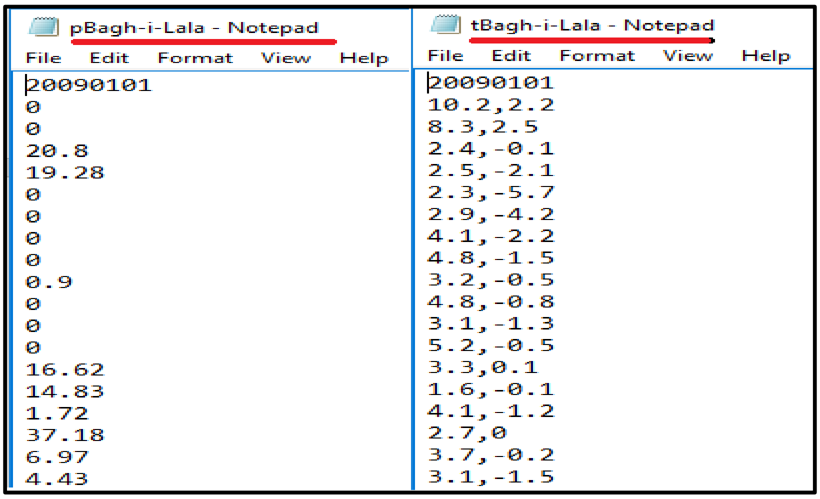

Figure 6. 9 Screenshot to illustrate format of weather data input text files of the Bagh-i-Lala station

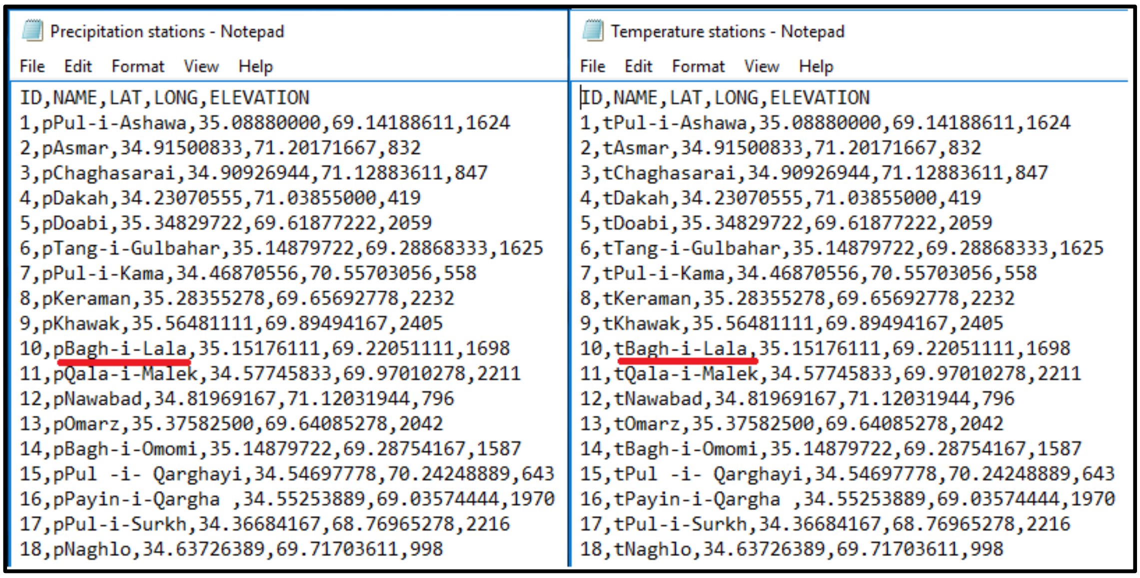

Precipitation stations - Notepad

File Edit Format View Help

```
ID,NAME,LAT,LONG,ELEVATION
1,pPul-i-Ashawa,35.08880000,69.14188611,1624
2,pAsmar,34.91500833,71.20171667,832
3,pChaghasarai,34.90926944,71.12883611,847
4,pDakah,34.23070555,71.03855000,419
5,pDoabi,35.34829722,69.61877222,2059
6,pTang-i-Gulbahar,35.14879722,69.28868333,1625
7,pPul-i-Kama,34.46870556,70.55703056,558
8,pKeraman,35.28355278,69.65692778,2232
9,pKhawak,35.56481111,69.89494167,2405
10,pBagh-i-Lala,35.15176111,69.22051111,1698
11,pQala-i-Malek,34.57745833,69.97010278,2211
12,pNawabad,34.81969167,71.12031944,796
13,pOmarz,35.37582500,69.64085278,2042
14,pBagh-i-Omomi,35.14879722,69.28754167,1587
15,pPul -i- Qarghayi,34.54697778,70.24248889,643
16,pPayin-i-Qargha ,34.55253889,69.03574444,1970
17,pPul-i-Surkh,34.36684167,68.76965278,2216
18,pNaghlo,34.63726389,69.71703611,998
```

Temperature stations - Notepad

File Edit Format View Help

```
ID,NAME,LAT,LONG,ELEVATION
1,tPul-i-Ashawa,35.08880000,69.14188611,1624
2,tAsmar,34.91500833,71.20171667,832
3,tChaghasarai,34.90926944,71.12883611,847
4,tDakah,34.23070555,71.03855000,419
5,tDoabi,35.34829722,69.61877222,2059
6,tTang-i-Gulbahar,35.14879722,69.28868333,1625
7,tPul-i-Kama,34.46870556,70.55703056,558
8,tKeraman,35.28355278,69.65692778,2232
9,tKhawak,35.56481111,69.89494167,2405
10,tBagh-i-Lala,35.15176111,69.22051111,1698
11,tQala-i-Malek,34.57745833,69.97010278,2211
12,tNawabad,34.81969167,71.12031944,796
13,tOmarz,35.37582500,69.64085278,2042
14,tBagh-i-Omomi,35.14879722,69.28754167,1587
15,tPul -i- Qarghayi,34.54697778,70.24248889,643
16,tPayin-i-Qargha ,34.55253889,69.03574444,1970
17,tPul-i-Surkh,34.36684167,68.76965278,2216
18,tNaghlo,34.63726389,69.71703611,998
```

Figure 6. 10 Creenshot to illustrate format of weather stations input text files

SWAT input files before reading and after reading are shown in Figure 6.11. The SWAT model takes a long time to read these files and some errors can occurr during this process. After the model's inputs are checked many times to find errors and eventually further corrected, the model reads all input files successfully. Before running the model, the initial input values of the watershed must be specified. Such values are spontaneously set based on the delineation of the watershed.

Once all the above procedures are done, the Edit SWAT Input menu becomes active where the user has the option to edit the input parameters before running the model. The Edit SWAT input menu contains the SWAT database, point source discharge, Inlet discharge, Reservoirs, etc. These can be edited if the default methods and parameters defined by the model are unsatisfactory to the user. The SWAT Edit Input menu can be used at any time whenever the user needs, but by editing any parameter the model must be re-run. For instance, if the land use and soils data are edited then the user must return to the watershed delineation menu and restart all processes from that point.

6.5 SWAT Simulation

All required input data such as meteorological, soil, and land use as mentioned in Chapter 4 were created in the format required by the SWAT model and loaded properly into the model. After watershed delineation and defining outlets and streams, the meteorological stations were linked to the corresponding sub-basins outlets in order to measure runoff in each outlet and compare with the observed runoff. Once the above processes were done the next step is to simulate the model, this task can be done by the SWAT simulation menu. The Simulation menu allows the user to finalize the setup of input for the SWAT model and run the model.

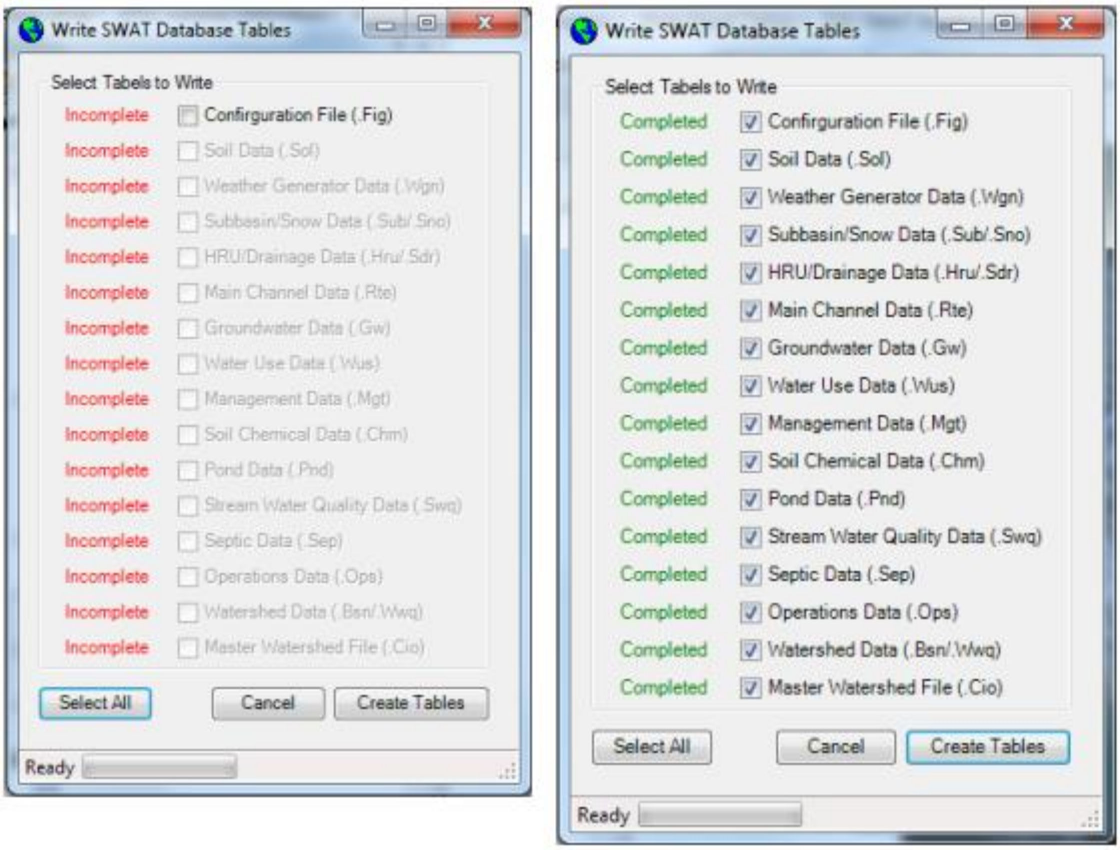

Figure 6. 11 Created Tables by SWAT Model (Source: M.Winchell et all, 2013)

The SWAT simulation menu is the last menu of the model, this menu generally focuses on the time interval in which the data are simulated by the model and it provides information about the SWAT output reports. The first command in the SWAT simulation menu is ‘Run SWAT’, by clicking this command the model simulation dialog box shown in Figure 6.12 is opened. This dialog box is the step where the user must be careful about the output data files and be aware of all the features shown in the window. The first command in the simulation dialog box is to set-up the starting and ending dates of the simulation. Generally, the model selects the starting and ending simulation dates directly from the uploaded data, but the user has the option to change the model simulation period to their target starting and ending dates. In this study, the starting and ending dates are set up from the loaded data (1/01/2009 and 12/31/2017) respectively.

Once the starting and ending dates of the simulation are defined, the next section is to define the rainfall distribution method. For the rainfall simulation, the model use two types of equations like the Skewed normal and Mixed exponential equations. These equations are described in more detail in Chapter 5 under the weather sub-title. Before selecting the rainfall distribution equation, the time step of the rainfall data must be set. The time step option is actived only in the case when the loaded rainfall data are on the sub-daily scale, otherwise, the option is off like in the present study where the rainfall and other uploaded data are on a daily scale. In the current study, the Skewed normal equation with daily rainfall data is used for the rainfall distribution.

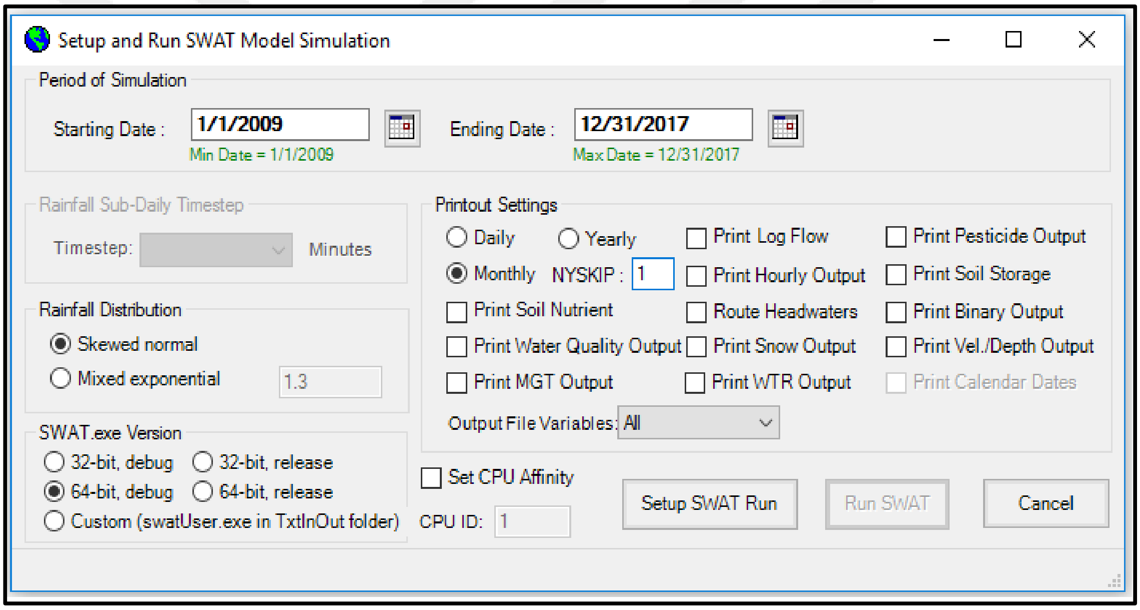

Figure 6. 12 SWAT simulation dialog box

The printout setting section includes several output files that can be printed by the model on a daily, monthly, or yearly base. The NYSKIP option can be used to define the warm-up period for the simulation process and the model does not print output files for this warm-up period. The warm-up period is significant to ensure that the model is not affected by the initial conditions. The length of the warm-up period varies from basin to basin and it can be selected based on the data interval for instance, for 30 years of data, the user can use a warm-up period of at least 5 years. The last section in the SWAT simulation dialog box is to choose the SWAT. exe Version. This section contains two versions of SWAT.exe for 32-bit and 64-bit operating systems. The debug version provides detailed massages in the case of a SWAT crash, where the release version does not include massaging during a crash (M. Winchell et al., 2013). However, the release versions run much faster than the debug version. In the current study, the warm-up period is selected to be a year and the 'All' option in the 'Printout Setting' is chosen to print all output files of the model on a monthly and daily time base.

Once all the required parameters in the SWAT simulation dialog box are defined, the next step is to create the watershed master control file (file.cio). This file can be generated by clicking the 'Setup SWAT run' command, which also creates a new set of input files for the model to be used during the running process. The watershed master control file (file.cio) provides general information about modeling options, climate inputs, databases, and output features as shown in Table 6.1.

Table 6. 1 Text file format of the watershed master control (file.cio) file

```
Master Watershed File: file.cio
Project Description:
General Input/Output section (file.cio):
12/17/2019 12:00:00 AM ARCGIS-SWAT interface AV

General Information/Watershed Configuration:
fig.fig
           8    | NBYR : Number of years simulated
        2009    | IYR : Beginning year of simulation
           1    | IDAF : Beginning julian day of simulation
         366    | IDAL : Ending julian day of simulation
Climate:
           0    | IGEN : Random number seed cycle code
           1        | PCPSIM : precipitation simulation code: 1=measured,
2=simulated
           0    | IDT : Rainfall data time step
           0    | IDIST : rainfall distribution code: 0 skewed, 1 exponential
       1.300    | REXP : Exponent for IDIST=1
```

6.6 Sensitivity Analysis

Once all the above procedures are done, the sensitivity of the model parameters is checked by applying SWAT Calibration and Uncertainty Program (SWAT-CUP). The SWAT Calibration and Uncertainty Program (SWAT-CUP) is a computer-based widely used program developed by Dr. Karim C. Abbaspour for the purpose of calibration, validation, and sensitivity analysis of the SWAT model. This program contains different methods such as the Sequential Uncertainty Fitting version 2 (SUFI2), Particle Swarm Optimization (PSO), Generalized Likelihood Uncertainty Estimation (GLUE), Parameter Solution (ParaSol), Markov Chain Monte Carlo (MCMC), that can be used for analyzing of SWAT outputs under several objective functions. The main function of SWAT-CUP is to provide a link between SWAT inputs and outputs. The SWAT-CUP program includes many parameters that can be easily applied based on the hydrological knowledge of the watershed, such as soil, management, crops, precipitation, temperature, and slope parameters (Karim C. Abbaspour, 2012).

A complex hydrological model can be influenced by different parameters, where most of these parameter's values are not precisely defined. There are several reasons, that is why the values of these parameters are not exactly known. It can be due to spatial variability, measurement errors, and incomplete description of both elements and processes present in the system. Accordingly, an important objective of obtaining a well representative hydrological model is to optimize the internal parameters of the model. These kinds of parameters can be optimized by calibrating the model outputs, where the calibration process is mostly supported by the sensitivity analysis. Sensitivity analysis is an important issue in hydrological modeling and it must be considered that which parameter in which range is more sensitive. Sensitivity analysis can be used to estimate the rate of change in model outputs related to the change in model inputs. In addition, sensitivity analysis makes it easier to select important and effective parameters for model calibration by specifying the parameters that represent the higher sensitivity of the model outputs related to the model input variance.

The Latine Hypercube Sampling-One At a Time approach is commonly used for sensitivity analysis. This approach considers the sensitivity of the variable to the parameter changes if all other parameters are held constant at some value. The Latine Hypercube Sampling-One At a Time approach can also be applied to get an idea about the ranges of the applied sensitive parameters, which can be set to the acceptable ranges for further analysis. In this analysis, 27 different sensitive parameters shown in Table 6.2 are tested under the Latine Hypercube Sampling-One At a Time approach. Out of these 27 sensitive parameters, the 20 most sensitive parameters that have a strong effect on the basin runoff are selected for the model calibration and validation analysis. Those 20 sensitive parameters with more details are presented in Chapter 7 Table 7.5.

In SWAT-CUP, three different methods (v, a, and r) can be used to indicate the type of change to be applied to the parameter. Where ("v_") means that the existing parameter value is replaced with the specified value, (“a_”) means that the specified value is added to the existing parameter value, and (“R_”) means that the existing value of the parameter is multiplied by (1+ a given value).

Table 6. 2 Set of tested sensitive parameters

No	Parameter Name	Parameter Name in SWAT-CUP
1	Treshold depth of water in the shallow aquifer required for return flow to occur (mm)	V__GWQMN.gw
2	Snow melt base temperature	V__SMTMP.bsn
3	SCS runoff curve number II	R__CN2.mgt
4	Precipitation lapse rate	V__PLAPS.sub
5	Average slope steepness	R__HRU_SLP.hru
6	Snowfall temperature	V__SFTMP.bsn
7	Minimum melt rate for snow during the year (occurs on winter solstice)	V__SMFMN.bsn
8	Average slope length	R__SLSUBBSN.hru
9	Groundwater delay (days)	V__GW_DELAY.gw
10	Temperature lapse rate	V__TLAPS.sub
11	Snow pack temperature lag factor	V__TIMP.bsn
12	Threshold depth of water in the shallow aquifer for "revap" to occur (mm)	V__REVAPMN.gw
13	Saturated hydraulic conductivity	R__SOL_K(..).sol
14	Soil evaporation compensation factor	R__ESCO.hru
15	Maximum melt rate for snow during year (occurs on summer solstice)	V__SMFMX.bsn
16	Surface runoff lag time	V__SURLAG.bsn
17	Available water capacity of the soil layer	R__SOL_AWC.sol
18	Manning's "n" value for overland flow	R__OV_N.hru
19	Baseflow alpha factor (days)	V__ALPHA_BF.gw
20	Groundwater "revap" coefficient	V__GW_REVAP.gw
21	Snow water equivalent that corresponds to 50% snow cover	V__SNO50COV.bsn
22	Manning's "n" value for the main channel	V__CH_N2.rte

(Continue on next page)

(table 6.2 cont.)

23	Effective hydraulic conductivity in main channel alluvium	V__CH_K2.rte
24	Minimum snow water content that corresponds to 100% snow cover	V__SNOCOVMX.bsn
25	Maximum rooting depth of soil profile	V__SOL_ZMX.sol
26	Initial depth of water in the deep aquifer (mm)	V__DEEPST.gw
27	Deep aquifer percolation fraction	V__RCHRG_DP.gw

6.7 Model Calibration

Calibration is a significant step in the development of hydrological models, providing both accurate and real depictions of the physical processes taking place in a watershed. As mentioned in the previous section, a set of parameters that affect the runoff process is set to execute the calibration process. The simulated discharge by the SWAT model and the time series of discharge at the outlets of each sub-basin is defined as inputs to the SWAT-CUP software to calibrate and validate the SWAT model outputs under the defined sensitive parameters. The purpose of using sensitive parameters in the calibration process is to minimize the difference between simulated and observed discharge. The most sensitive parameters of the present study for the process of calibration are presented in Chapter 7 at Table 7.5, ordered from a more sensitive one to the less sensitive one. The calibration of the model outputs is deemed to be necessary due to the possible existence of some uncertainties in the model inputs. In order to calibrate and validate the discharge data simulated by the SWAT model, the available observed discharge data of the station located at the outlet of the basin must be divided into two groups, one for calibration and other for the validation process. These data (observed data) must be divided in such a manner that each part of the data must contain wet, moderate, and dry years. Most of the researchers recommended that two-third of the simulated and available observed data can be used for calibration and the remaining one-third of the data for the validation process.

In this study, two-third of the observed discharge data with one year of the warm-up period is used for calibration (2010-2014). SWAT-CUP is run several times to get a better result. The simulation interval of the SWAT-CUP is set to 300 and further iterations are performed to get a good match between the simulated and observed discharge.

6.8 Model Validation

The model is checked against an independent set of observed discharge data to utilize a calibrated model to estimate the effectiveness of possible management practices in the future. This test of the model on a separate set of datasets is often called model validation. The validation process is carried out at the same hydrological stations, that are used previously for the calibration, located at the sub-basins outlets. During the validation, the same input parameters in the same ranges used for the calibration process remained unchanged.

In this study, SWAT-CUP is run under the same number of simulations defined as for the calibration. One-third of the observed data are used for the validation, for a time period of three years from 2015 to 2017. For a better understanding, the entire process of setting up the SWAT model is shown in the below flowchart.

6.9 Model Performance Evaluation

SWAT-CUP software is used in order to analyze the performance of the SWAT model. SWAT-CUP uses ten different statically measures to check the performance of the SWAT model and to compare the simulated SWAT data with observed data. Among these ten statically measures; three of them Nash-Sutcliffe efficiency (NSE), coefficient of determination (R^2), and RMSE standard deviation ratio (RSR) are selected for this study. The SWAT-CUP is run for each of them to see which one provides a better result. Several iterations are carried out for everyone and finally, the model indicates that the NSE can be used as an objective function where it is provided a good result compared to the others.

The Nash-Sutcliffe efficiency (NSE) shows that how much of a graph of observed and simulated data corresponds to the 1: 1 line and it is a normalized statistic that determines the relative magnitude of the residual variance compared to the measured data variance. The values of Nash-Sutcliffe efficiency (NSE) ranges from $-\infty$ to 1.

Values between 0 and 1 are commonly regarded as an acceptable level of model performance, while values below zero mean that the observed average value is a better predictor than the simulated value indicating unacceptable results. The NSE is computed as follows.

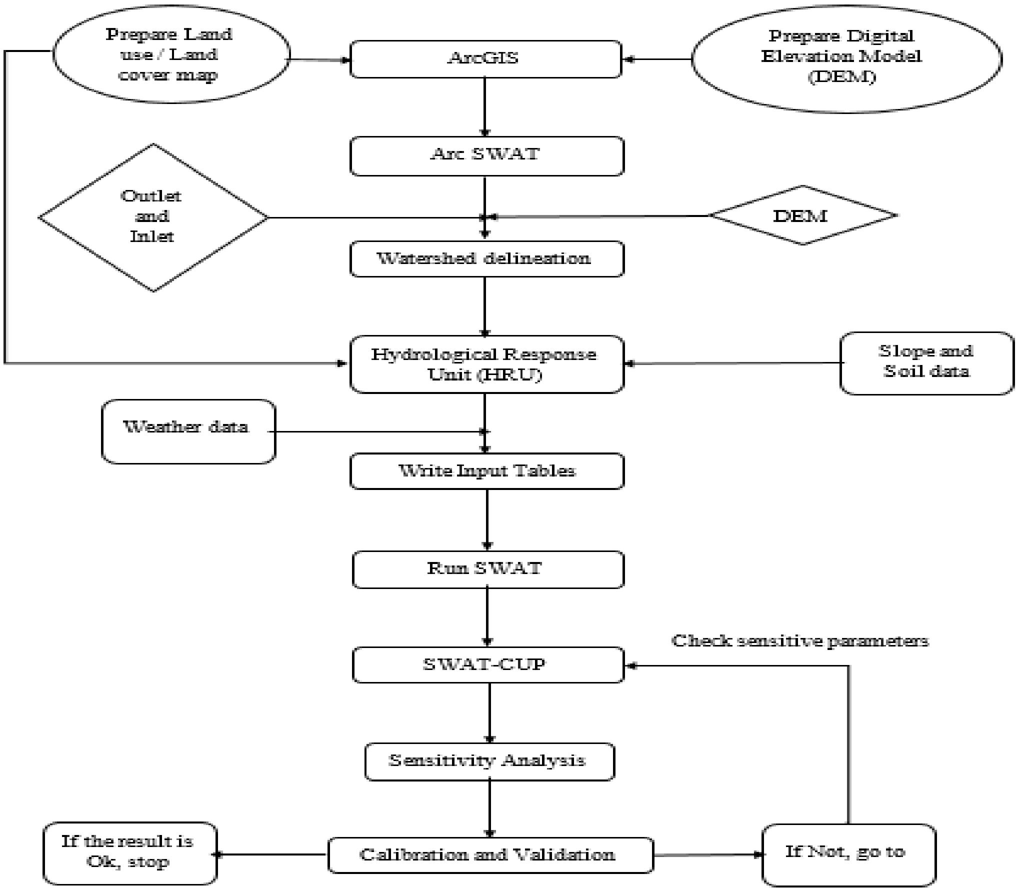

Figure 6. 13 Flowchart of Arc SWAT processing steps

$$NSE = 1 - \frac{\sum_{i=1}^{n}(Q_o - Q_s)^2}{\sum_{i=1}^{n}(Q_o - Q_{om})^2} \quad (6.1)$$

Where, Q_o and Q_s represent the observed and simulated values respectively, and Qom represents the mean observed values.

The coefficient of determination (R^2) is one of the widely used norms for determining the ratio of the total variability in the observed data that can be explained by the model. The values of R^2 are defined in the interval from zero to one, where the closest value to 1 represents a better match between the observed and simulated values. The coefficient of determination (R^2) can be calculated as follow.

$$R^2 = \frac{[\sum_{i=1}^{n}(Q_s - Q_{sm}) * (Q_o - Q_{om})]^2}{\sum_{i=1}^{n}(Q_s - Q_{sm})^2 * \sum_{i=1}^{n}(Q_o - Q_{om})^2} \quad (6.2)$$

Where, Q_{sm} is the mean simulated value.

Root mean square and standard deviation ratio (RSR) is another commonly used statistical measure. The RSR is defined as the ratio of root mean square error (RMSE) and the standard deviation of observed data. The values of RSR are defined in the interval from zero to one, where the lower value of RSR represents a better performance of the model simulation. The RSR can be computed by applying the following equation.

$$RSR = \frac{\left[\sqrt{\sum_{i=1}^{n}(Q_o - Q_S)^2}\right]}{\left[\sqrt{\sum_{i=1}^{n}(Q_{om} - Q_{sm})^2}\right]} \tag{6.3}$$

CHAPTER 7

RESULT AND DISCUSSION

In this chapter, the results obtained by the SWAT model is discussed. These results include the processes of watershed delineation, model calibration and validation, and the most sensitive runoff parameters and the range of these parameters. Each of them is discussed step by step.

7.1 Land Use and Land Cover Reclassification Map

As mentioned in the Materials and dataset chapter, the land use map is used to see which crop or urban parameters occupy the basin area or which land use classes are located in the basin. In the present study, the land use digital map of Asia is downloaded from the USGS Land Cover Institute (LCI), which contains sixteen different land use classes. The specific study area (Kabul River Basin) is extracted from the map and the SWAT model is used to reclassify the defined land use classes of the region. After SWAT reclassification, it is found that the basin has thirteen different land-use classes. These classes were Barren or Sparsely Vegetated, Croplands, Deciduous Needle leaf Forest, Evergreen Needle leaf Forest, Grasslands, Mixed Forests, Shrublands, Permanent Wetland, Savannas, Snow and Ice, Urban, Water, and Woody Savannas. Among the thirteen land use classes, it is found that Shrublands and Grasslands area are dominating with coverage of 1607052.1547 ha and 2477559.2072 ha of the total basin area respectively followed by Barren or Sparsely Vegetated. The land use land cover (LULC) distribution of the Kabul River Basin is shown in Table 7.1., and the digital (LULC) map of the basin is presented in Figure 7.1. From Table 7.1, and Figure 7.2 it can be seen that the Shrublands and Grassland are the most extensive land cover in the basin, accounting for about 33% and 51% of the total basin area, respectively. Barren or Sparsely Vegetated is the third extensive land cover in the basin which occupies 8.74 percent of the total basin area.

Table 7. 1 Land Use distribution in Kabul River Basin

Lan use Classes	Area (ha)	Area (acres)	%Wat.Area
Water	602.6930	1489.2846	0.01
Evergreen Needle leaf forest	91153.3667	225244.5268	1.88
Deciduous Needle leaf forest	1730.6135	4276.4324	0.04
Mixed forests	3379.6114	8351.1887	0.07
Shrublands	1607052.1547	3971106.2268	33.22
Woody Savannas	911.4316	2252.1932	0.02
Savannas	43147.3229	106619.1923	0.89
Grasslands	2477559.2072	6122172.6789	51.21
Permanent Wetland	308.1334	761.4131	0.01
Croplands	176598.8300	436384.5390	3.65
Urban	1 2642.3748	31239.9403	0.26
Snow and Ice	155.0177	383.0566	0.00
Barren or Sparsely vegeted	422854.5716	1044894.7892	8.74

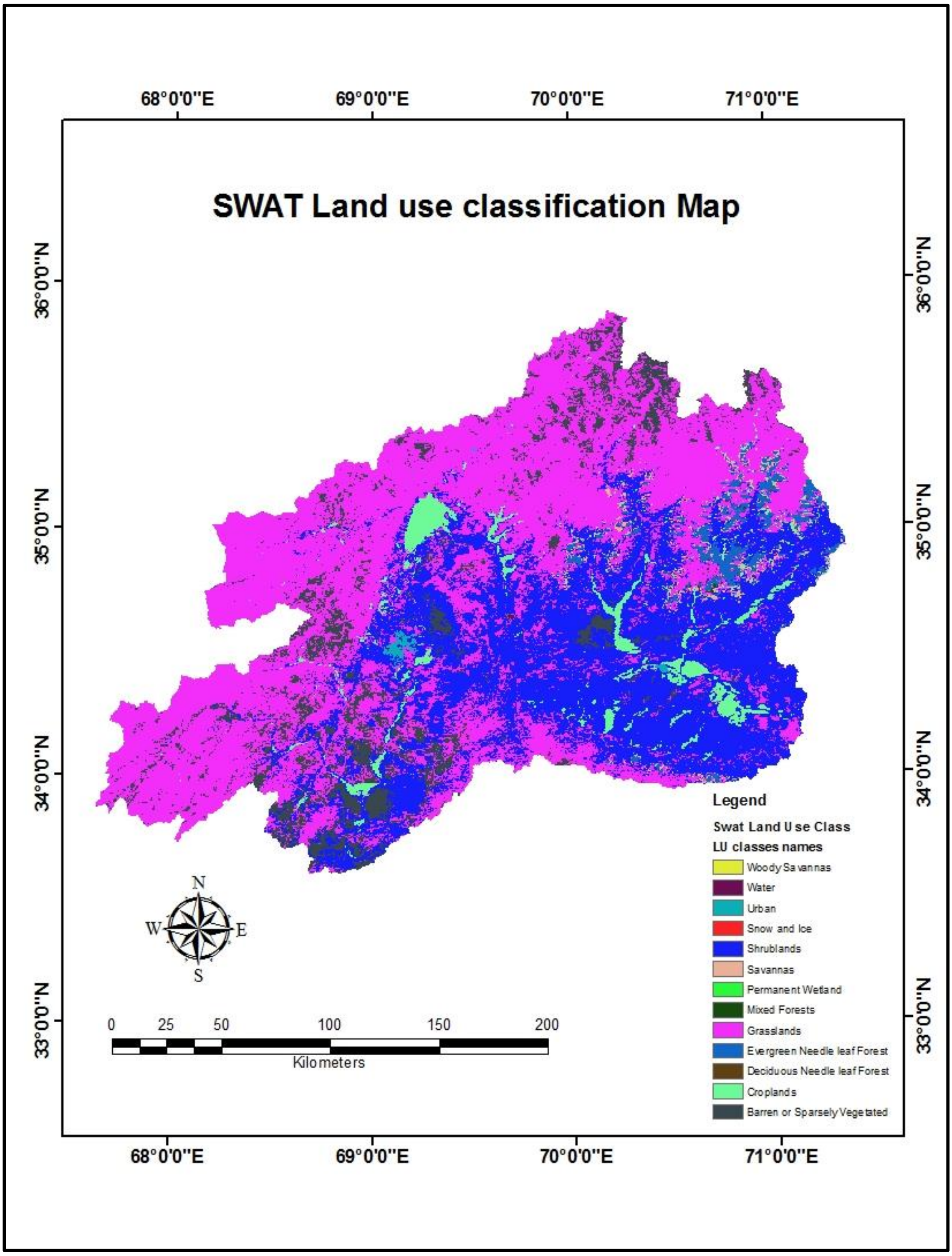

Figure 7. 1 Land Use Map of the Kabul River Basin

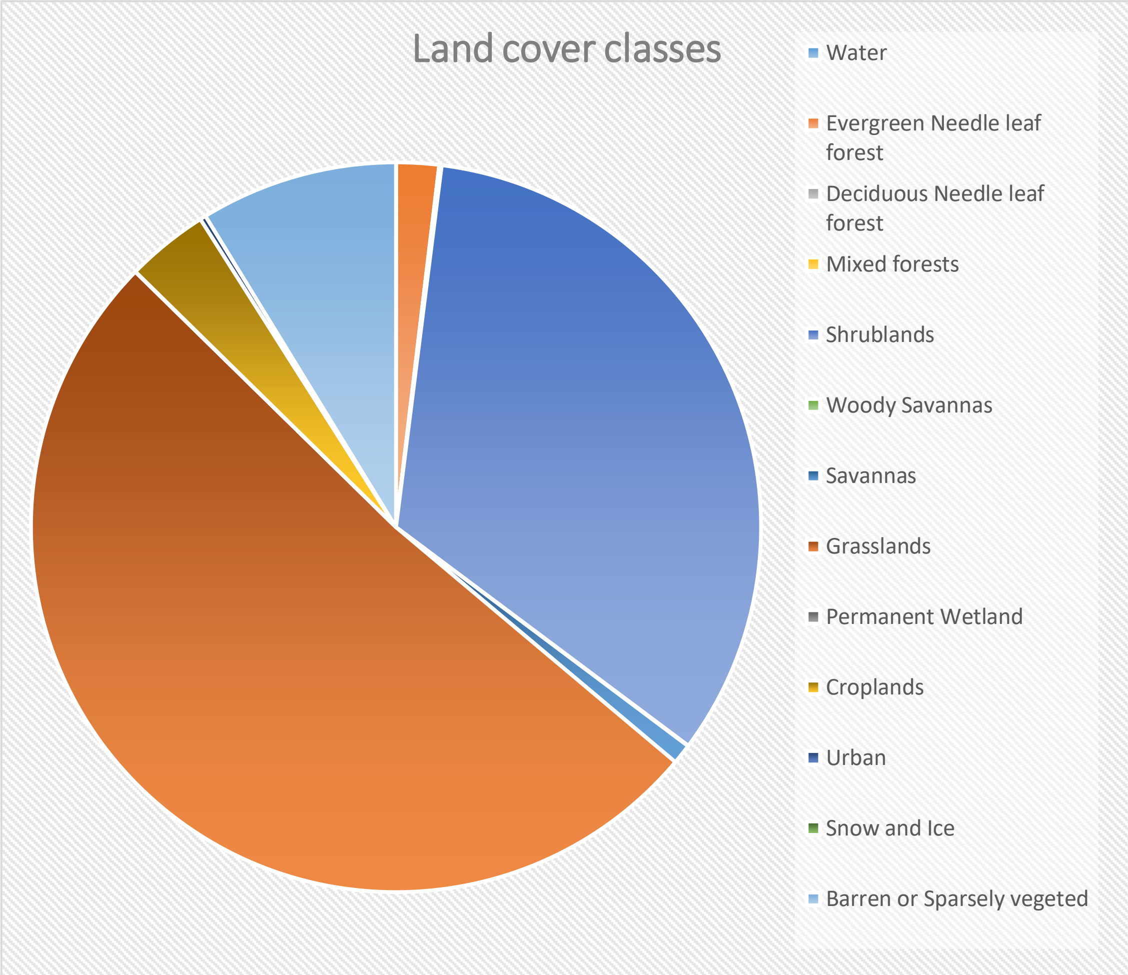

Figure 7. 2 Land cover Classification Pie chart of the Basin

7.2 Soil Classes and Soil Map

The Food and Agriculture Organization of the United Nations (FAO) database is used for soil classification in the SWAT model. Based on the FAO soil classification map and from the reclassification of the SWAT model processes the Kabul River Basin contains six major soil groups, (Be73-2c-3673, GLACIER-6998, I-B-U-2c-3503, I-X-c-3512, Jc37-2a-3525, Xh18-bc-3870), as shown in Figure 7.3. More details such as texture, Hydrologic group, soil combination, etc. of the above soil classes are presented in Table 7.2. As observed in Figure 7.4, LITHOSOL2 (I-X-c-3512) soil covers around 44.33 percent area of the Basin and LITHOSOL1 (I-B-U-2c-3503) is the second-largest soil group which covers about 33.37 percent of the basin area. The distribution of the soil classes of the Kabul river basin is shown in Table 7.3.

Table 7. 2 FAO soil combination

Soil	Name	Hydrologic Group	Texture	Clay percent	Silt percent	Sand percent	Rock percent
Be73-2c-3673	Eutric Cambisols	D	LOAM	23	35	41	0
GLACIER-6998	Gleysols	D	UWB	5	25	70	98
I-B-U-2c-3503	Lithosol 1	C	LOAM	26	30	44	0
I-X-c-3512	Lithosol 2	D	LOAM	22	33	45	0
Jc37-2a-3525	Calcaric Fluvisol	D	LOAM	18	35	47	0
Xh18-bc-3870	Haplic Xerosols	D	SILT-LOAM	21	54	26	0

Table 7. 3 Soil distribution in Kabul River Basin

Soil	Area (ha)	Area (acres)	%Wat.Area
Be73-2c-3673	4927.4544	12175.9861	0.10
GLACIER-6998	35302.7753	87234.9228	0.73
I-B-U-2c-3503	1614410.9270	3989290.1213	33.37
I-X-c-3512	2144955.3387	5300291.8898	44.33
Jc37-2a-3525	572862.9089	1415572.8911	11.84
Xh18-bc-3870	470563.3787	1162785.6370	9.73

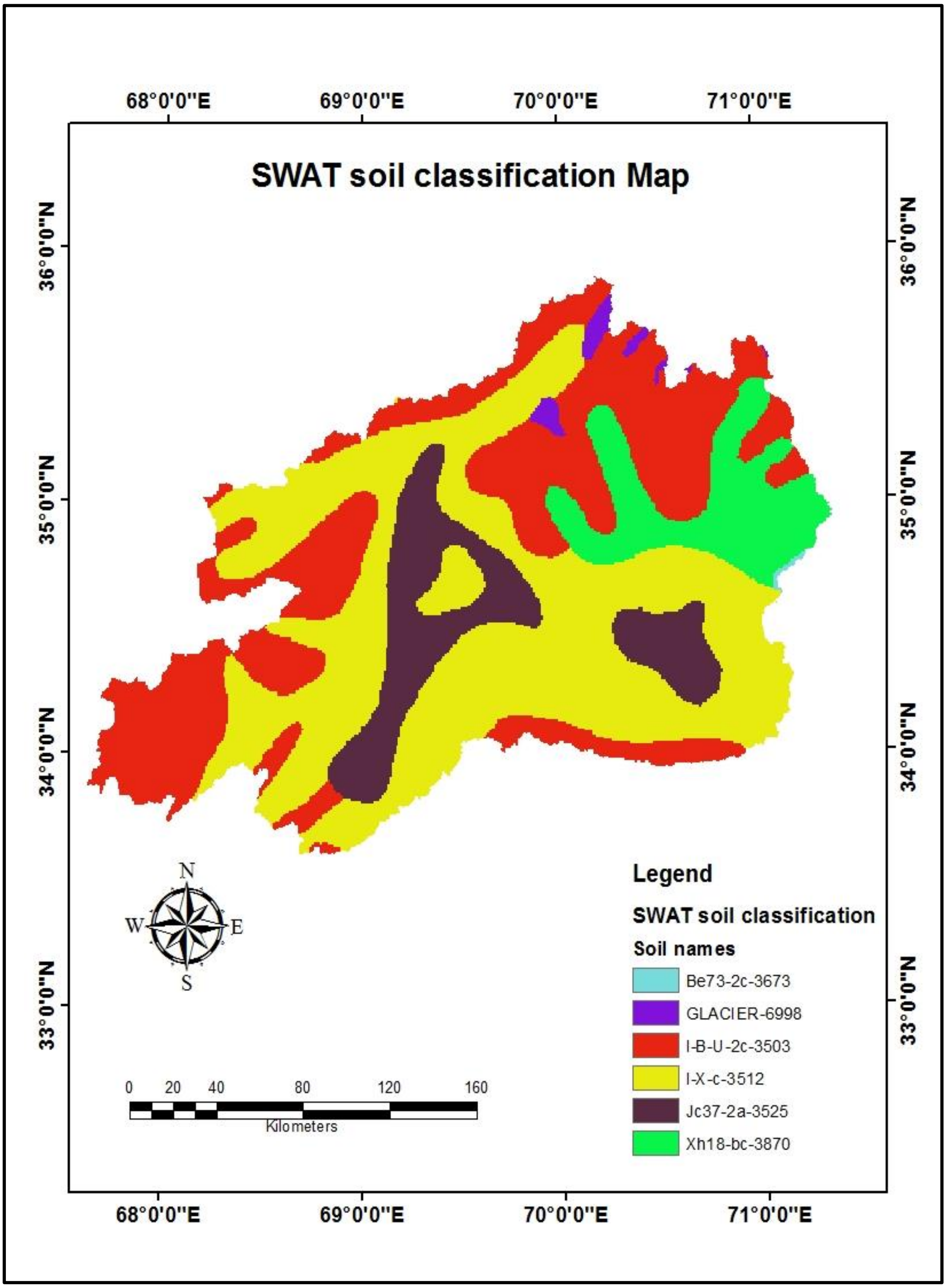

Figure 7. 3 Soil Classification Map of the Kabul River Basin

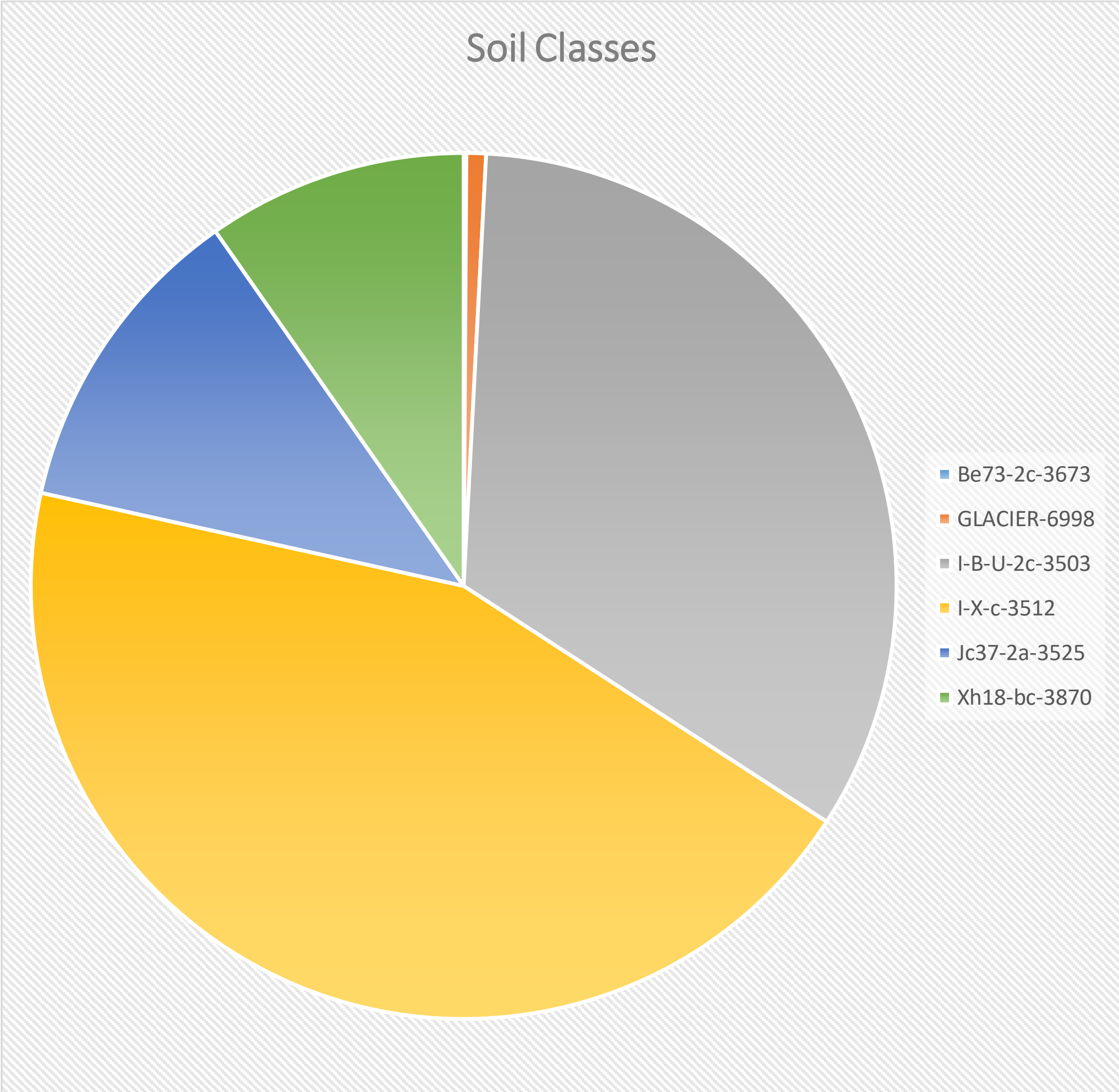

Figure 7. 4 Soil Classification Pie Chart of the Basin

7.3 Drainage Map of the Kabul River Basin

The first step in setting up a SWAT model is the delineation of Watershed. After setting up the model and defining the projected coordinate system of the DEM file for the study area (Kabul River Basin), DEM-based flow direction and accumulation process is performed to generate a drainage network taking into account various outlets. For the defined sub-basins outlets, the entire basin is divided into 48 different sub-basins. Figure 7.5 shows a drainage map of the study area in which SWAT considers different outlets for each sub-basin.

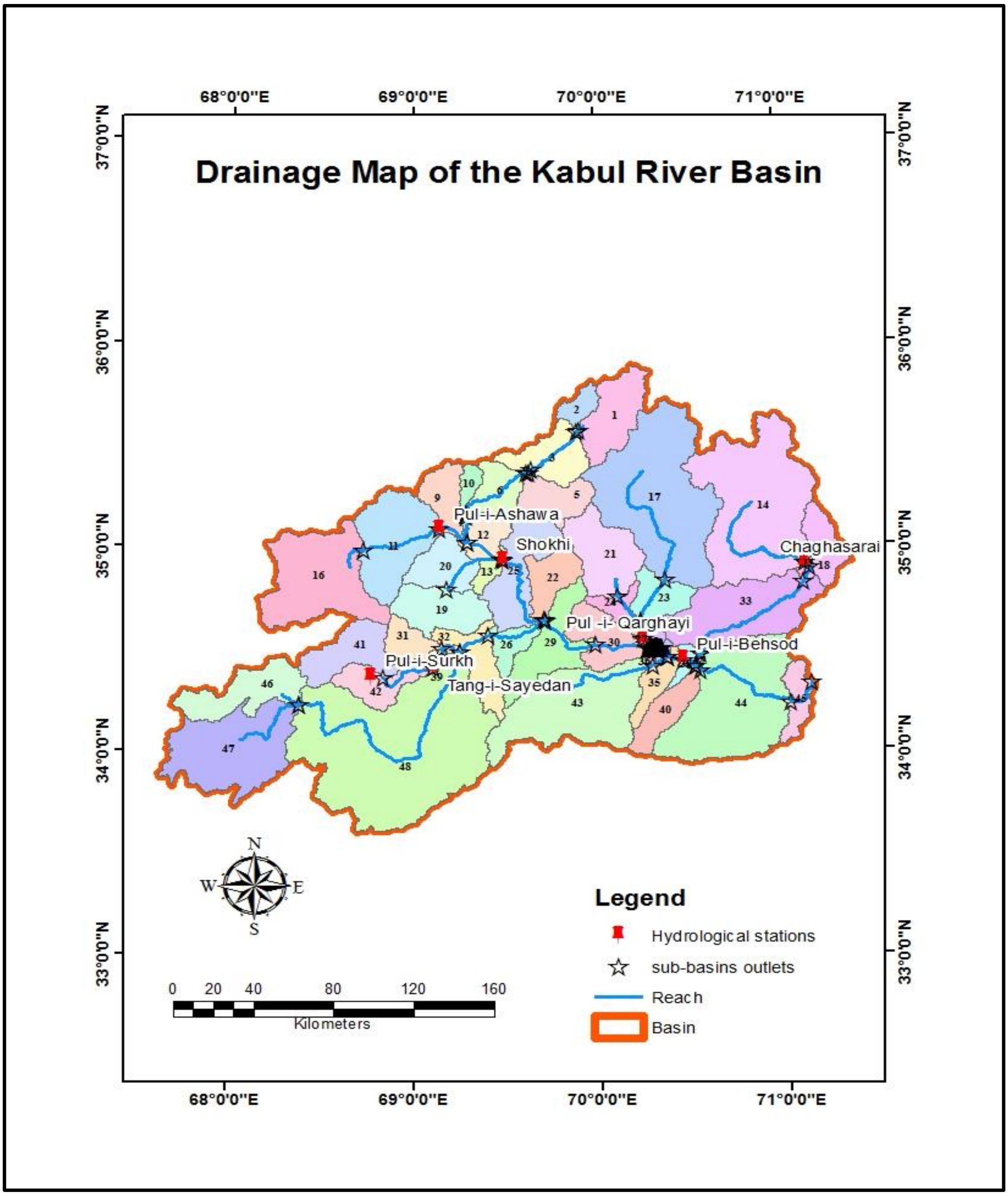

Figure 7. 5 Drainage Map of the Kabul River Basin

7.4 HRU Analysis

The hydrological response units have been defined as parts of the subbasin that contains unique land use, soil, and management attributes. The SWAT model divides the basin area into sub-basins and each sub-basin into several HRUs. The model calculates runoff, sediment, etc individually for each HRU, and then combines them to assess the overall loading from the sub-basin, such as runoff, sediment, etc.

Dividing the basin into regions of unique land use, soil, and slope combinations allow us to examine differences in evapotranspiration and other hydrological conditions at different land covers, soils, and slopes. For the HRUs analysis process, the SWAT model requires land use, soil, and slope as input parameters. Land use and soil maps of the study area are inserted into the model and it is reclassified for the defined soil and land cover classes. In the slope theme, three different slope classes under the multiple slope option are selected for the entire basin, ranging from 0 - 15%, 15% - 30%, 30% - 45% and 45% - 9999% as shown in Figure 7.6. After successfully reclassifying and overlying the land use, soil, and slope datasets, the model creates 770 HRUs with a unique combination of land use, soil and slope with an overlap of 99.98 % basin boundaries.

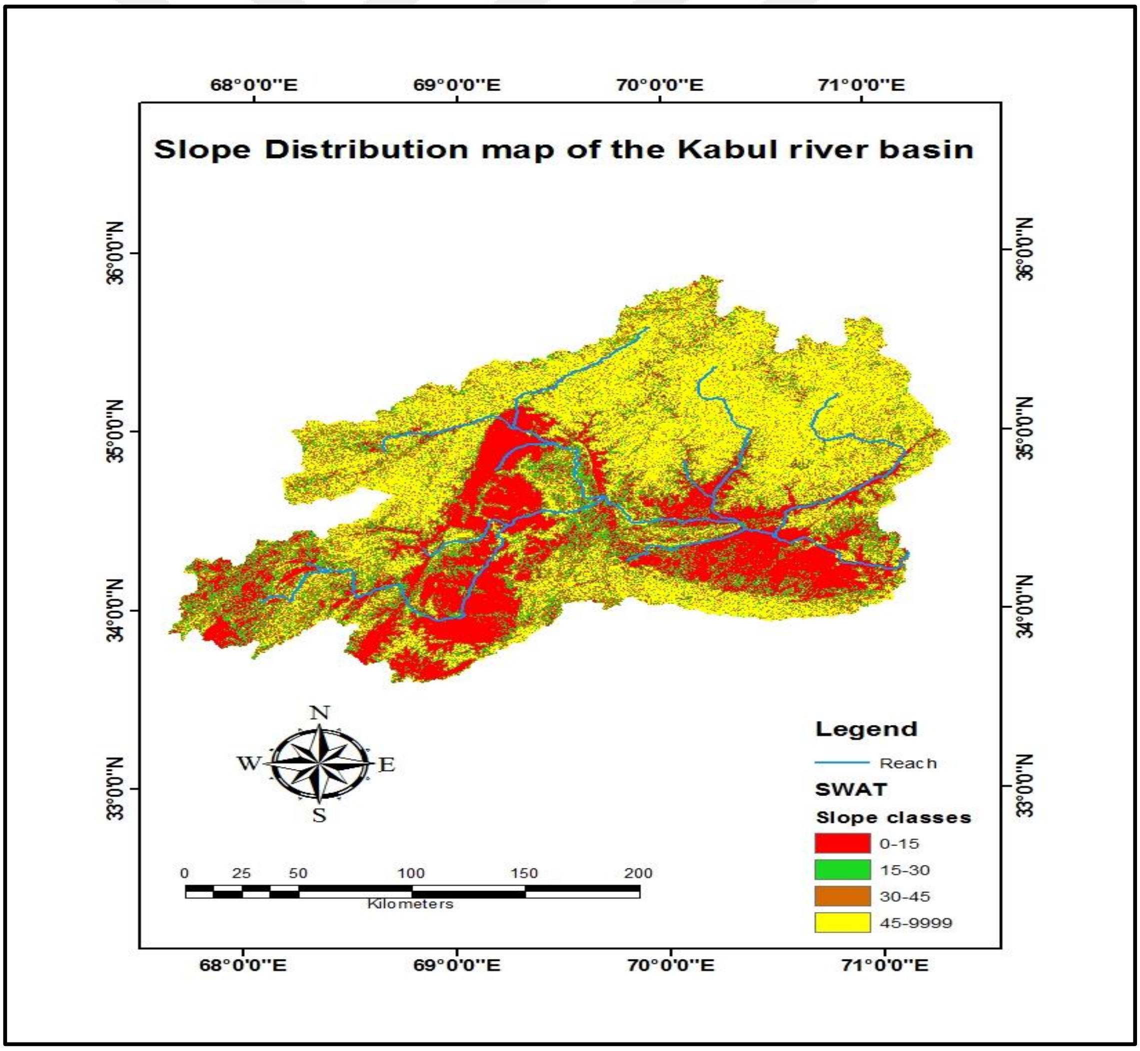

Figure 7. 6 Slope Distribution map of the Kabul River Basin

7.5 Water Balance of Kabul River Basin Generated by SWAT

The most important part of rainfall-runoff modeling is to use the observed rainfall data to predict catchment hydrological components such as surface runoff, evapotranspiration, lateral flow and percolation generated in the basin.

After properly defining the HRUs distribution, land use, soil, and slope the weather database files are provided as input to the SWAT model. The model simulation date is set based on observed weather data interval from 01/01/2009 to 31/12/2017 and Run SWAT is selected under the SWAT simulation menu with one year of the warm-up period. The model is run both on a monthly and daily basis and the model output results for the entire basin, for each sub-basin or for each HRU are printed daily and monthly. Finally, the water balance components of the Kabul River Basin are generated by SWAT Check. From the result obtained by SWAT, as shown in Figure 7.7 the annual average rainfall in the Kabul River Basin is estimated to be 484.7mm/year, evaporation and transpiration, and potential evapotranspiration are estimated 52.6mm/year and 59.6mm/year, respectively. The average monthly hydrology components of the study area obtained by SWAT is presented in Table 7.4.

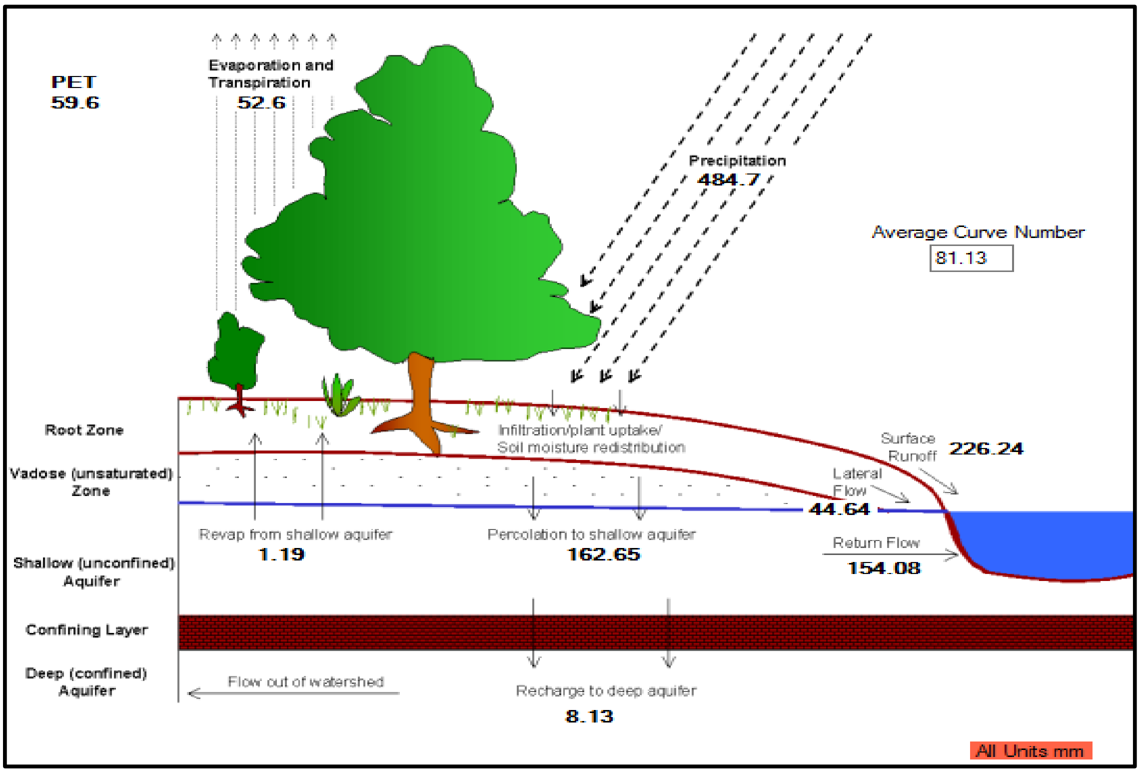

Figure 7. 7 Water balance of Kabul River Basin by SWAT Check

Table 7. 4 Average monthly hydrology components of the study area over the period 2009 to 2017

Month	Rain (mm)	Snow fall (mm)	SURF Q (mm)	LAT Q (mm)	Water Yield (mm)	ET (mm)	PET (mm)
1	33.79	16.67	8.63	2.39	18.49	0.53	0.55
2	75.86	35.69	24.55	5.65	40.4	1.37	1.53
3	67.77	11.91	36.07	8.84	65.68	3.89	4.45
4	59.78	1.42	15.58	9.88	54.37	6.52	7.32
5	30.95	0	4.56	6.07	41.1	9.46	10.21
6	9.64	0	1.13	2.18	24.8	6.73	7.48
7	11.68	0	1.62	1.08	15.45	8.88	10.09
8	13.37	0	2.63	1.4	11.88	7.29	8.64
9	115.33	0.03	106.02	1.15	83.36	5.1	6.16
10	15.72	0.8	2.03	1.75	37.32	2.11	2.37
11	20.1	1.31	3.19	2.7	11.77	0.64	0.68
12	30.07	4.26	20	1.5	28.26	0.12	0.12
TOTAL	**484.06**	**72.09**	**226.01**	**44.59**	**432.88**	**52.64**	**59.6**
percentage out of rainfall		**14.8 %**	**46.6 %**	**9.21 %**	**89.4 %**	**10.87 %**	**12.3 %**

From Table 7.4 it can be seen that the highest flows are observed from December to April. While during the summer season, the river generally dries out due to a long drought period. For the simulated period (2009 to 2017), the total amount of water yield in the basin is estimated by SWAT as 432.88mm/year, which is around 89.42 percentage out of rainfall.

7.6 Results of Sensitivity Analysis

With the help of SWAT-CUP , the sensitivity analysis is performed for the period of calibration and validation including warming up period. A set of sensitive parameters are initially tested with default upper and lower bound values. The number of parameters that can be used for the period of calibration and validation must be less in number and more impactful. These sensitive parameters also help to assess the capacity of the model and understand the behavior of the system being modeled.

The sensitivity analysis of the present study is carried out in order to specify the effect of a set of parameters on the flow simulated by the model. For the sensitivity analysis, the Latine Hypercube Sampling-One At a Time method is used to determine the sensitivity of each parameter. Observed monthly discharge data from different stations are defined to be inputs for the sensitivity analysis process. The simulated monthly and daily discharge data obtained from the model for a time period of 9 years (2009-2017) and the upper and lower limits of each sensitive parameter is set initially. In this study, 27 different sensitive parameters with the upper and lower bound for runoff are selected for sensitivity analysis.

After setting up the sensitive parameters and the lower and upper values of the parameters, The Global sensitivity analysis is run for the selected hydrological stations located at the outlet of each sub-basin. Out of the 27 selected sensitive parameters, the 20 most sensitive parameters as shown in Table 7.5 are taken in to account for the calibration process which is described in the upcoming section. The upper and lower values of the parameters of the simulated flow (obtained from the model) are changed several times in order to match the observed flow (gauge flow). Finally, the sensitivity analysis is conducted for a time period of 9 years (2009-2017), including both calibration and validation periods.

Table 7. 5 Selected 20 most sensitive parameters for calibration

Parameter Name	Parameter Name in SWAT-CUP	t-Stat	p-Value	Sensitivity rank
Treshold depth of water in the shallow aquifer required for return flow to occur (mm)	V__GWQMN.gw	-19.098	0.00000000000	1
Snow melt base temperature	V__SMTMP.bsn	7.210	0.00000000001	2
SCS runoff curve number II	R__CN2.mgt	6.724	0.00000000010	3
Precipitation lapse rate	V__PLAPS.sub	-5.319	0.00000066823	4
Average slope steepness	R__HRU_SLP.hru	4.652	0.00000502240	5
Snowfall temperature	V__SFTMP.bsn	4.494	0.00001199410	6
Minimum melt rate for snow during the year (occurs on winter solstice)	V__SMFMN.bsn	-4.163	0.00004710428	7
Average slope length	R__SLSUBBSN.hru	-4.058	0.00006390336	8
Groundwater delay (days)	V__GW_DELAY.gw	-3.168	0.00169879485	9
Temperature lapse rate	V__TLAPS.sub	-3.000	0.00342889059	10

(Continue on next page)

(table 7.5 cont.)

Snow pack temperature lag factor	V__TIMP.bsn	-1.952	0.05232394017	11
Threshold depth of water in the shallow aquifer for "revap" to occur (mm)	V__REVAPMN.gw	1.672	0.09560430432	12
Saturated hydraulic conductivity	R__SOL_K(..).sol	1.599	0.11083127065	13
Soil evaporation compensation factor	R__ESCO.hru	-1.597	0.11117353011	14
Maximum melt rate for snow during year (occurs on summer solstice)	V__SMFMX.bsn	-1.496	0.13622178625	15
Surface runoff lag time	V__SURLAG.bsn	-0.701	0.48385707278	16
Available water capacity of the soil layer	R__SOL_AWC(..).sol	-0.657	0.51112244224	17
Manning's "n" value for overland flow	R__OV_N.hru	-0.516	0.60567708018	18
Baseflow alpha factor (days)	V__ALPHA_BF.gw	-0.509	0.61110162320	19
Groundwater "revap" coefficient	V__GW_REVAP.gw	-0.429	0.66815111108	20

The ranks of the sensitive parameters are obtained according to the objective function Nash-Sutcliffe (NS), the greater the t-state and the smaller the P-value, the more sensitive the parameter. From the parameters set, it is clear that the streamflow is influenced by groundwater, sub basins, and management parameters of the study area. This shows that the study region has a very complex hydrological variability. Treshold depth of water in the shallow aquifer required for return flow to occur (GWQMN.gw), Snowmelt base temperature (SMTMP.bsn), SCS runoff curve number for moisture condition II (CN2.mgt), Precipitation lapse rate (PLAPS.sub), and Average slope steepness (HRU_SLP.hru) were found the most sensitive parameters among the other parameters. The dotty plots as shown in Figure 7.8, Figure 7.9, and Figure 7.10 are another representation of the most sensitive parameters. Those are parameter values plots or relative adjustments to the objective function. The main goal of these graphs is to demonstrate the distribution of the sampling points and to explain the sensitivity of the parameters (Karim C. Abbaspour, 2012).

From the processes of calibration, the PLAPS.sub, TLAPS.sub, snow parameters, and the other sensitive parameters are calibrated individually. From the dotty plots shown in Figure 7.8, it can be seen a nice trend for PLAPS.sub as it increases which indicates that PLAPS.sub is more sensitive compare to TLAPS.sub. In the group of snow parameters (SMTMP.bsn, SFTMP.bsn, SMFMN.bsn, SMFMX.bsn, TIMP.bsn) it can be observed nice trends for SMTMP.bsn, SFTMP.bsn, SMFMN.bsn as it increases, which shows that these three parameters are more sensitive among the five snow parameters as shown in Figure 7.9. In the group of other sensitive parameters (GWQMN.gw, CN2.mgt, HRU_SLP.hru, SLSUBBSN.hru, and GW_DELAY.gw) represents the most sensitive parameters shown in Figure 7.10. The graphical representation of the most 20 sensitive parameters based on t-state and P-value is shown in Figure 7.11.

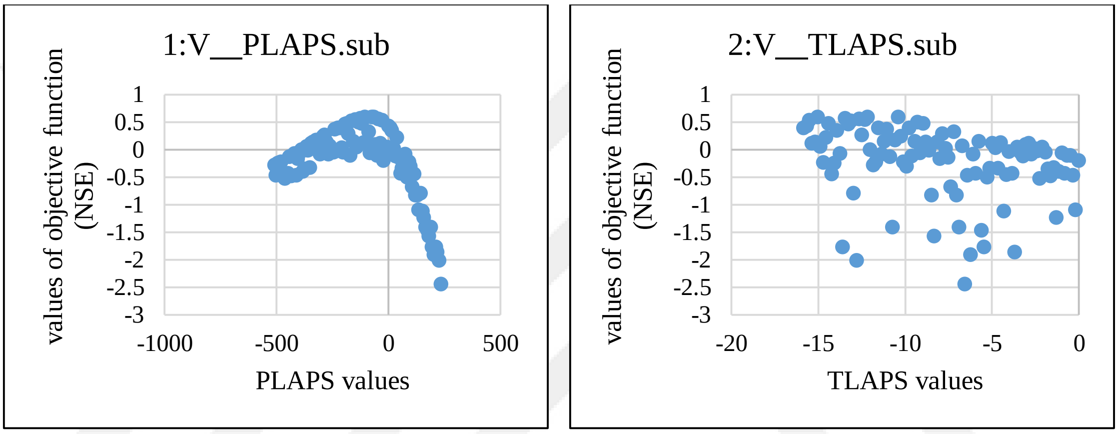

Figure 7. 8 Dotty plot of Precipitation and Temperature lapse rate

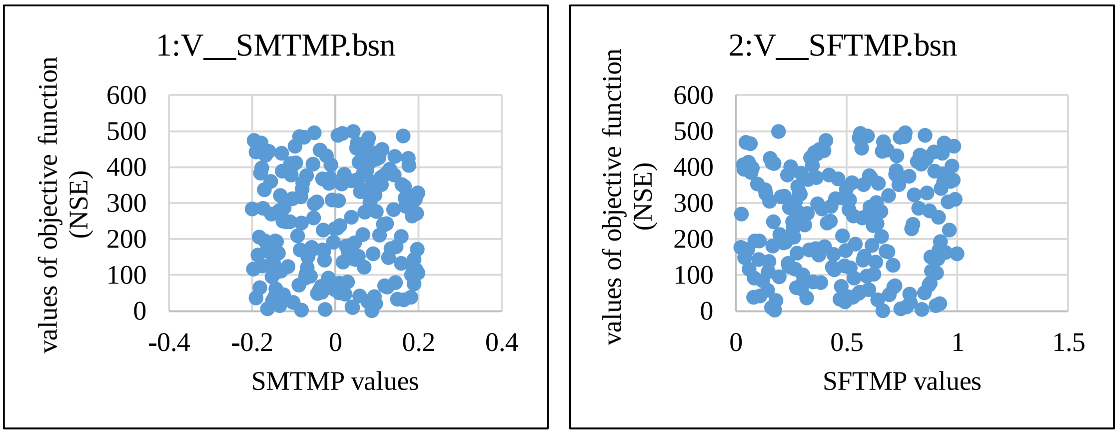

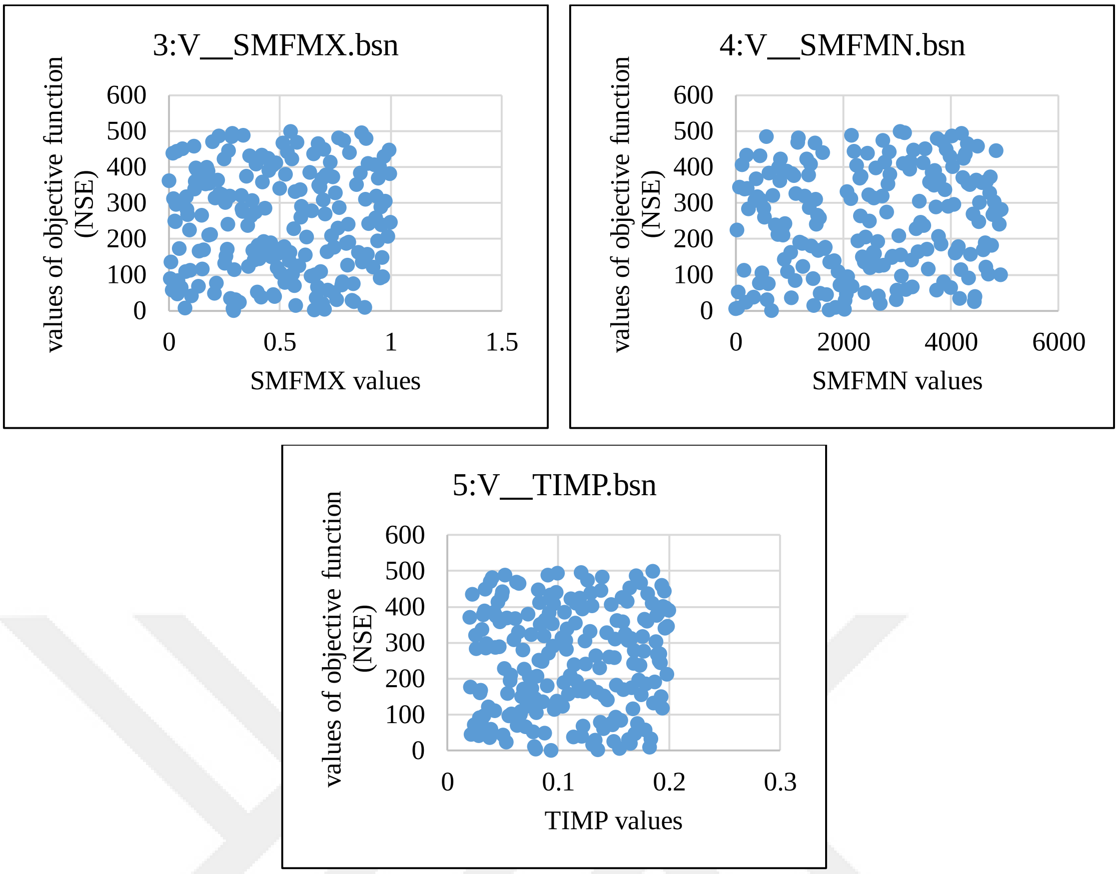

Figure 7. 9 Dotty plots of the snow parameters

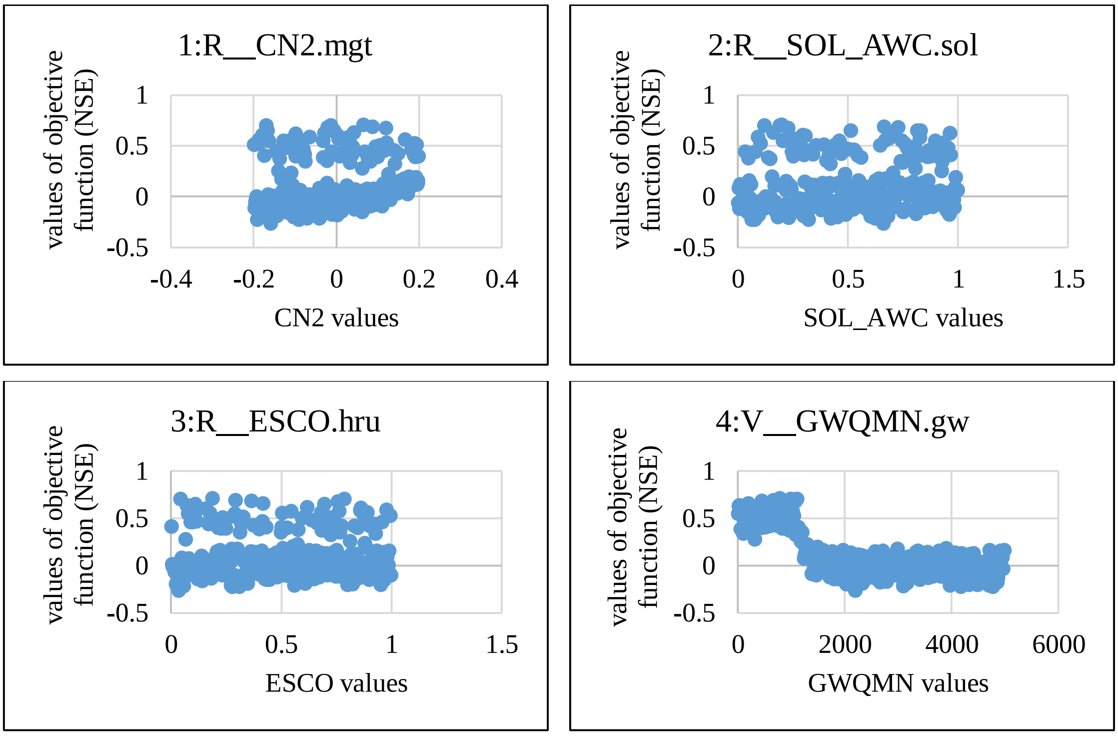

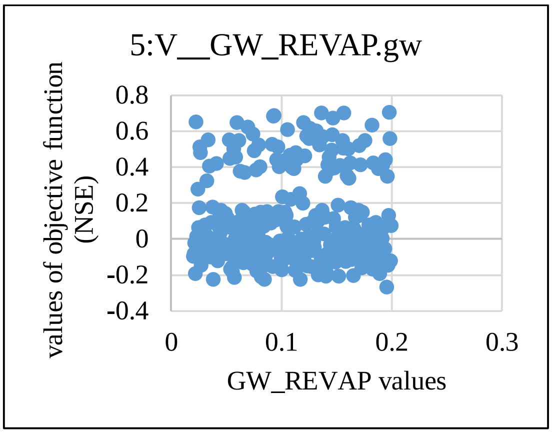
5:V__GW_REVAP.gw
values of objective function (NSE)
0.8
0.6
0.4
0.2
0
-0.2
-0.4
0
0.1
0.2
0.3
GW_REVAP values

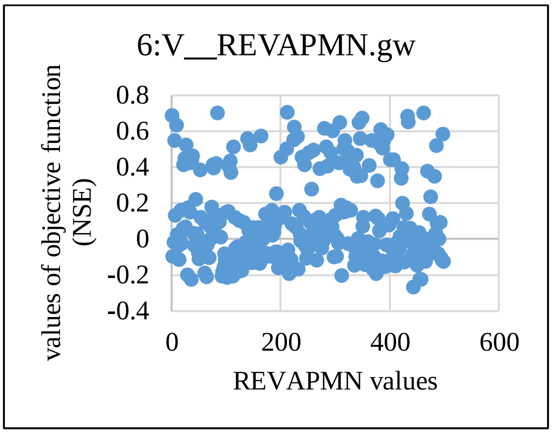
6:V__REVAPMN.gw
values of objective function (NSE)
0.8
0.6
0.4
0.2
0
-0.2
-0.4
0
200
400
600
REVAPMN values

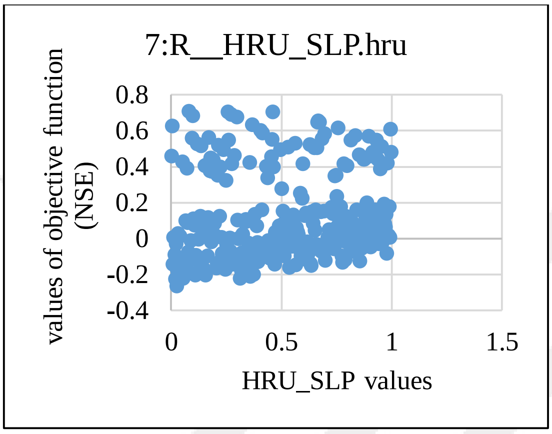
7:R__HRU_SLP.hru
values of objective function (NSE)
0.8
0.6
0.4
0.2
0
-0.2
-0.4
0
0.5
1
1.5
HRU_SLP values

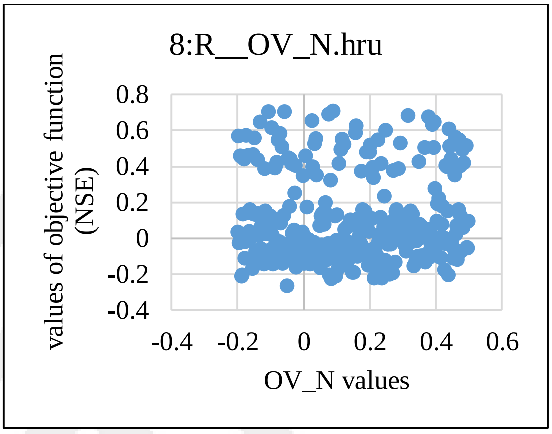
8:R__OV_N.hru
values of objective function (NSE)
0.8
0.6
0.4
0.2
0
-0.2
-0.4
-0.4
-0.2
0
0.2
0.4
0.6
OV_N values

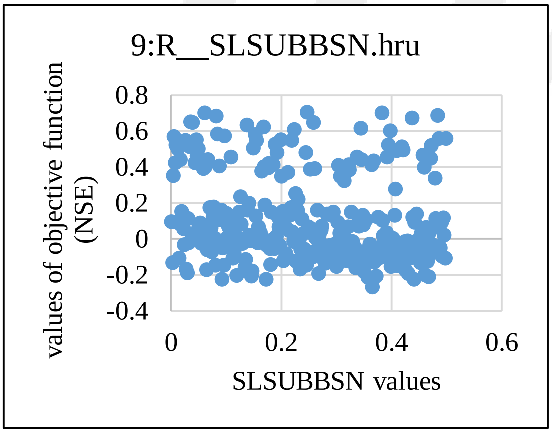
9:R__SLSUBBSN.hru
values of objective function (NSE)
0.8
0.6
0.4
0.2
0
-0.2
-0.4
0
0.2
0.4
0.6
SLSUBBSN values

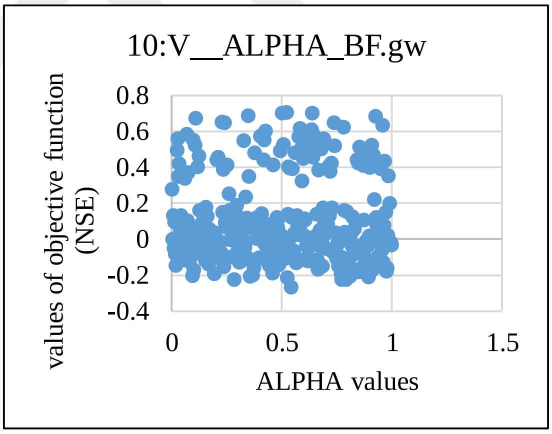
10:V__ALPHA_BF.gw
values of objective function (NSE)
0.8
0.6
0.4
0.2
0
-0.2
-0.4
0
0.5
1
1.5
ALPHA values

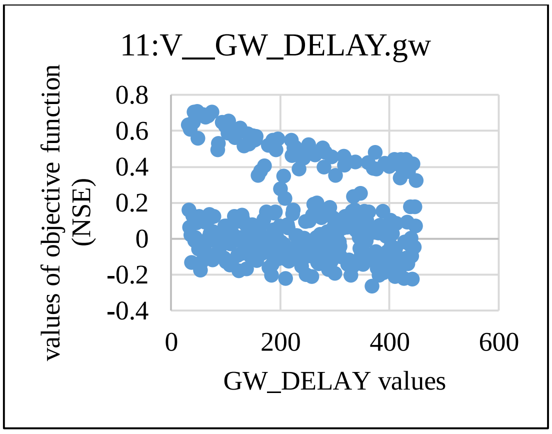
11:V__GW_DELAY.gw
values of objective function (NSE)
0.8
0.6
0.4
0.2
0
-0.2
-0.4
0
200
400
600
GW_DELAY values

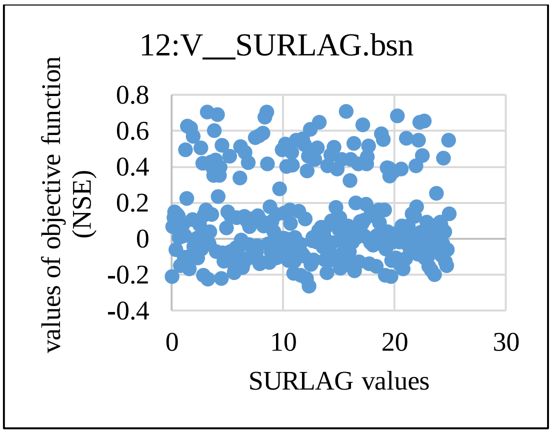
12:V__SURLAG.bsn
values of objective function (NSE)
0.8
0.6
0.4
0.2
0
-0.2
-0.4
0
10
20
30
SURLAG values

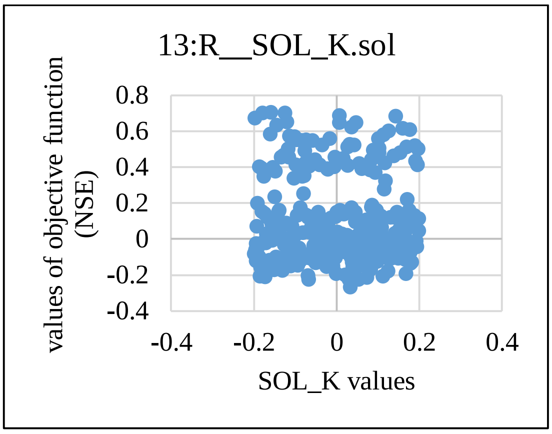

Figure 7. 10 Dotty plots of the other effective sensitive parameters

Figure 7. 11 Graphical representation of the most sensitive parameters

7.7 Calibration Analysis

The calibration process is performed on the 20 most sensitive flow parameters found from the sensitivity analysis, and the values of these parameters are iteratively changed to the acceptable range. In this study, two-thirds of the available runoff data (2010-2014), with one year of the warm-up period from seven different hydrological stations in the basin are used for the calibration, and the rest of the data are used for the validation purposes. The observed discharge data are given as input to SWAT-CUP, and each hydrological station is linked to their corresponding sub-basin. From the hydrological knowledge, the Kabul River Basin is located in the mountain region, and most of the area is covered by snow. Based on that, the five main snow parameters Snow melt base temperature (SMTMP.bsn), Snowfall temperature (SFTMP.bsn), Minimum melt rate for snow during the year (SMFMN.bsn), Snow pack temperature lag factor (TIMP.bsn), and Maximum melt rate for snow during year (SMFMX.bsn) are set to their acceptable upper and lower range.

In the process of calibration, the Precipitation lapse rate (PLAPS.sub), Temperature lapse rate (TLAPS.sub), and the five snow parameters are calibrated individually. These parameters cannot be calibrated with other parameters at the same time. After setting up these parameters to the best-simulated values, SWAT-CUP is run for the other sensitive parameters individually. Initially, SWAT-CUP is run both on a monthly and daily time scale with the initial default values. The coefficients of determination (R^2) for hydrological stations (Pul-i-Ashawa, Pul-i-Behsod, Pul-i-Qarghayi, Shokhi, Pul-i-Surkh, Tang-i-Sayedan, and Chaghasarai) initially are found to be 0.42, 0.23, 0.32, 0.24, 0.53, 0.46, 0.28 for the monthly data scale simulation respectively, and for daily scale simulation are found to be 0.18, 0.11, 0.24, 0.14, 0.42, 0.50, 0.19, respectively. The model is run several times to get a better result, and the number of simulations is set to 300. Further iterations are performed with a new range of parameters to get a good match between simulated and observed discharge. The calibration ranges of the calibrated parameters with their fitted values are shown in Table 7.6, Table 7.7, Table 7.8, Table 7.9, Table 7.10, Table 7.11, and Table 12.

The scatter plots between observed and simulated discharge during the calibration period for both monthly and daily calibration are shown in Figure 7.12 and Figure 7.13, which indicates a good correlation between the measured and simulated flow (see Table 7.13).

Table 7. 6 Calibrated and fitted values of parameters of Pul-i-Ashawa catchment

Calibrated range and fitted values of parameters of Pul-i-Ashawa catchment							
	Monthly			Daily			
Parameter	Lower value	Upper value	Fitted value	Lower value	Upper value	Fitted value	Method
V__GWQMN.gw	0	5000	791.66	-343.3	1923.8	166.7	Replace
V__SMTMP.bsn	-5	5	2.775	-5	5	4.17	Replace
R__CN2.mgt	-0.2	0.2	0.066	-9.511	-0.063	-2.945	Relative
V__PLAPS.sub	-513.2	237.24	-74.20	-466.3	174.6	-142.6	Replace
R__HRU_SLP.hru	0	1	0.081	0.108	0.28	0.27	Relative
V__SFTMP.bsn	-5	5	-4.625	-5	5	1.025	Replace
V__SMFMN.bsn	0	10	0.125	0	10	0.2750	Replace
R__SLSUBBSN.hru	0	0.5	0.2475	0.614	1.73	1.18	Relative
V__GW_DELAY.gw	30	450	47.5	-61.29	143.73	38.144	Replace
V__TLAPS.sub	-15.89	0.057	-12.14	-22.27	-7.145	-15.99	Replace
V__TIMP.bsn	0	1	0.447	0	1	0.2525	Replace
V__REVAPMN.gw	0	500	212.5	-212.3	124.1	8.040	Replace
R__SOL_K(..).sol	-0.20	0.20	-0.159	-0.429	-0.117	-0.290	Relative
R__ESCO.hru	0	1	0.188	0.0049	0.19	0.0472	Relative
V__SMFMX.bsn	0	10	1.775	0	10	3.225	Replace
V__SURLAG.bsn	0	25	15.70	6.356	18.46	13.562	Replace
R__SOL_AWC(..).sol	0	1	0.201	-0.148	0.0627	-0.119	Relative
R__OV_N.hru	-0.20	0.50	0.090	-0.14	0.975	-0.013	Relative
V__ALPHA_BF.gw	0	1	0.521	0.358	0.758	0.452	Replace
V__GW_REVAP.gw	0.02	0.2	0.197	0.059	0.169	0.135	Replace

Table 7. 7 Calibrated range and fitted value of parameters of Pul-i-Behsod catchment

Calibrated range and fitted values of parameters of Pul-i-Behsod catchment							
	Monthly			Daily			
Parameter	Lower value	Upper value	Fitted value	Lower value	Upper value	Fitted value	Method
V__GWQMN.gw	-1447.5	1070.5	-763.4	370.7	2793.6	1295.4	Replace
V__SMTMP.bsn	-5	5	2.675	-1.99	4.042	2.15	Replace
R__CN2.mgt	-0.281	-0.106	-0.24	-0.14	0.015	-0.113	Relative
V__PLAPS.sub	-962.00	86	-893.8	-964.1	88.155	-895.7	Replace
R__HRU_SLP.hru	0.00028	0.001	0.0004	0.17	0.54	0.28	Relative
V__SFTMP.bsn	-5	5	3.725	-0.717	7.86	7.67	Replace
V__SMFMN.bsn	0	10	0.175	1.183	7.06	1.22	Replace
R__SLSUBBSN.hru	5.925	38.451	7.931	0.35	0.69	0.43	Relative
V__GW_DELAY.gw	15.867	161.136	100.84	-104	129.4	21.59	Replace
V__TLAPS.sub	-0.2182	15.418	13.15	-0.218	15.41	13.15	Replace
V__TIMP.bsn	0	1	0.402	-0.19	0.60	0.35	Replace
V__REVAPMN.gw	68.54	202.58	170.18	66.3	447.2	150.8	Replace
R__SOL_K(..).sol	-0.0003	0.129	0.129	-0.28	-0.07	-0.227	Relative
R__ESCO.hru	0.554	0.854	0.767	-0.83	0.069	-0.76	Relative
V__SMFMX.bsn	0	10	9.175	-0.241	6.59	1.58	Replace
V__SURLAG.bsn	14.02	19.59	14.07	-3.52	10	8.95	Replace
R__SOL_AWC(..).sol	-0.035	0.344	0.053	-0.65	0.15	0.06	Relative
R__OV_N.hru	-40.8	-10	-21.7	-0.22	0.129	-0.08	Relative
V__ALPHA_BF.gw	0.486	0.954	0.713	0.565	1.058	0.799	Replace
V__GW_REVAP.gw	0.066	0.121	0.082	0.093	0.18	0.104	Replace

Table 7. 8 Calibrated range and fitted value of parameters of Pul-i-Qarghayi catchment

Calibrated range and fitted values of parameters of Pul-i-Qarghayi catchment							
	Monthly			Daily			
Parameter	Lower value	Upper value	Fitted value	Lower value	Upper value	Fitted value	Method
V__GWQMN.gw	-2609.9	993.8	-1102	-188.7	3272.1	1962.7	Replace
V__SMTMP.bsn	2.495	9.065	3.228	-7.94	0.69	-2.04	Replace
R__CN2.mgt	-0.1968	-0.005	-0.174	-0.14	0.085	-0.08	Relative
V__PLAPS.sub	-945.00	86.70	-891.8	-959.4	83.46	-735.2	Replace
R__HRU_SLP.hru	-0.790	0.105	-0.463	-0.482	0.50	-0.17	Relative
V__SFTMP.bsn	-5	5	3.234	-0.24	9.29	4.26	Replace
V__SMFMN.bsn	1.987	8.642	5.703	-3.91	5.36	1.86	Replace
R__SLSUBBSN.hru	0.121	0.413	-0.167	-0.131	0.289	0.239	Relative
V__GW_DELAY.gw	-5.557	178.95	86.39	-158	247.4	15.64	Replace
V__TLAPS.sub	-0.223	13.518	10.15	-0.22	15.42	13.93	Replace
V__TIMP.bsn	0.869	1.725	1.501	0.06	0.68	0.07	Replace
V__REVAPMN.gw	20.812	226.59	60.25	3.642	334.69	306.5	Replace
R__SOL_K(..).sol	-0.217	-0.018	-0.209	-0.09	0.1210	-0.02	Relative
R__ESCO.hru	0.072	0.530	0.514	0.067	0.689	0.103	Relative
V__SMFMX.bsn	0	10	8.234	2.157	7.39	5.15	Replace
V__SURLAG.bsn	5.623	20.022	16.206	8.307	24.94	11.27	Replace
R__SOL_AWC(..).sol	0.237	0.584	0.306	0.458	1.37	0.530	Relative
R__OV_N.hru	-0.520	-0.057	-0.167	-0.24	0.25	0.049	Relative
V__ALPHA_BF.gw	0.487	0.871	0.631	0.117	0.706	0.571	Replace
V__GW_REVAP.gw	0.038	0.134	0.0571	0.089	0.228	0.139	Replace

Table 7. 9 Calibrated range and fitted value of parameters of Shokhi catchment

Calibrated range and fitted values of parameters of Shokhi catchment							
	Monthly			Daily			
Parameter	Lower value	Upper value	Fitted value	Lower value	Upper value	Fitted value	Method
V__GWQMN.gw	0	5000	1108.3	-1565	2815	267.2	Replace
V__SMTMP.bsn	-5	5	4.375	-5	5	1.87	Replace
R__CN2.mgt	-0.2	0.2	-0.014	-0.36	0.01	-0.324	Relative
V__PLAPS.sub	-63.134	356.54	136.21	-246	474	88.7	Replace
R__HRU_SLP.hru	0	1	0.461	0.49	1.49	0.86	Relative
V__SFTMP.bsn	-5	5	4.475	-5	5	4.7	Replace
V__SMFMN.bsn	0	10	2.325	0	10	0.075	Replace
R__SLSUBBSN.hru	0	0.5	0.382	0.497	1.49	0.086	Relative
V__GW_DELAY.gw	30	450	41.90	-172.7	242	34.2	Replace
V__TLAPS.sub	-19.157	-6.208	-10.93	-12.04	-14.6	0.45	Replace
V__TIMP.bsn	0	1	0.122	0	1	0.692	Replace
V__REVAPMN.gw	0	500	84.16	192	576.3	265.6	Replace
R__SOL_K(..).sol	-0.2	0.2	-0.124	-0.011	0.36	0.003	Relative
R__ESCO.hru	0	1	0.0416	0.43	1.292	1.262	Relative
V__SMFMX.bsn	0	10	7.975	0	2	2.67	Replace
V__SURLAG.bsn	0	25	8.541	6.18	18.73	15.40	Replace
R__SOL_AWC(..).sol	0	1	0.121	-0.05	0.64	0.082	Relative
R__OV_N.hru	-0.20	0.50	-0.105	0.608	0.120	0.76	Relative
V__ALPHA_BF.gw	0	1	0.638	0.317	0.952	0.55	Replace
V__GW_REVAP.gw	0.02	0.2	0.1565	0.058	0.152	0.076	Replace

Table 7. 10 Calibrated range and fitted value of parameters of Pul-i-Surkh catchment

Calibrated range and fitted values of parameters of Pul-i-Surkh catchment							
	Monthly			Daily			
Parameter	Lower value	Upper value	Fitted value	Lower value	Upper value	Fitted value	Method
V__GWQMN.gw	169.28	2116.9	1165.8	-2438.8	2522	-363.49	Replace
V__SMTMP.bsn	-4.694	3.422	-2.597	-5	5	-3.575	Replace
R__CN2.mgt	-0.2772	-0.050	-0.252	-0.079	0.16	-0.050	Relative
V__PLAPS.sub	-72.231	400.25	235.11	-600	600	-138	Replace
R__HRU_SLP.hru	0.701	1.363	0.786	0.052	0.68	0.29	Relative
V__SFTMP.bsn	-5	5	3.49	-5	5	0.875	Replace
V__SMFMN.bsn	2.942	5.845	3.904	0	10	0.425	Replace
R__SLSUBBSN.hru	0.284	0.545	0.429	-0.04	0.318	0.053	Relative
V__GW_DELAY.gw	4.567	220.21	127.12	-179	240	30	Replace
V__TLAPS.sub	-20.57	-7.354	-10.30	-8	8	-7.92	Replace
V__TIMP.bsn	0.014	0.871	0.370	0	1	0.052	Replace
V__REVAPMN.gw	453.03	877.2	590.89	-236.3	254.6	-142.24	Replace
R__SOL_K(..).sol	-0.116	0.100	0.088	-0.32	0.027	-0.3027	Relative
R__ESCO.hru	0.020	0.772	0.663	-0.39	0.536	0.50	Relative
V__SMFMX.bsn	0	10	5.762	0	10	6.225	Replace
V__SURLAG.bsn	14.761	24.685	17.986	8.59	26	21.25	Replace
R__SOL_AWC(..).sol	0.716	1.407	1.372	-0.257	0.58	-0.091	Relative
R__OV_N.hru	-0.019	0.444	0.356	0.094	0.683	0.54	Relative
V__ALPHA_BF.gw	-0.120	0.410	0.360	0.478	1.437	0.83	Replace
V__GW_REVAP.gw	0.116	0.189	0.162	0.10	0.26	0.132	Replace

Table 7. 11 Calibrated range and fitted value of parameters of Tang-i-Sayedan catchment

Calibrated range and fitted values of parameters of Tang-i-Sayedan catchment							
	Monthly			Daily			
Parameter	Lower value	Upper value	Fitted value	Lower value	Upper value	Fitted value	Method
V__GWQMN.gw	0	5000	625	0	5000	425	Replace
V__SMTMP.bsn	-5	5	0.650	-5	5	2.275	Replace
R__CN2.mgt	-0.2	0.2	-0.179	-0.2	0.2	-0.64	Relative
V__PLAPS.sub	-500	500	419.24	-600	600	18	Replace
R__HRU_SLP.hru	0	1	0.995	0	1	0.415	Relative
V__SFTMP.bsn	-5	5	4.128	-5	5	0.675	Replace
V__SMFMN.bsn	0	10	2.650	0	10	4.625	Replace
R__SLSUBBSN.hru	0	0.5	0.224	0	0.5	0.084	Relative
V__GW_DELAY.gw	30	450	34.90	30	450	103.5	Replace
V__TLAPS.sub	-15.459	-6.30	-12.38	-8	8	-5.52	Replace
V__TIMP.bsn	0	1	0.585	0	1	0.732	Replace
V__REVAPMN.gw	0	500	384.16	0	500	497	Replace
R__SOL_K(..).sol	-0.20	0.20	0.176	-0.2	0.2	-0.16	Relative
R__ESCO.hru	0	1	0.861	0	1	0.98	Relative
V__SMFMX.bsn	0	10	8.89	0	10	8.775	Replace
V__SURLAG.bsn	0	25	12.458	0	25	8.21	Replace
R__SOL_AWC(..).sol	0	1	0.295	0	1	0.092	Relative
R__OV_N.hru	-0.2	0.5	0.440	-0.2	0.5	0.16	Relative
V__ALPHA_BF.gw	0	1	0.635	0	1	0.068	Replace
V__GW_REVAP.gw	0.02	0.2	0.105	0.02	0.2	0.074	Replace

Table 7. 12 Calibrated range and fitted value of parameters of Chaghasarai catchment

Calibrated range and fitted values of parameters of Chaghasarai catchment							
	Monthly			Daily			
Parameter	Lower value	Upper value	Fitted value	Lower value	Upper value	Fitted value	Method
V__GWQMN.gw	0	5000	1108	0	5000	625	Replace
V__SMTMP.bsn	-5	5	-3.575	-5	5	-2.32	Replace
R__CN2.mgt	-0.2	0.2	-0.014	-0.2	0.2	-0.179	Relative
V__PLAPS.sub	-217.73	565.73	115.24	-218	566	84	Replace
R__HRU_SLP.hru	0	1	0.461	0	1	0.995	Relative
V__SFTMP.bsn	-5	5	0.875	-5	5	1.325	Replace
V__SMFMN.bsn	0	10	0.425	0	1	1.575	Replace
R__SLSUBBSN.hru	0	0.5	0.382	0	0.5	0.224	Relative
V__GW_DELAY.gw	30	450	41.90	30	450	34.90	Replace
V__TLAPS.sub	-15.41	0.218	-12.83	-15.42	0.22	-15.340	Replace
V__TIMP.bsn	0	1	0.052	0	1	0.057	Replace
V__REVAPMN.gw	0	500	84.16	0	500	384.17	Replace
R__SOL_K(..).sol	-0.20	0.20	-0.124	-0.2	0.2	0.176	Relative
R__ESCO.hru	0	1	0.0416	0	1	0.861	Relative
V__SMFMX.bsn	0	10	6.225	0	10	5.125	Replace
V__SURLAG.bsn	0	25	8.541	0	25	12.45	Replace
R__SOL_AWC(..).sol	0	1	0.121	0	1	0.295	Relative
R__OV_N.hru	-0.2	0.5	-0.105	-0.2	0.5	0.44	Relative
V__ALPHA_BF.gw	0	1	0.638	0	1	0.635	Replace
V__GW_REVAP.gw	0.02	0.2	0.156	0.02	0.2	0.1055	Replace

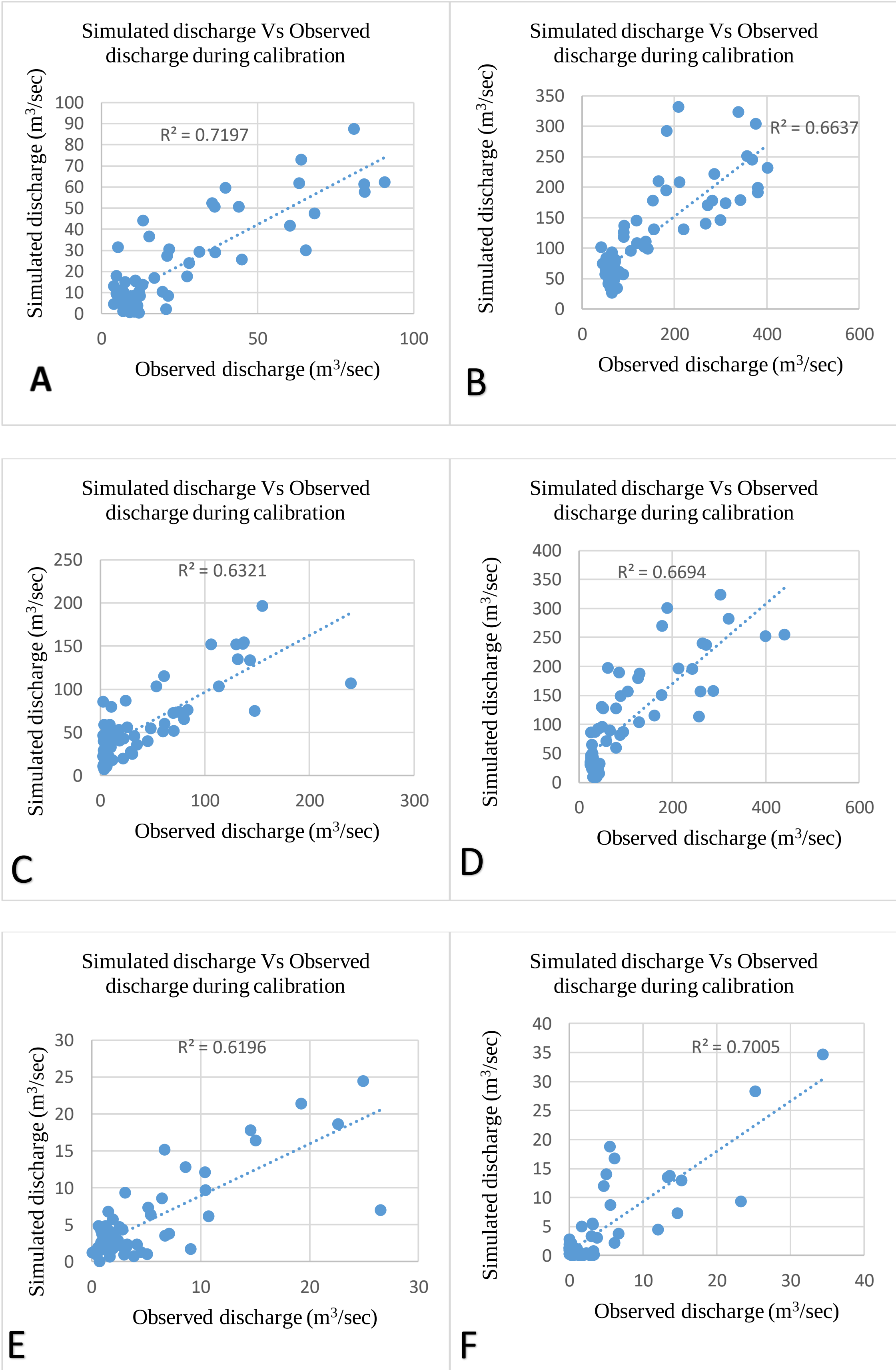
Simulated discharge Vs Observed discharge during calibration
Simulated discharge (m³/sec)
Observed discharge (m³/sec)
R² = 0.7197
A
Simulated discharge Vs Observed discharge during calibration
Simulated discharge (m³/sec)
Observed discharge (m³/sec)
R² = 0.6637
B
Simulated discharge Vs Observed discharge during calibration
Simulated discharge (m³/sec)
Observed discharge (m³/sec)
R² = 0.6321
C
Simulated discharge Vs Observed discharge during calibration
Simulated discharge (m³/sec)
Observed discharge (m³/sec)
R² = 0.6694
D
Simulated discharge Vs Observed discharge during calibration
Simulated discharge (m³/sec)
Observed discharge (m³/sec)
R² = 0.6196
E
Simulated discharge Vs Observed discharge during calibration
Simulated discharge (m³/sec)
Observed discharge (m³/sec)
R² = 0.7005
F

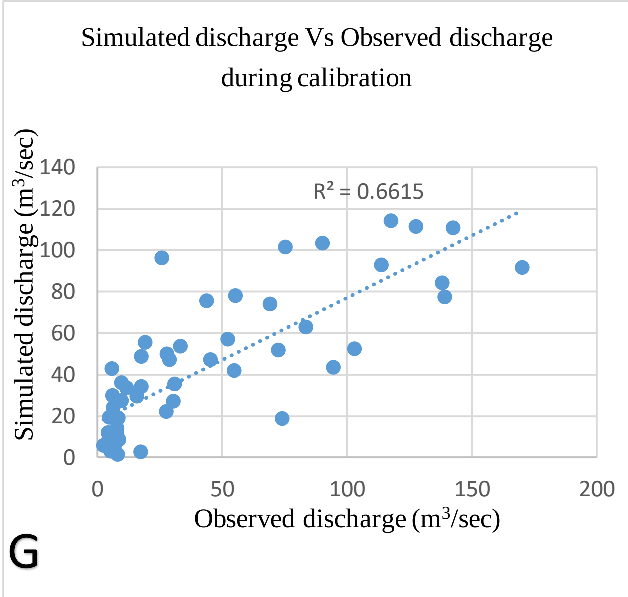

Figure 7. 12 Comparison of calibrated model output and observed monthly runoff at stations Pul-i-Ashawa (A), Pul-i-Behsod (B), Pul -i- Qarghayi (C), Shokhi (D), Pul-i-Surkh (E), Tang-i-Sayedan (F), Chaghasarai (G), during the calibration period of 2010-2014.

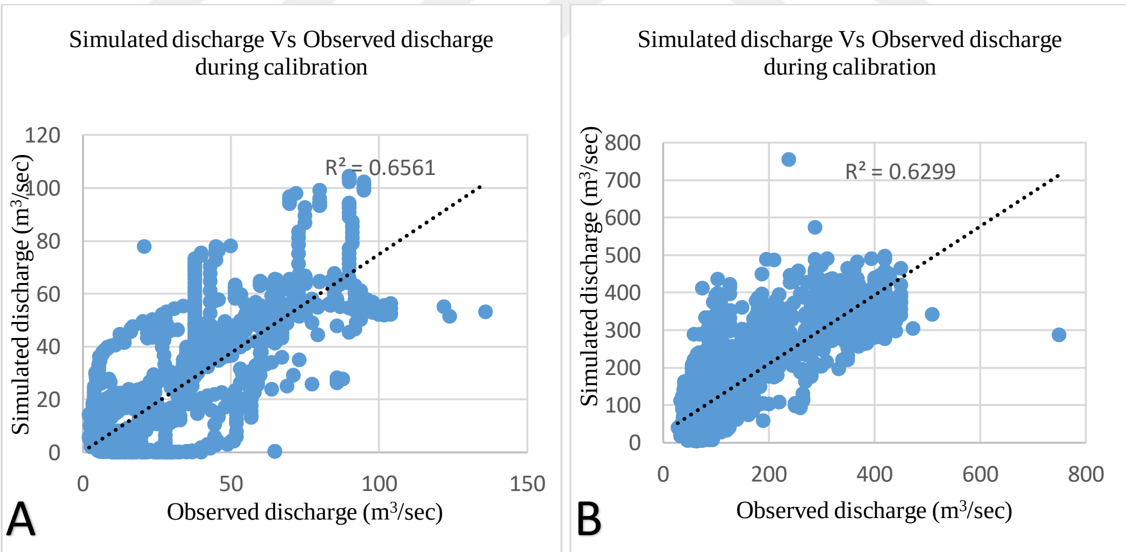

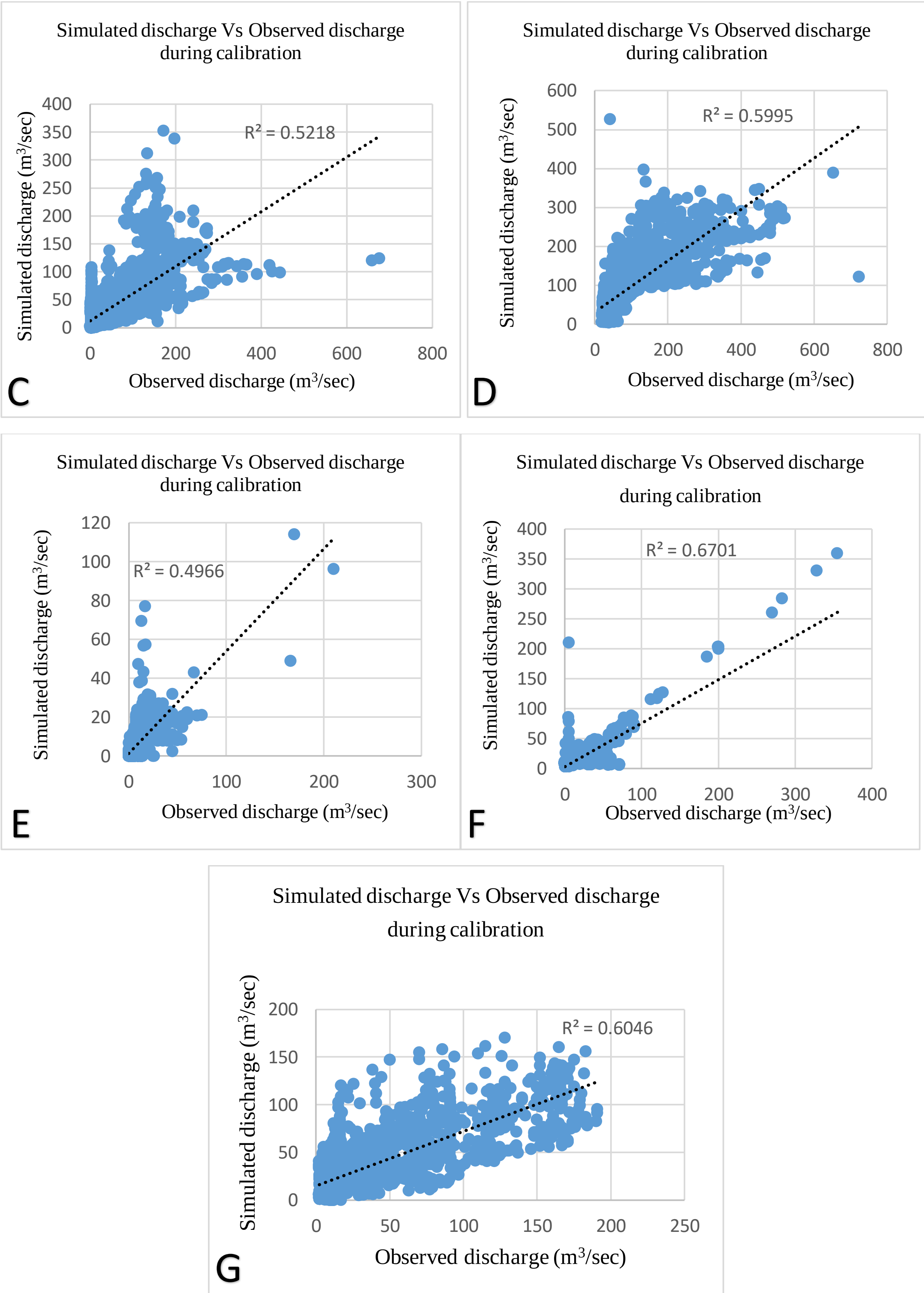

Figure 7. 13 Comparison of calibrated model output and observed daily runoff at stations Pul-i-Ashawa (A), Pul-i-Behsod (B), Pul-i-Qarghayi (C), Shokhi (D), Pul-i-Surkh (E), Tang-i-Sayedan (F), Chaghasarai (G) during the calibration period of 2010-2014

7.8 Validation Analysis

In the processes of validation, the rest of the data (2015-2017) of the same observation stations are used. Discharge data for the period of validation are provided to SWAT-CUP, and the ranges of the parameters are remained unchanged from the calibration processes. After setting up the input discharge data and parameters, SWAT-CUP is run both on a monthly and daily time scale with the same number of simulations of 300 used previously for calibration. From the scatter plots shown in Figure 7.14 and Figure 7.15, it can be seen that the observed and simulated discharge values match very well. Table 7.13 shows the model performance statistics of the measured and simulated discharge for both calibration and validation. This shows that there is a good correlation between the measured and simulated flows. Based on the three different statistics values as shown in Table 7.13, the model provides better results for monthly calibration and validation compared to the daily calibration and validation.

Table 7. 13 Calibration and Validation statistics values at Kabul river basin

	Monthly						Daily					
	Calibration			Validation			Calibration			Validation		
Station	R^2	NSE	RSR	R^2	NSE	RSR	R^2	NSE	RSR	R^2	NSE	RSR
Pul-i-Ashawa	0.72	0.71	0.54	0.72	0.63	0.61	0.66	0.59	0.64	0.73	0.63	0.61
Pul-i-Behsod	0.66	0.60	0.64	0.68	0.61	0.62	0.63	0.45	0.74	0.56	0.51	0.70
Pul-i-Qarghayi	0.63	0.53	0.68	0.70	0.69	0.56	0.52	0.48	0.72	0.85	0.44	0.75
Shokhi	0.67	0.67	0.58	0.71	0.65	0.59	0.60	0.59	0.64	0.64	0.61	0.62
Pul-i-Surkh	0.62	0.60	0.63	0.84	0.81	0.43	0.50	0.47	0.73	0.47	0.40	0.77
Tang-i-Sayedan	0.70	0.66	0.58	0.64	0.63	0.61	0.67	0.57	0.51	0.60	0.55	0.50
Chaghasarai	0.66	0.65	0.59	0.66	0.48	0.72	0.60	0.60	0.63	0.63	0.43	0.76

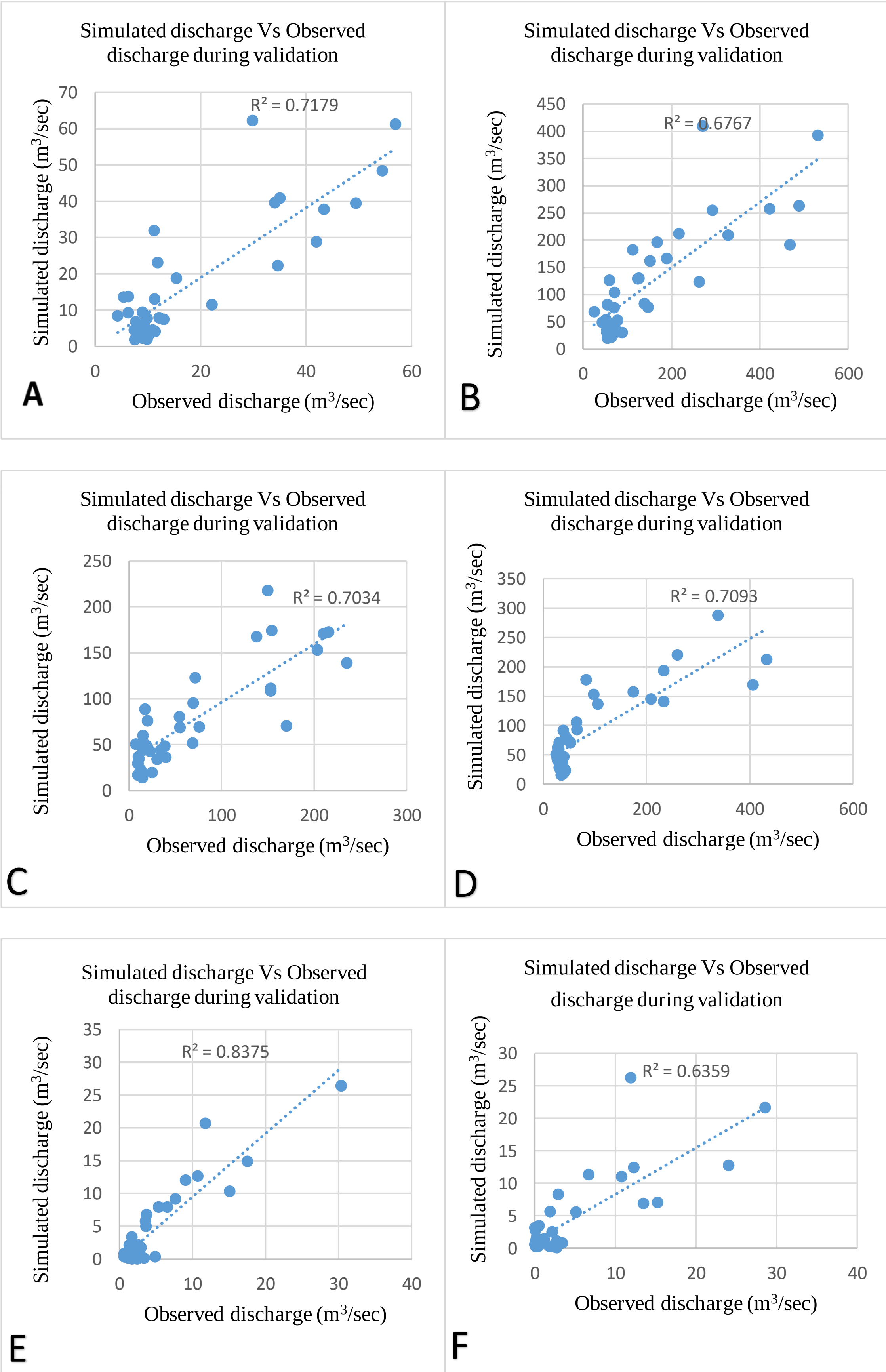
Simulated discharge Vs Observed discharge during validation
R² = 0.7179
Simulated discharge (m³/sec)
Observed discharge (m³/sec)
0 10 20 30 40 50 60 70
0 20 40 60
A
Simulated discharge Vs Observed discharge during validation
R² = 0.6767
Simulated discharge (m³/sec)
Observed discharge (m³/sec)
0 50 100 150 200 250 300 350 400 450
0 200 400 600
B
Simulated discharge Vs Observed discharge during validation
R² = 0.7034
Simulated discharge (m³/sec)
Observed discharge (m³/sec)
0 50 100 150 200 250
0 100 200 300
C
Simulated discharge Vs Observed discharge during validation
R² = 0.7093
Simulated discharge (m³/sec)
Observed discharge (m³/sec)
0 50 100 150 200 250 300 350
0 200 400 600
D
Simulated discharge Vs Observed discharge during validation
R² = 0.8375
Simulated discharge (m³/sec)
Observed discharge (m³/sec)
0 5 10 15 20 25 30 35
0 10 20 30 40
E
Simulated discharge Vs Observed discharge during validation
R² = 0.6359
Simulated discharge (m³/sec)
Observed discharge (m³/sec)
0 5 10 15 20 25 30
0 10 20 30 40
F

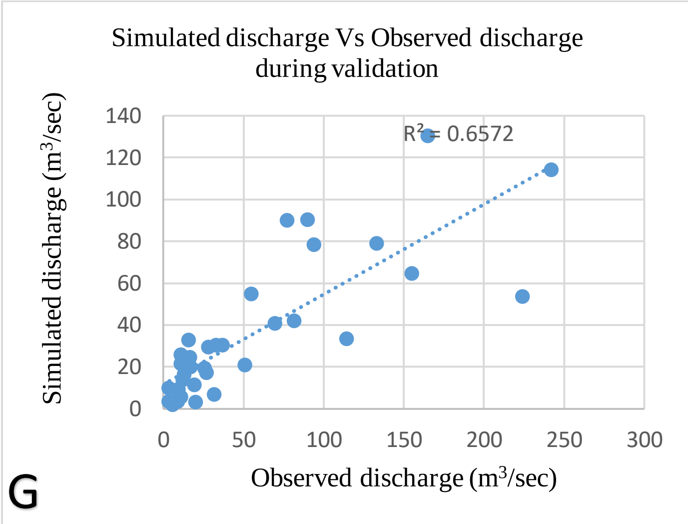

Figure 7. 14 Comparison of validated model output and observed monthly runoff at stations Pul-i-Ashawa (A), Pul-i-Behsod (B), Pul -i- Qarghayi (C), Shokhi (D), Pul-i-Surkh (E), Tang-i-Sayedan (F), Chaghasarai (G), during the validation period of 2015-2017.

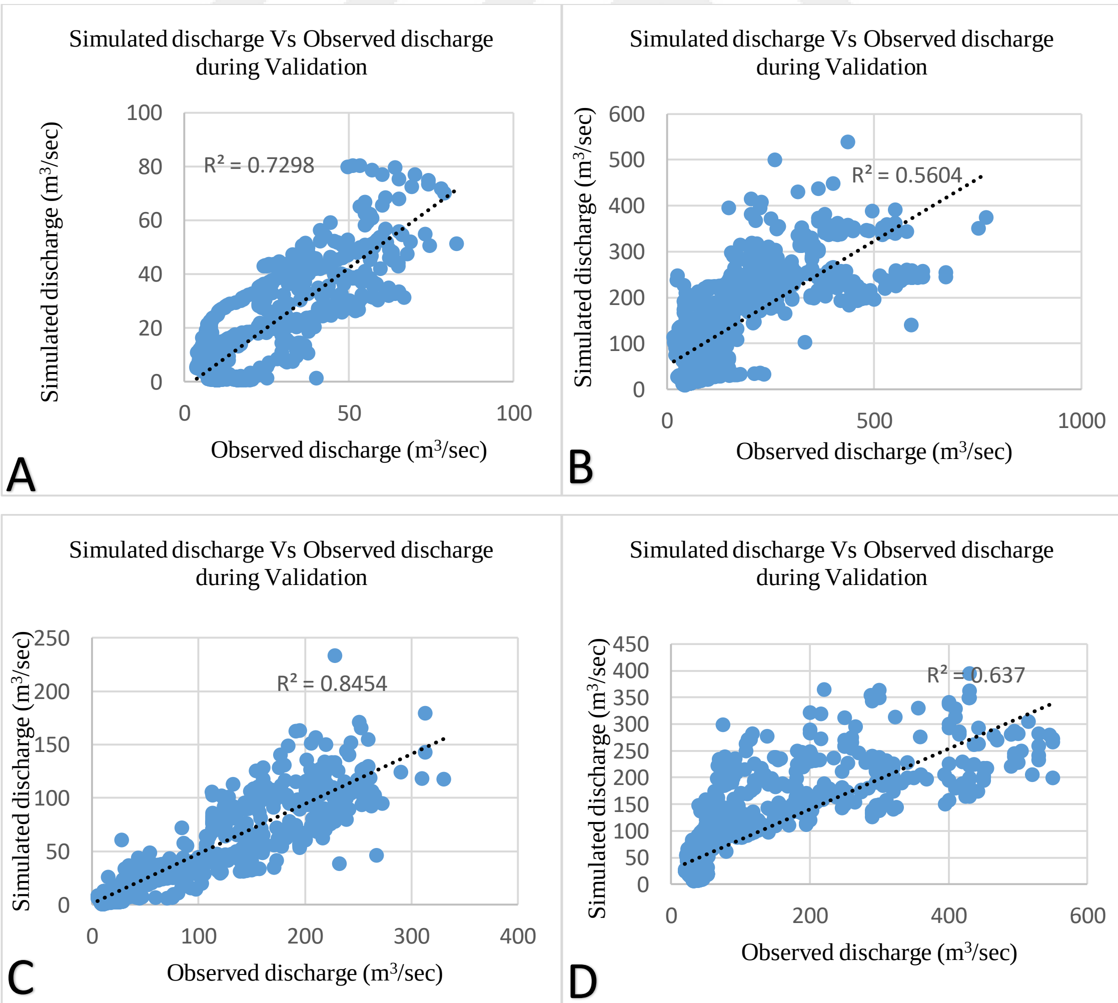

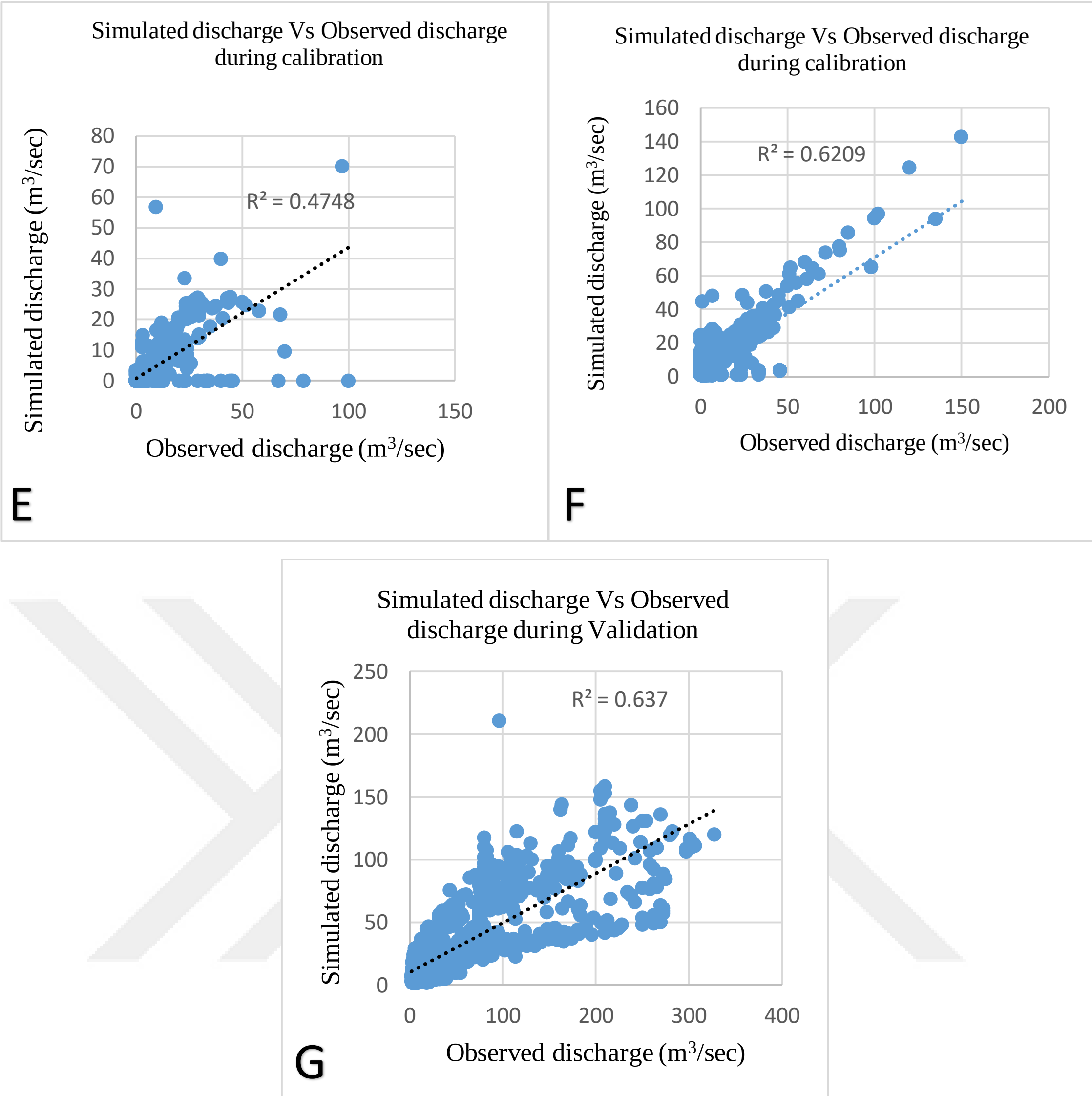

Figure 7. 15 Comparison of validated model output and observed daily runoff at stations Pul-i-Ashawa (A), Pul-i-Behsod (B), Pul -i- Qarghayi (C), Shokhi (D), Pul-i-Surkh (E), Tang-i-Sayedan (F), Chaghasarai (G), during the validation period of 2015-2017.

Graphical representation of the comparison between observed and simulated stream flow during calibration (2010-2014) and validation (2015-2017) is carried out as shown in Figure 7.16 and Figure 7.17. Initially, in some cases, the simulated base flows are too high and simulated peaks are too low and in some cases, the simulated flows shifts to the left. In the case of high simulated base flow and low simulated peaks, some relevant parameters SCS runoff curve number II (CN2.mgt), Available water capacity of the soil layer (SOL_AWC(..).sol), Soil evaporation compensation factor (ESCO.hru), Treshold depth of water in the shallow aquifer required for return flow to occur (GWQMN.gw), Groundwater "revap" coefficient (GW_REVAP.gw), Threshold depth of water in the shallow aquifer for "revap" to occur (REVAPMN.gw) are increased and decreased. To decrease base flow and increase peaks flow, increase CN2.mgt, decrease SOL_AWC(..).sol, decrease ESCO.hru, increase GW_REVAP.gw, increase GWQMN.gw, and decrease REVAPMN.gw, match the simulated and observed flow in the good agreement. To match the shift between the observed and simulated flows, decreased HRU_SLP, increased OV_N.hru, and increased SLSUBBSN.hru.

Overall, the model gives satisfactory results for both calibration and validation steps. This shows that the model has sufficient capacity to represent the Kabul river basin.

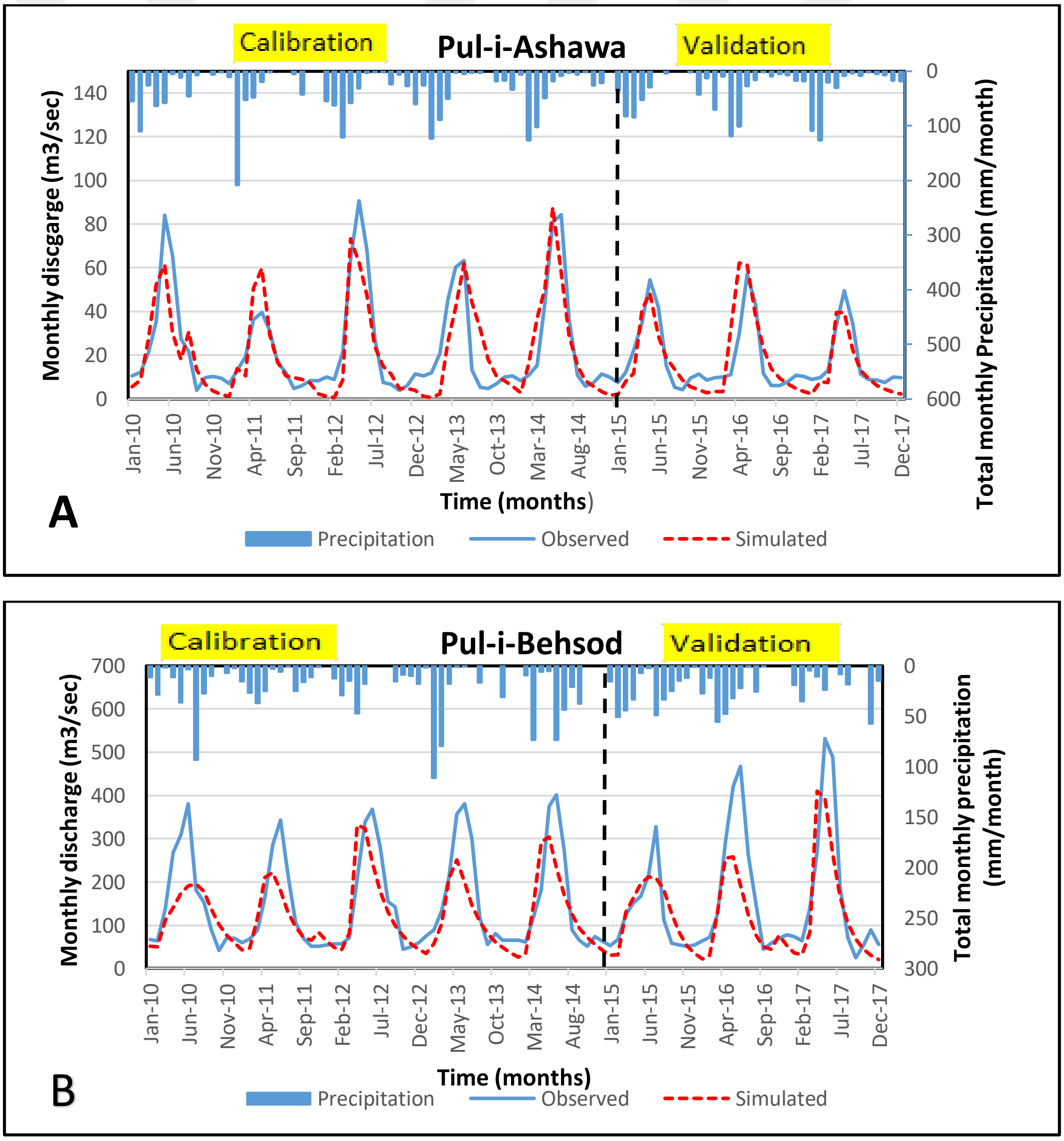

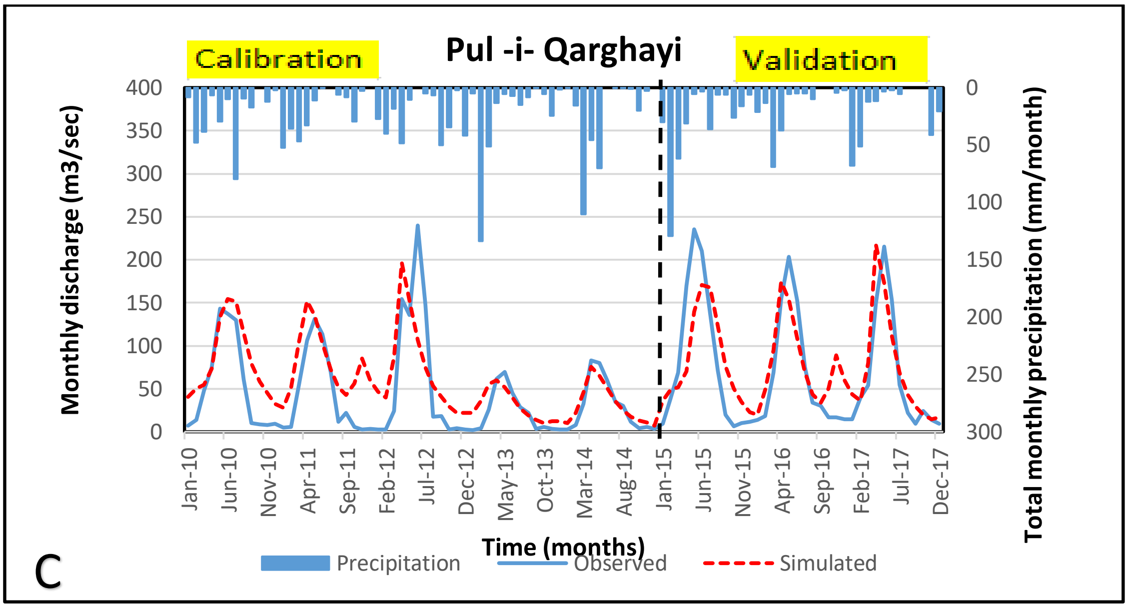

Calibration
Pul -i- Qarghayi
Validation
Monthly discharge (m3/sec)
Total monthly precipitation (mm/month)
Time (months)
Precipitation
Observed
Simulated
C

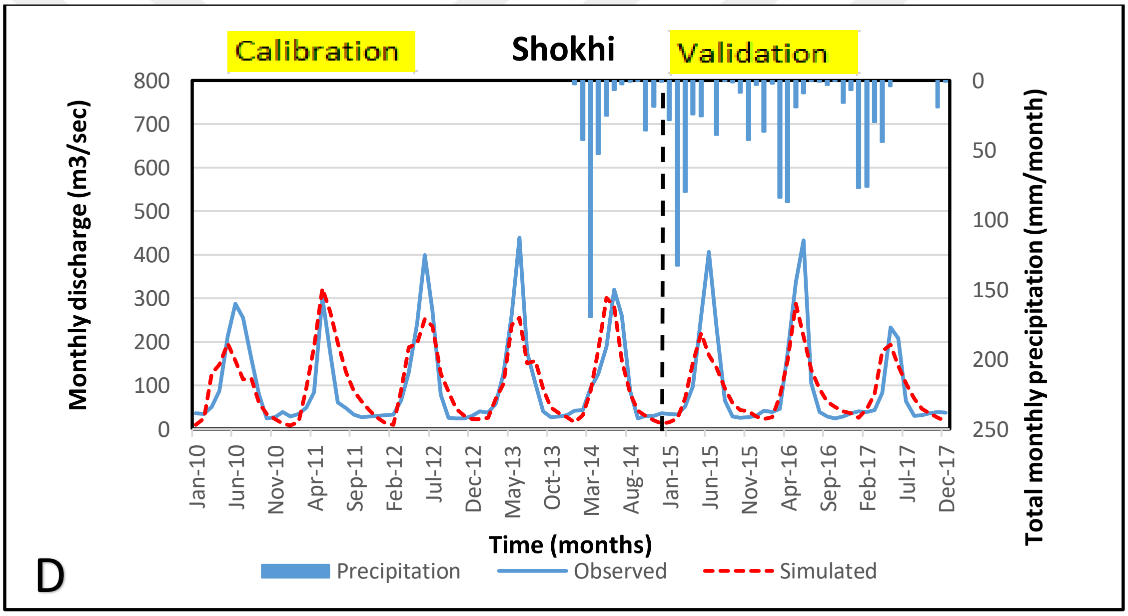

Calibration
Shokhi
Validation
Monthly discharge (m3/sec)
Total monthly precipitation (mm/month)
Time (months)
Precipitation
Observed
Simulated
D

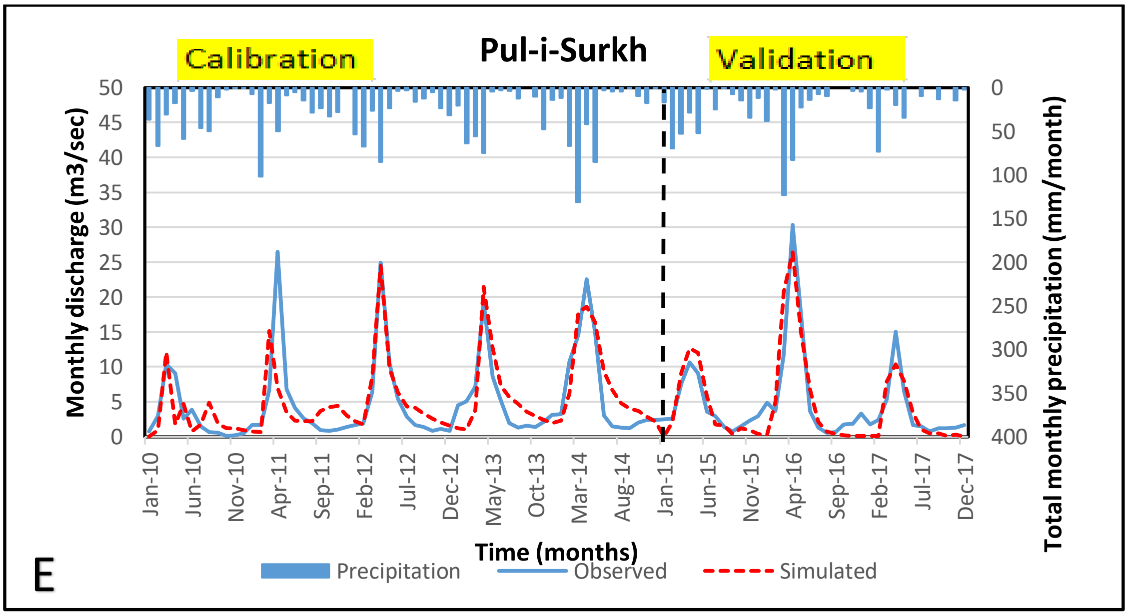

Calibration
Pul-i-Surkh
Validation
Monthly discharge (m3/sec)
Total monthly precipitation (mm/month)
Time (months)
Precipitation
Observed
Simulated
E

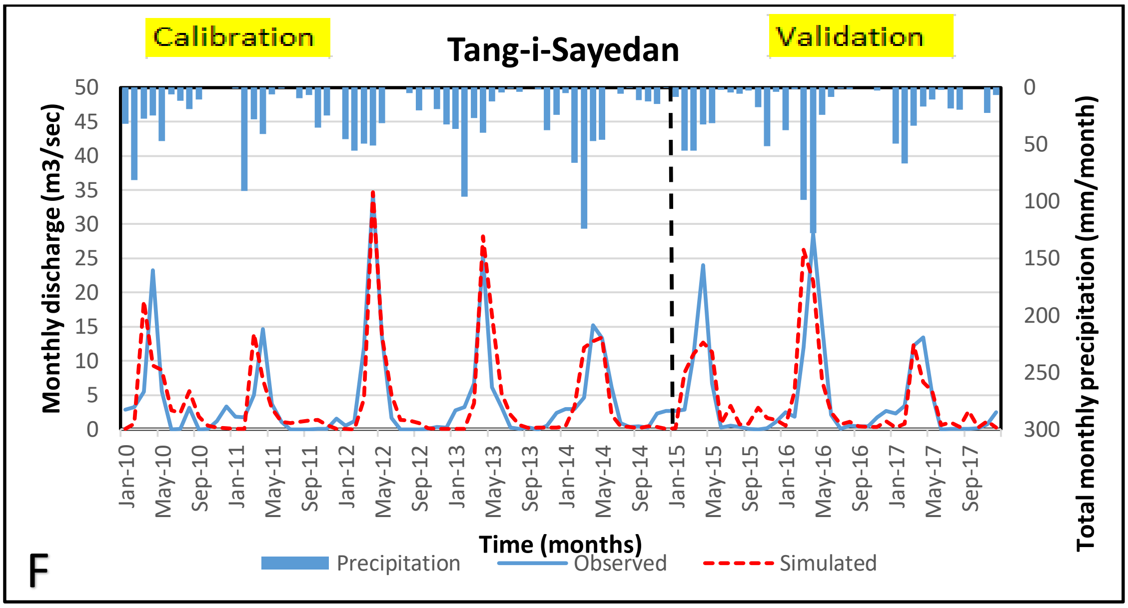

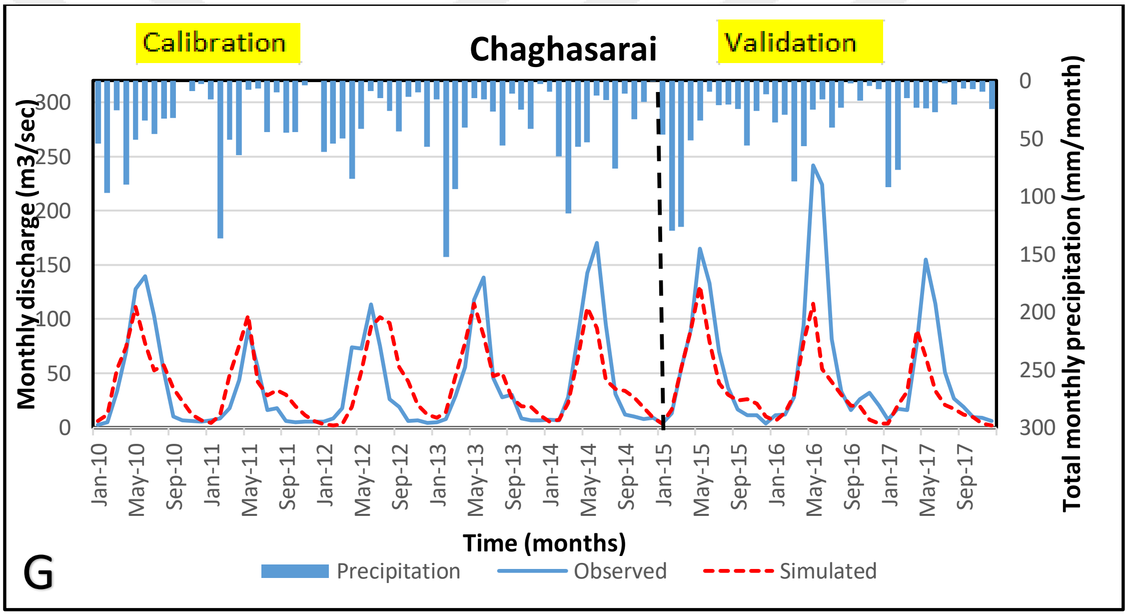

Figure 7. 16 Comparison between observed and simulated monthly discharge during calibration (2010-2014) and validation (2015-2017), at stations Pul-i-Ashawa (A), Pul-i-Behsod (B), Pul -i- Qarghayi (C), Shokhi (D), Pul-i-Surkh (E), Tang-i-Sayedan (F), Chaghasarai (G)

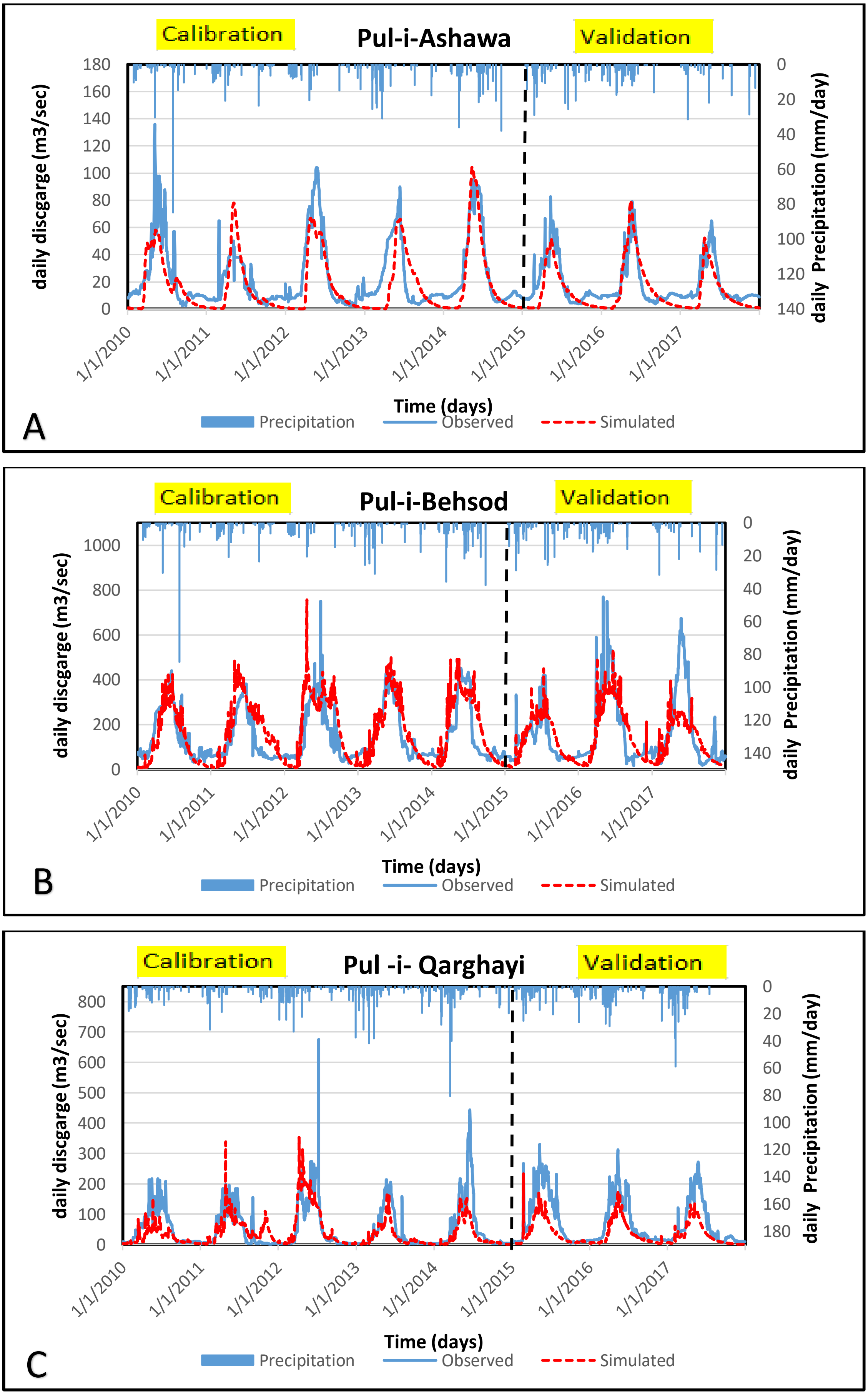
Calibration
Pul-i-Ashawa
Validation
daily discgarge (m3/sec)
daily Precipitation (mm/day)
0
20
40
60
80
100
120
140
160
180
0
20
40
60
80
100
120
140
1/1/2010
1/1/2011
1/1/2012
1/1/2013
1/1/2014
1/1/2015
1/1/2016
1/1/2017
Time (days)
Precipitation
Observed
Simulated
A
Calibration
Pul-i-Behsod
Validation
daily discgarge (m3/sec)
daily Precipitation (mm/day)
0
200
400
600
800
1000
0
20
40
60
80
100
120
140
1/1/2010
1/1/2011
1/1/2012
1/1/2013
1/1/2014
1/1/2015
1/1/2016
1/1/2017
Time (days)
Precipitation
Observed
Simulated
B
Calibration
Pul -i- Qarghayi
Validation
daily discgarge (m3/sec)
daily Precipitation (mm/day)
0
100
200
300
400
500
600
700
800
0
20
40
60
80
100
120
140
160
180
1/1/2010
1/1/2011
1/1/2012
1/1/2013
1/1/2014
1/1/2015
1/1/2016
1/1/2017
Time (days)
Precipitation
Observed
Simulated
C

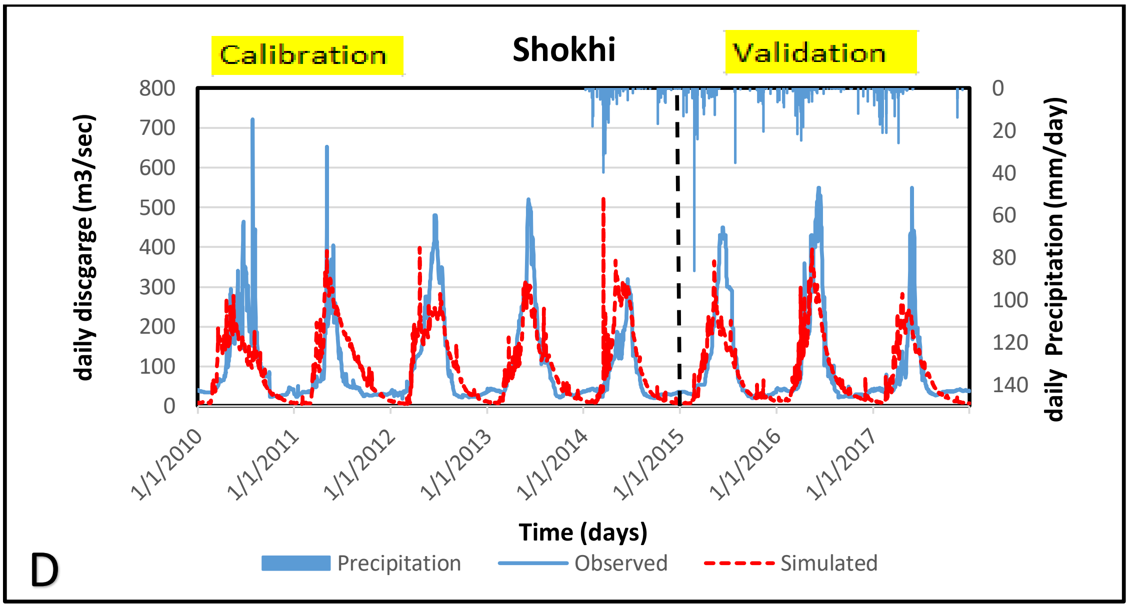
Calibration
Shokhi
Validation
daily discgarge (m3/sec)
daily Precipitation (mm/day)
800
700
600
500
400
300
200
100
0
0
20
40
60
80
100
120
140
1/1/2010
1/1/2011
1/1/2012
1/1/2013
1/1/2014
1/1/2015
1/1/2016
1/1/2017
Time (days)
Precipitation
Observed
Simulated
D

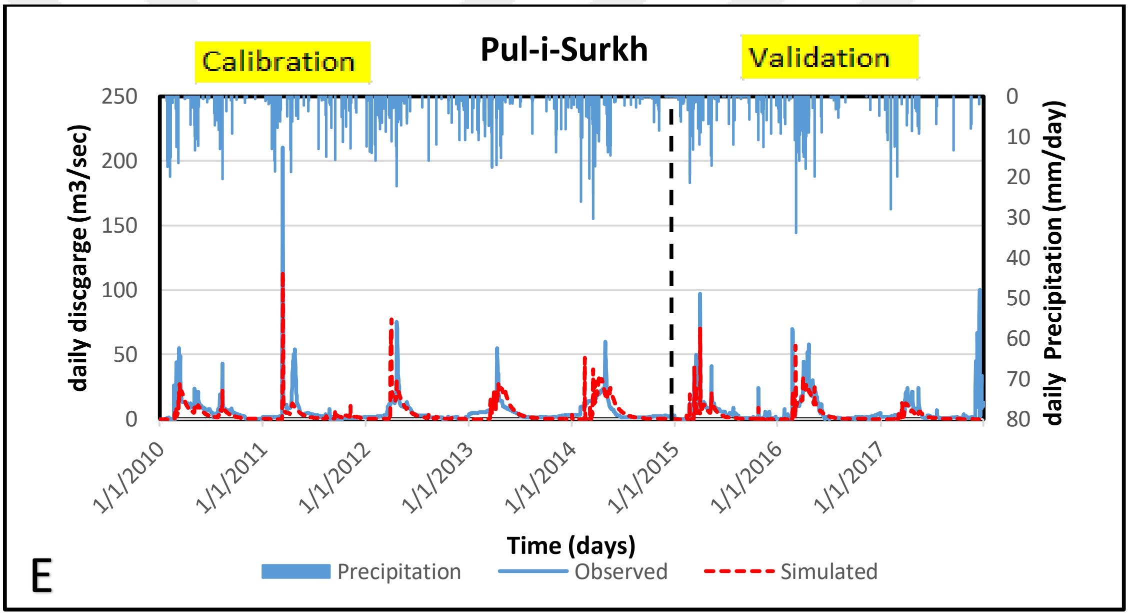
Calibration
Pul-i-Surkh
Validation
daily discgarge (m3/sec)
daily Precipitation (mm/day)
250
200
150
100
50
0
0
10
20
30
40
50
60
70
80
1/1/2010
1/1/2011
1/1/2012
1/1/2013
1/1/2014
1/1/2015
1/1/2016
1/1/2017
Time (days)
Precipitation
Observed
Simulated
E

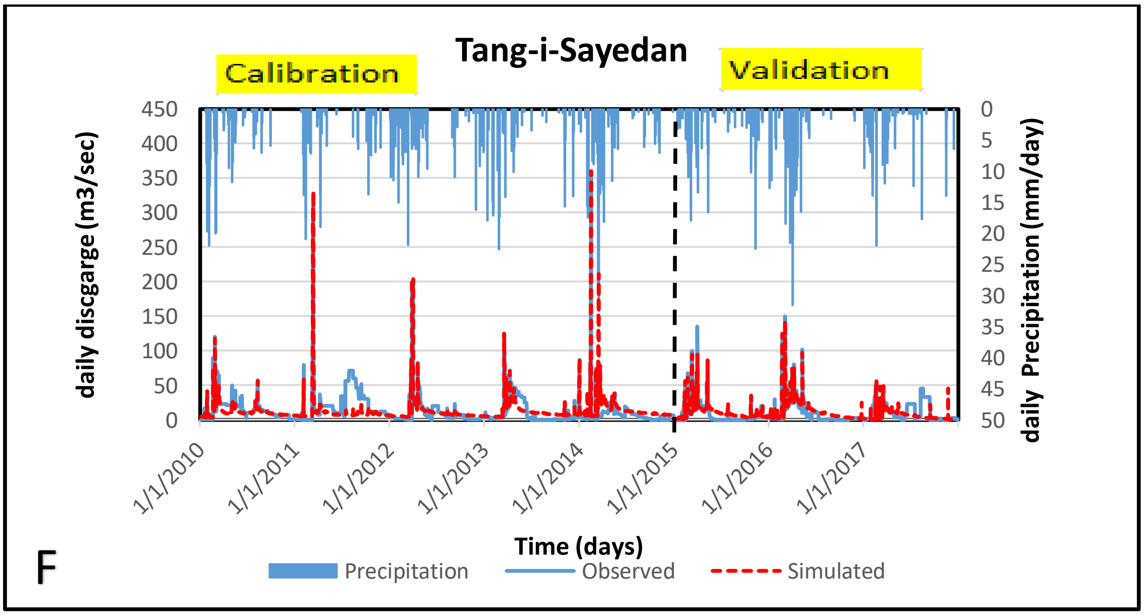
Tang-i-Sayedan
Calibration
Validation
daily discgarge (m3/sec)
daily Precipitation (mm/day)
450
400
350
300
250
200
150
100
50
0
0
5
10
15
20
25
30
35
40
45
50
1/1/2010
1/1/2011
1/1/2012
1/1/2013
1/1/2014
1/1/2015
1/1/2016
1/1/2017
Time (days)
Precipitation
Observed
Simulated
F

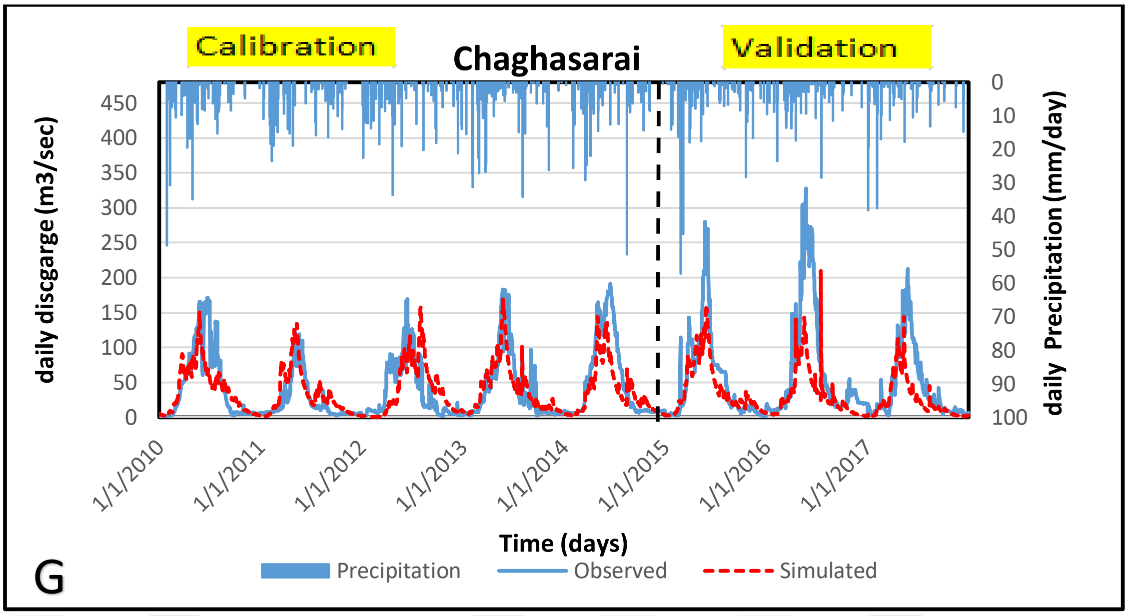

Figure 7. 17 Comparison between observed and simulated daily discharge during calibration (2010-2014) and validation (2015-2017), at stations Pul-i-Ashawa (A), Pul-i-Behsod (B), Pul -i- Qarghayi (C), Shokhi (D), Pul-i-Surkh (E), Tang-i-Sayedan (F), Chaghasarai (G)

CHAPTER 8

CONCLUSIONS AND RECOMMENDATIONS

Population growth, industrialization, deforestation, and unplanned human activities can rapidly alter climate parameters and land use, adversely affecting the hydrologic processes and hydrological cycle of the region in a long run. As such, land use, land cover, soil type, and climate of a specific region play an important role in analyzing basin flow. The most important part of the processes of streamflow analysis is to understand the hydrological processes and design an effective hydrologic model to represent the properties of the entire basin. In the field of water resource development, watershed based hydrologic models can be applied to assess the quantity and quality of water.

In the current study, rainfall-runoff modeling of the study area (Kabul river basin) was conducted using the ArcSWAT model together with remote sensing (GIS) techniques. Kabul river basin, which encompasses the majority land of the country, has been regularly faced with threats of hydro-meteorological disasters such as floods, droughts, etc in recent times. In order to understand the various hydrological processes taking place in the Kabul river basin, which covers an area of approximately 72000 km^2 with a very complex hydrological variability, a hydrological study of the basin was carried out using the SWAT model. The required SWAT input data, such as DEM, soil, land use/land cover were downloaded from the available global database and was cut to the specific study region (Kabul river basin), and another set of SWAT input data such as meteorological and hydrological data were taken from the ministry of energy and water. Available meteorological data (precipitation, maximum and minimum temperature) of 18 different meteorological stations were given as inputs to the model.

After the data were processed, SWAT 2012 was used to create parameters together with hydrologic components needed in the hydrological SWAT model. The entire basin was divided into 48 sub-basins and a total of 770 HRUs were generated by applying threshold values of 10 percent for land use, soil, and slope classes.

Finally, SWAT 2012 was run for a time period of 9 years (2009-2017) both on a monthly and daily time scales with a warm-up period of one year. The discharge values of each HRUs or each sub-basin were generated by the SWAT model on a monthly and daily time scale. SWAT-CUP with the SUFI-2 algorithm was used to calibrate the model output flow and to find the most sensitive parameters that have an effect on stream flow.

For the sensitivity analysis, the Latine Hypercube Sampling-One At a Time method was used to determine the sensitivity of each parameter. With the help of SWAT-CUP, the sensitivity analysis was performed on 27 different flow parameters. Out of 27 calibrated parameters, GWQMN.gw, SMTMP.bsn, CN2.mgt, PLAPS.sub, HRU_SLP.hru, SFTMP.bsn , SMFMN.bsn , SLSUBBSN.hru, GW_DELAY.gw, TLAPS.sub, TIMP.bsn, REVAPMN.gw, SOL_K(..).sol, ESCO.hru, SMFMX.bsn, SURLAG.bsn, SOL_AWC(..).sol, OV_N.hru, ALPHA_BF.gw, GW_REVAP.gw were found the most sensitive parameters and were taken into account for the process of calibration. A closer look at these sensitive parameters indicated that the flow characteristics of this region were highly influenced by groundwater, sub basins, and management parameters.

For the calibration process, SWAT-CUP with the SUFI-2 algorithm was run for seven different hydrological stations data with a number of simulation of 300. Observed stream flow data from each station for a period of 5 years (2010-2014) were given as input through auto calibration tool (SWAT-CUP). The values of Nash Sutcliff efficiency (NSE), R^2, and RSR for monthly scale simulation were found to be (0.71, 0.60, 0.53, 0.67, 0.60, 0.66, 0.65), (0.72, 0.66, 0.63, 0.67, 0.62, 0.70, 0.66), (0.54, 0.64, 0.68, 0.58, 0.63, 0.58, 0.59), respectively for Pul-i-Ashawa, Pul-i-Behsod, Pul-i-Qarghayi, Shokhi, Pul-i-Surkh, Tang-i-Sayedan, Chaghasarai stations and for daily scale simulation were found (0.59, 0.45, 0.48, 0.59, 0.47, 0.67, 0.60), (0.66, 0.63, 0.52, 0.60, 0.50, 0.57, 0.60), (0.64, 0.74, 0.72, 0.64, 0.73, 0.51, 0.63), respectively. The validation was also carried out by using the data of 3 years (2015-2017) and the values of Nash Sutcliff efficiency (NSE), R^2, and RSR for monthly scale simulation were found (0.63, 0.61, 0.69, 0.65, 0.81, 0.63, 0.48), (0.72, 0.68, 0.70, 0.71, 0.84, 0.64, 0.66), (0.61, 0.62, 0.56, 0.59, 0.43, 0.61, 0.72), respectively for Pul-i-Ashawa, Pul-i-Behsod, Pul-i-Qarghayi, Shokhi, Pul-i-Surkh, Tang-i-Sayedan, Chaghasarai stations and for daily scale simulation were found (0.63, 0.51, 0.44, 0.61, 0.47, 0.55, 0.63), (0.73, 0.56, 0.85, 0.64, 0.47, 0.60, 0.43), (0.61, 0.70, 0.75, 0.62, 0.77, 0.50, 0.76), respectively. This indicates that the model has sufficient capacity to represent the Kabul River basin.

Results in the study clearly indicates that the calibrated model sufficiently reveals the phenomena occurring within the hydrological regime. Although the data are limited, the final calibration and validation results for the Kabul river basin are acceptable. The time verse flow plots of the observed and simulated flows from various hydrological stations located within the basin show that the catchment rainfall-runoff is sufficiently simulated by the SWAT model. Finally, the following findings are concluded from SWAT modeling experience during the study:

1. The SWAT model is a useful tool that helps to accurately estimate various water balance components.
2. The SWAT modeling technique is useful in many aspects, such as analyzing of watershed hydrology, identifying hydrologically sensitive parameters, and it can delegate appropriate management activities in the basin.
3. This model can be applied to investigate the climatic, spatial, and temporal changes occurring within the study area and it can relate them to reality in a high accuracy manner.
4. The SWAT model is an appropriate tool that can be used to predict future flows with limited meteorological data and it is an effective tool for many different types of water resource and land management problems.
5. In the present study, two sub-basins (Gomal and Shamal) and some part of the Kunar sub-basins are not included in the analysis due to insufficient meteorological and hydrological data, that may effect on the total catchment runoff processes.

In the present study, only meteorological data, land use land cover data, soil data, and flow data for calibration and validation are used, all other things remained constant. However, changes in some parameters can also have a significant impact on catchment rainfall-runoff processes. These parameters, which have an impact on the rainfall-runoff process, may include changes in climate and soil management activities and other variables of land use.

In the present study, the following recommendations are suggested in future studies.

1. Further investigation should be done with complete land use land cover, soil, and meteorological data in the catchment area to check the overall accuracy.
2. In the present study, the SWAT model is calibrated only by observed flow data at seven different hydrological stations. To improve model performance, both in terms of quality and quantity, the weather stations should be improved. It is therefore highly recommended that a good network of both hydrological and meteorological stations should be established.

3. Since only river flows are calibrated and validated, it must be highlighted that other outputs presented in this study, such as sediment dynamics in response to land-use change, should be handled with care and, therefore, further study must be conducted in order to check the model performance for the available sediment data.
4. For better results, the government needs to place more meteorological and hydrological stations within the basin, especially in the upstream part of the basin.
5. In this study, only available rainfall, maximum and minimum temperature data are used. For a better simulation, other meteorological data such as wind speed, solar radiation, relative humidity must be applied, in order to get an appropriate result.

REFERENCES

Abdullah Aini. "Water Conservation in Afghanistan." *Developments in Sustainable Agriculture* 2 (2007): 51-58.

Abouabdillah Aziz. "Hydrological Modeling in a Data-Poor Mediterranean Catchment (Mergullil, Tunisia) Assessing Scenarios of Land Managment and Climate Change." PHD Thesis, Tuscia University of Viterbo, ITALY, 2009.

Afera Halefom, Ermias Sisay, Deepak Khare, Lakhwinder Singh, and Tesfa Worku. "Hydrological Modeling of Urban Catchment Using Semi-Distributed Model." *Journal of Modeling Earth Systems and Environment, Springer* Volume 3 (2017): 683-92.

Aggarwal Ashish, Srivastava P.K, Tiwari Aman, Chatterjee R.S, and Gupta D.K. "ArcSWAT Based Geospatial Modeling of Rainfall-Runoff Processes in Rupen Basin, Mehsana District, Gujarat." *Journal of Disaster Advances* Volume 12 (2019).

Ahmad Shukran Sahaar. "Erosion Mapping and Sediment Yield of the Kabul River Basin, Afghanistan." Master Thesis Colorado State University, 2013.

Bob Rout. "Water Management, Livestock and the Opium Economy How the Water Flows a Typology of Irrigation Systems in Afghanistan." Afghanistan Research and Evaluation Unit Issue Paper Series, 2008.

David Pullar , and Darren Springer "Towards Integrating Gis and Catchment Models." *Journal of Environmental Modelling and Software* 15 (2000): 451-59.

FAO. "Aquastat Country Profile – Afghanistan." Food and Agriculture Organization of the United Nations (FAO),Rome, Italy: 2012.

FAO. "Computation of Long-Term Annual Renewable Water Resources (Rwr)." 2016, http://www.fao.org/nr/water/aquastat/data/wrs/readPdf.html?f=AFG-WRS_eng.pdf.

FAO. "Soil Map of the World." International Soil Reference and Information Centre (ISRIC), Wageningen: 1997.

FAO, and Ministry of Energy and Water. "Water Availability and Management in Afghanistan." (2015).

Fazlullah Akhtar. "Water Availability and Demand Analysis in the Kabul River Basin, Afghanistan." PHD, thesis Rheinischen Friedrich-Wilhelms-Universität Bonn, 2017.

Goyal, Manish Kumar. "Engineering Hydrology.", 2016.

H. B. Manguerra, and B. A. Engel. "Hydrological Parameterization of Watersheds for Runoff Prediction Using SWAT." *Journal of the American Water Resources Association* volume 34, NO.5 (1998).

Hafizullah Rasoul, Rijan B. Kayastha, Bikas C. Bhattarai, Ahuti Shrestha, Hedayatullah Arian, and Richard Armstrong. "Estimation of Discharge from Upper Kabul River Basin, Afghanistan Using the Snowmelt Runoff Model." *Journal of Hydrology and Meteorology* Volume 9, No.1 (2015).

Icarda. "Needs Assessment on Soil and Water in Afghanistan Future Harvest Consortium to Rebuild Agriculture in Afghanistan." International Center for Agricultural Research in the Dry Areas, Aleppo, Syria, 2002.

J. R. Peterson, and J. M. Hamlett. "Hydrologic Calibration of the Swat Model in a Watershed Containing Fragipan Soil." *Journal of the American water resources association* Volume 34, NO.3 (1998).

Jan Sitterson, Chris Knightes, Rajbir Parmar, Kurt Wolfe, Muluken Muche, and Brian Avant. "An Overview of Rainfall-Runoff Model Types" United States Enviromental Protection Agency,Athens, Georgia, 2017.

Jurgen D. Garbrech, Jeanne M. Schneider, and Michael W. Van Liew. "Monthly Runoff Predictions Based on Rainfall Forecasts in a Small Oklahoma Watershed." *Journal of The American Water Resources Association* (2006).

Karim C. Abbaspour. "Swat Calibration and Uncertainty Programs (Swat Cup) User Manual." (2012).

M. P. Tripathi, R. K. Panda, N. S. Raghuwanshi, and R. Singh. "Hydrological Modelling of a Small Watershed Using Generated Rainfall in the Soil and Water Assessment Tool Model." *Journal of Hydrological Processes* Volume 18 (2004): 1811-21.

M. T. Vu, S. V. Raghavan, and S. Y. Liong. "SWAT Use of Gridded Observations for Simulating Runoff – a Vietnam River Basin Study." *Journal of Hydrology and Earth System Sciences* Volume 16 (2011): 2801–11.

M. Winchell , R. Srinivasan, M. Diluzio, and J. Arnold. "Arcswat Interface for Swat2012, User's Guide.", (2013).

Michael W. Van Liew, and Jurgen Garbrecht. "Hydrologic Simulation of the Little Washita River Experimental Watershed Using Swat." *Journal of the American Water Resources Association* Volume 39(2) (2003): 413-26.

Mohammad Tayib Bromand. "Impact Assessment of Climate Change on Water Resources in the Kabul River Basin, Afghanistan." Master thesis, Ritsumeikan University, 2015.

Mohsen Pourreza Bilondi, Karim C. Abbaspour , and Bijan Ghahraman. " Application of Three Different Calibration-Uncertainty Analysis Methods in a Semi-Distributed Rainfall-Runoff Model Application.". *Journal of Middle-East Scientific Research* Volume 15, NO.9 (2013): 1255-63.

Patricia Jimeno-Sáez, Javier Senent-Aparicio, Julio Pérez-Sánchez, and David Pulido-Velazquez. "A Comparison of Swat and Ann Models for Daily Runoff Simulation in Different Climatic Zones of Peninsular Spain." *Journal of water* (2018).

Qureshi, Asad Sarwar. "Water Resources Management in Afghanistan the Issues and Options." Pakistan, 2002).

R. L. Bingner, J. Garbrecht, J. G. Arnold, and R. Srinivasan. " Effect of Watershed Subdivision on Simulation Runoff and Fine Sediment Yield." *Transactions of the American Society of Agricultural Engineers* Volume 40, NO.5 (1997): 1329-35.

Raphy Favre, and Golam Monowar Kamal. "Watershed Atlas of Afghanistan.", 2004.

Rientjes, Thomas Henricus Maria. "Inverse Modelling of the Rainfall-Runoff Relation a Multi Objective Model Calibration Approach." PHD thesis, Deift University, 2004.

Rohtash, Dr. L. N. Thakural, Dr. M.K.Choudhary, and Dipti Tiwari. "Rainfall Runoff Modeling Using Swat Model for Chaliyr Basin Kerala , India." *Journal of International Science and Research* Volume 8, no. 5 (2018).

S.L.Neitsch, J.G. Arnold, J.R. Kiniry, and J.R. Williams. "Soil and Water Assessment Tool Theoretical Documentation." Grassland, Soil and Water Research Laboratory of Agricultural Research Service,TEMPLE, TEXAS, 2005.

Shanbor Kurbah, and Manoj Jain. " Rainfall-Runoff Modeling of a River Basin Using SWAT Model." *Journal of Engineering Research and Technology (IJERT)* Volume 6., no. 12 (2017).

Taha Aawar, and Deepak Khare. "Assessment of Climate Change Impacts on Streamflow through Hydrological Model Using SWAT Model a Case Study of Afghanistan." *Journal Modeling Earth Systems and Environment* Volume 6 (2020): 1427-37.

Tesfa Worku, Deepak Khare, and S. K. Tripathi. "Modeling Runoff–Sediment Response to Land Use/Land Cover Changes Using Integrated Gis and SWAT Model in the Beressa Watershed." *journal of Environmental Earth Sciences* 76:550 (2016). https://doi.org/DOI 10.1007/s12665-017-6883-3.

Thomas Pagano, and Soroosh Sorooshian. "Hydrologic Cycle." *Journal of the Earth system* Volume 1 (2002).

Tooryalay Ayoubi, and Dongshik Kang. "Assessing Impacts of Landuse/Landcover Change on Surface Runoff for Panjshir Watershed: A Watershed Modelling Approach." *International Journal of Engineering and Technical Research (IJETR)* Volume 6, Issue 1 (2016).

Tooryalay Ayoubi, and Kang Dongshik. "Panjshir Watershed Hydrologic Model Using Integrated Gis and Arcswat Interface." *International Journal of Geology, Earth & Environmental Sciences* Volume 6 (1) (2016): 145-61.

Torge Tünnermeier, and Georg Houben. "Hydrogeology of the Kabul Basin Part 1", Federal Institute for Geosciences and Natural Resources (BGR), Germany, 2003.

Umit Duru, Mazdak Arabi, and Ellen E. Wohl. "Modeling Stream flow and Sediment Yield Using the SWAT Model a Case Study of Ankara River Basin, Turkey." *Journal of Physical Geography* Volume 39, NO. 3 (2017): 264–89.

Valentin Aich, Noor Ahmad Akhundzadah, Alec Knuerr, Ahmad Jamshed Khoshbeen, Fred Hattermann, Heiko Paeth, Andrew Scanlon, and Eva Nora Paton. "Climate Change in Afghanistan Deduced from Reanalysis and Coordinated Regional Climate Downscaling Experiment (Cordex)—South Asia Simulations." *Journal of Climate* 5, no. 38 (2017).

Vikash Shivhare, M K Goel, and C K Singh. "Simulation of Surface Runoff for Upper Tapi Subcatchment Area (Burhanpur Watershed) Using SWAT." *The International Archives of the Photogrammetry, Remote Sensing and Spatial Information Sciences,Hyderabad, India* Volume XL-8, 2014 (2014).

World Bank. "Scoping Strategic Options for Development of the Kabul River Basin.", (2010).

Z. Simić, N. Milivojević, D. Prodanović, V. Milivojević, and N. Perović. "SWAT-Based Runoff Modeling in Complex Catchment Areas –Theoretical Background and Numerical Procedures." *Journal of the Serbian Society for Computational Mechanics* Volume 3, NO.1 (2009): 38-63.

APPENDIX A

Pul-i-Ashawa STATION					
Date	Observed Flow	SWAT simulated Flow	Date	Observed Flow	SWAT simulated Flow
Jan-10	10.55806	5.615	Jan-14	8.435484	2.672
Feb-10	12.2	8.677	Feb-14	10.83929	15.87
Mar-10	21.02903	27.379999	Mar-14	15.14516	36.759998
Apr-10	35.38334	52.41	Apr-14	43.86667	50.73
May-10	84.13677	61.490002	May-14	80.87096	87.639999
Jun-10	65.39	30.24	Jun-14	84.19666	57.740002
Jul-10	27.31613	17.870001	Jul-14	36.40323	29.059999
Aug-10	21.66455	30.58	Aug-14	10.87871	15.32
Sep-10	3.912333	13.21	Sep-14	5.726	8.412
Oct-10	9.770323	6.667	Oct-14	7.296774	5.969
Nov-10	10.2	3.755	Nov-14	11.33333	3.317
Dec-10	9.32258	2.092	Dec-14	9.870968	1.625
Jan-11	6.879355	1.23	Jan-15	7.519355	1.939
Feb-11	13.00929	13.79	Feb-15	12.075	7.968
Mar-11	19.41936	10.45	Mar-15	22.09355	11.56
Apr-11	36.23333	50.73	Apr-15	34.99	40.880001
May-11	39.60645	59.759998	May-15	54.39032	48.5
Jun-11	31.24667	29.440001	Jun-15	41.96	28.879999
Jul-11	16.92258	17	Jul-15	15.3371	18.84
Aug-11	11.92839	10.46	Aug-15	5.412903	13.72
Sep-11	4.663333	9.58	Sep-15	4.241333	8.501
Oct-11	6.145806	8.751	Oct-15	9.323871	5.477
Nov-11	8.32	7.34	Nov-15	11.29667	4.151
Dec-11	8.380645	2.185	Dec-15	8.629032	2.747
Jan-12	9.892903	1.238	Jan-16	9.729033	3.409
Feb-12	8.972414	0.7323	Feb-16	9.948276	3.375
Mar-12	21.22581	8.641	Mar-16	11.1129	31.98
Apr-12	63.94	73.160004	Apr-16	29.82833	62.310001
May-12	90.6129	62.400002	May-16	56.94194	61.330002
Jun-12	68.20667	47.560001	Jun-16	43.345	37.880001
Jul-12	28.06129	24.02	Jul-16	11.78387	23.209999
Aug-12	7.471613	15.04	Aug-16	6.214516	13.76
Sep-12	6.659333	11.26	Sep-16	6.257	9.357
Oct-12	3.863871	4.8	Oct-16	7.710968	6.874
Nov-12	6.128667	4.868	Nov-16	10.83	4.608
Dec-12	11.38581	3.91	Dec-16	10.32903	3.424
Jan-13	10.45714	1.029	Jan-17	8.939355	2.364
Feb-13	11.89032	0.6657	Feb-17	9.758572	7.818
Mar-13	20.68387	2.183	Mar-17	12.93903	7.523
Apr-13	44.96667	25.82	Apr-17	34.08	39.650002
May-13	60.25806	41.810001	May-17	49.41613	39.509998
Jun-13	63.25667	61.990002	Jun-17	34.59	22.379999
Jul-13	13.22129	44.150002	Jul-17	11.2729	13.15
Aug-13	5.207097	31.690001	Aug-17	8.976774	9.442
Sep-13	4.7	18	Sep-17	8.514667	6.084
Oct-13	7.002581	10.31	Oct-17	7.425161	4.594
Nov-13	10.09333	8.444	Nov-17	9.941334	3.126
Dec-13	10.5871	5.967	Dec-17	9.832258	2.136

APPENDIX B

Pul-i-Behsod STATION					
Date	Observed Flow	SWAT simulated Flow	Date	Observed Flow	SWAT simulated Flow
Jan-10	67.5742	51.33	Jan-14	64.81935	26.99
Feb-10	64.23572	50.45	Feb-14	60.78571	35.19
Mar-10	137.9355	111.1	Mar-14	118.0645	146
Apr-10	267.6667	140.2	Apr-14	182.8667	292.6
May-10	309.8387	174	May-14	375.5807	304.6
Jun-10	380.3333	191.6	Jun-14	401.2333	232.3
Jul-10	181.7097	194.7	Jul-14	271.3226	170.5
Aug-10	153.5484	178.3	Aug-14	89.70968	126
Sep-10	90.94666	137.4	Sep-14	64.83334	93.75
Oct-10	41.59355	102.3	Oct-14	52.03226	72.09
Nov-10	71.42	77.18	Nov-14	74.08	55.65
Dec-10	69.21935	58.04	Dec-14	62.00645	41.87
Jan-11	60.22581	43.05	Jan-15	53.46452	30.41
Feb-11	68.86429	47.52	Feb-15	66.30714	32.29
Mar-11	89.53548	118.9	Mar-15	123.871	129.5
Apr-11	164.9667	210	Apr-15	151	161.7
May-11	285.8065	221.7	May-15	167.4194	196.1
Jun-11	342.9333	179.2	Jun-15	216.9	212.4
Jul-11	219.6194	131.4	Jul-15	328.3548	209.4
Aug-11	105.6129	96.22	Aug-15	112.5806	182.1
Sep-11	69.39333	72.38	Sep-15	59.16667	126.8
Oct-11	51.12903	65.45	Oct-15	54.35484	81.68
Nov-11	52.02	84.11	Nov-15	50.96667	53.61
Dec-11	54.67742	63.47	Dec-15	54.03226	35.19
Jan-12	57.57419	48.18	Jan-16	64.22581	22.65
Feb-12	57.13104	42.62	Feb-16	72.79311	30.56
Mar-12	71.56129	81.74	Mar-16	125.9032	130.4
Apr-12	208.9333	331.7	Apr-16	292	255
May-12	338.3871	323.9	May-16	421.4839	258.2
Jun-12	368.3333	245.3	Jun-16	467.4	192.2
Jul-12	281.8387	178.4	Jul-16	262.0968	123.9
Aug-12	155	131	Aug-16	146.4113	77.3
Sep-12	142.1333	99.53	Sep-16	43.98	49.54
Oct-12	44.67419	75.02	Oct-16	58.94839	44.58
Nov-12	50.2	57.09	Nov-16	69.56667	76.34
Dec-12	60.46129	43.91	Dec-16	78.03226	53.23
Jan-13	75.90323	34.61	Jan-17	73.3	35.82
Feb-13	89.28571	57.69	Feb-17	64.53214	32.56
Mar-13	133.7097	103.1	Mar-17	139.1129	83.94
Apr-13	210.6667	208.2	Apr-17	270.3667	410.2
May-13	356.9355	251.1	May-17	531.2903	393
Jun-13	380.3333	199.2	Jun-17	488	263.2
Jul-13	299.8387	146.4	Jul-17	189.2258	166.4
Aug-13	118.2258	108.4	Aug-17	70.39677	104.7
Sep-13	55.16667	80.72	Sep-17	24.80967	68.4
Oct-13	80.32258	61.56	Oct-17	54.73064	44.76
Nov-13	65	48.48	Nov-17	88.635	30.19
Dec-13	65.70968	36.8	Dec-17	55.20807	20.79

APPENDIX C

Pul -i- Qarghayi STATION					
Date	Observed Flow	SWAT simulated Flow	Date	Observed Flow	SWAT simulated Flow
Jan-10	7.496774	40.53	Jan-14	2.628387	10.55
Feb-10	14.08214	50.56	Feb-14	8.111786	22.33
Mar-10	48.15807	54.63	Mar-14	32.23484	45.99
Apr-10	75.19	73.41	Apr-14	83.37	75.84
May-10	143.0774	133.8	May-14	80	65.35
Jun-10	137.2533	154.7	Jun-14	60	51.37
Jul-10	129.9129	151.8	Jul-14	35	35.51
Aug-10	60.99677	115	Aug-14	30.32258	25.05
Sep-10	10.30667	79.45	Sep-14	11.5	17.87
Oct-10	9.190323	58.83	Oct-14	4.084516	13.65
Nov-10	8.387333	44.89	Nov-14	5.912667	10.93
Dec-10	9.828387	32.87	Dec-14	3.449032	7.38
Jan-11	5.200645	28.49	Jan-15	9.612904	36.66
Feb-11	5.913571	51.26	Feb-15	38.62143	48.72
Mar-11	53.31936	103.3	Mar-15	68.71935	52
Apr-11	105.8967	152.3	Apr-15	169.8	70.46
May-11	131.3774	135	May-15	235.129	139.2
Jun-11	113.24	103.2	Jun-15	210.0667	170.9
Jul-11	69.67742	72.56	Jul-15	137.3548	167.6
Aug-11	12.08323	52.09	Aug-15	71.50967	123.1
Sep-11	21.938	43.08	Sep-15	20	76.18
Oct-11	6.147097	56.45	Oct-15	6.954839	50.46
Nov-11	2.606	85.58	Nov-15	10.23333	34.67
Dec-11	3.572903	59.07	Dec-15	11.81936	22.96
Jan-12	2.585806	46.4	Jan-16	14.3871	19.93
Feb-12	3.228966	40.12	Feb-16	18.82759	48.81
Mar-12	24.06839	86.95	Mar-16	68.87096	95.21
Apr-12	154.5167	196.5	Apr-16	154.2633	174.2
May-12	135.9355	152.6	May-16	203.1194	153.4
Jun-12	239.5667	107	Jun-16	152.75	108.9
Jul-12	147.6	75.14	Jul-16	75.73548	69.53
Aug-12	17.79484	53.17	Aug-16	34.21774	44.03
Sep-12	18.12667	40.52	Sep-16	30.385	34.38
Oct-12	3.046774	29.42	Oct-16	16.70968	50.6
Nov-12	4.077333	22.29	Nov-16	16.96667	89.04
Dec-12	2.517419	22.52	Dec-16	14.6129	60.27
Jan-13	2.423226	22.35	Jan-17	14.85968	43.87
Feb-13	4.741071	36.46	Feb-17	39.69286	36.19
Mar-13	25.6471	55.96	Mar-17	54.20968	80.31
Apr-13	61.30667	60.05	Apr-17	149.4667	217.8
May-13	70	51.74	May-17	215.5484	172.9
Jun-13	45	39.99	Jun-17	152.975	111.2
Jul-13	29.03871	27.52	Jul-17	54.78548	68.99
Aug-13	21.91484	19.46	Aug-17	22.35	42.94
Sep-13	3.869333	13.93	Sep-17	9.398	29.95
Oct-13	5.710968	10.14	Oct-17	24.72387	19.94
Nov-13	3.481333	12.61	Nov-17	14.162	14.4
Dec-13	2.939355	12.71	Dec-17	9.537742	17.12

APPENDIX D

Shokhi STATION					
Date	Observed Flow	SWAT simulated Flow	Date	Observed Flow	SWAT simulated Flow
Jan-10	36.78064	9.326	Jan-14	43	15.94
Feb-10	34.85714	24.53	Feb-14	44	32.5
Mar-10	51.49032	127.7	Mar-14	94.5	86.84
Apr-10	88.44666	148.6	Apr-14	126	180.2
May-10	212.5161	196.8	May-14	189	300.7
Jun-10	287.3667	157.5	Jun-14	320	282.1
Jul-10	256.0645	113.9	Jul-14	260	156.4
Aug-10	161.5936	115.5	Aug-14	87.6	82.1
Sep-10	78.54667	59.91	Sep-14	25.2	42.14
Oct-10	24.67742	35.37	Oct-14	30	29.96
Nov-10	27.03333	23.07	Nov-14	31	20.59
Dec-10	39.48387	12.71	Dec-14	36	12.94
Jan-11	29.19677	8.982	Jan-15	34.80645	15.39
Feb-11	35.53929	16.88	Feb-15	33.32143	23.94
Mar-11	48.93548	95.93	Mar-15	52.64516	71.05
Apr-11	85.27	189.3	Apr-15	97.5	153.3
May-11	302.8065	323.8	May-15	260	220.8
Jun-11	177.2833	269.9	Jun-15	406.3333	169.5
Jul-11	61.05484	197.6	Jul-15	233.1613	140.8
Aug-11	48.18065	130.7	Aug-15	65.32258	93.72
Sep-11	33.66667	87.16	Sep-15	29.5	59.92
Oct-11	27.46774	64.83	Oct-15	26.80645	44.13
Nov-11	29.33333	42.87	Nov-15	27.9	40.97
Dec-11	30.09678	26.28	Dec-15	31.03226	28.5
Jan-12	32.49677	14.77	Jan-16	42.16129	23.5
Feb-12	32.99655	9.326	Feb-16	38.93103	28.02
Mar-12	65.72581	89.41	Mar-16	46.25806	76.19
Apr-12	129.8667	187.4	Apr-16	174.33	157.6
May-12	241.871	196	May-16	338.3452	287.8
Jun-12	399.4516	252	Jun-16	432.9667	212.5
Jul-12	271.5333	236.9	Jul-16	105.3839	136.5
Aug-12	78.54516	127.9	Aug-16	39.08387	92.17
Sep-12	25.43333	86.5	Sep-16	28.4	62.58
Oct-12	25.32258	46.05	Oct-16	25.06452	51.35
Nov-12	24.5	30.8	Nov-16	28.86667	40.23
Dec-12	30.67742	22.9	Dec-16	35.90323	35.8
Jan-13	40.7129	22.59	Jan-17	41.48387	25.44
Feb-13	37.80357	26.02	Feb-17	39.97143	46.99
Mar-13	58.64516	70.73	Mar-17	43.54839	80.86
Apr-13	128	103.4	Apr-17	83.23666	178.5
May-13	264.3548	239.4	May-17	233.7645	193.4
Jun-13	439.2	254.8	Jun-17	208.6267	145.2
Jul-13	176.2323	151	Jul-17	64.39032	105.4
Aug-13	104.6129	157.1	Aug-17	30.77581	70.81
Sep-13	40.6	92.74	Sep-17	32.72333	47.43
Oct-13	28.06452	49.88	Oct-17	36.6129	36.31
Nov-13	28.8	36.2	Nov-17	39.72333	26.36
Dec-13	32.57097	27.68	Dec-17	38.49355	18.81

APPENDIX E

Pul-i-Surkh STATION					
Date	Observed Flow	SWAT simulated Flow	Date	Observed Flow	SWAT simulated Flow
Jan-10	0.707097	0.0476	Jan-14	3.258065	2.308
Feb-10	2.9625	0.9457	Feb-14	10.735714	6.151
Mar-10	10.383871	12.09	Mar-14	14.567742	17.8
Apr-10	9.083333	1.714	Apr-14	22.593334	18.6
May-10	2.557419	4.685	May-14	15.048388	16.39
Jun-10	3.880333	0.7194	Jun-14	3.05	9.311
Jul-10	1.439032	1.78	Jul-14	1.500645	6.74
Aug-10	0.641935	4.832	Aug-14	1.284194	4.814
Sep-10	0.581333	1.861	Sep-14	1.234	4.048
Oct-10	0.080323	1.232	Oct-14	2.03871	3.638
Nov-10	0.229333	1.159	Nov-14	2.4	2.896
Dec-10	0.427419	0.9242	Dec-14	2.370645	2.256
Jan-11	1.670968	0.7356	Jan-15	2.472903	0.0318
Feb-11	1.655714	0.623	Feb-15	2.546429	2.143
Mar-11	6.700645	15.16	Mar-15	7.654516	9.143
Apr-11	26.483334	6.937	Apr-15	10.663333	12.63
May-11	6.752258	3.491	May-15	9.060645	12.05
Jun-11	4.142334	2.332	Jun-15	3.556333	5.765
Jul-11	2.59871	2.177	Jul-15	2.944516	1.784
Aug-11	1.89871	2.181	Aug-15	1.352258	1.545
Sep-11	0.968333	3.713	Sep-15	0.781	0.4175
Oct-11	0.84129	4.191	Oct-15	1.438387	1.209
Nov-11	1.064	4.375	Nov-15	2.333667	0.9048
Dec-11	1.374194	3.027	Dec-15	2.9	0.3697
Jan-12	1.624194	2.21	Jan-16	4.897742	0.3326
Feb-12	1.955172	1.742	Feb-16	3.646552	4.985
Mar-12	6.465806	8.579	Mar-16	11.749355	20.68
Apr-12	24.92	24.44	Apr-16	30.363333	26.41
May-12	10.438709	9.679	May-16	17.531612	14.91
Jun-12	5.414333	6.363	Jun-16	3.671667	6.793
Jul-12	2.845806	4.346	Jul-16	1.292194	2.115
Aug-12	1.635484	4.117	Aug-16	0.607742	0.786
Sep-12	1.367333	3.301	Sep-16	0.619	0.3597
Oct-12	0.846452	2.558	Oct-16	1.725806	0.1662
Nov-12	1.1025	1.983	Nov-16	1.81	0.1197
Dec-12	0.831452	1.568	Dec-16	3.325806	0.1145
Jan-13	4.545161	1.238	Jan-17	1.739355	0.0643
Feb-13	5.092857	1.024	Feb-17	2.352857	0.0858
Mar-13	7.112903	3.737	Mar-17	5.343871	7.936
Apr-13	19.216667	21.41	Apr-17	15.0535	10.36
May-13	8.596774	12.77	May-17	6.518774	7.963
Jun-13	5.183333	7.272	Jun-17	1.658067	3.364
Jul-13	1.922581	5.733	Jul-17	1.509419	0.9853
Aug-13	1.316129	4.648	Aug-17	0.775452	0.4327
Sep-13	1.55	3.568	Sep-17	1.2291	0.4565
Oct-13	1.353226	2.923	Oct-17	1.215161	0.1364
Nov-13	2.15	2.376	Nov-17	1.276533	0.2964
Dec-13	3.145161	1.901	Dec-17	1.684968	0.0431

APPENDIX F

Tang-i-Sayedan STATION					
Date	Observed Flow	SWAT simulated Flow	Date	Observed Flow	SWAT simulated Flow
Jan-10	2.890645	0.0274	Jan-14	2.993548	0.4399
Feb-10	3.237857	0.762	Feb-14	2.982143	3.298
Mar-10	5.48	18.78	Mar-14	4.647097	11.96
Apr-10	23.292	9.279	Apr-14	15.192	12.91
May-10	5.580645	8.684	May-14	13.3529	13.46
Jun-10	0	2.732	Jun-14	6.117333	2.125
Jul-10	0.076452	2.43	Jul-14	0.907742	0.4385
Aug-10	3.107742	5.547	Aug-14	0.367419	0.3337
Sep-10	0	1.853	Sep-14	0.412	0.1614
Oct-10	0.068065	0.5631	Oct-14	0.226452	0.3845
Nov-10	1.137	0.2375	Nov-14	2.294	0.3504
Dec-10	3.335484	0.1064	Dec-14	2.639032	0.0972
Jan-11	1.88	0.0461	Jan-15	2.709677	0.1351
Feb-11	1.718214	0.017	Feb-15	2.863571	8.295
Mar-11	4.971935	14	Mar-15	10.7829	11
Apr-11	14.672	7.288	Apr-15	24.01267	12.73
May-11	3.74129	3.057	May-15	6.673548	11.32
Jun-11	1.069333	1.101	Jun-15	0.2785	0.836
Jul-11	0	0.8584	Jul-15	0.47971	3.428
Aug-11	0	1.096	Aug-15	0.370806	0.7236
Sep-11	0	1.282	Sep-15	0.077233	0.7611
Oct-11	0.021613	1.372	Oct-15	0.002419	3.135
Nov-11	0.095	0.6476	Nov-15	0.182	1.615
Dec-11	1.514194	0.1009	Dec-15	1.127097	1.402
Jan-12	0.550323	0.0192	Jan-16	2.496774	0.5678
Feb-12	1.217586	0.0037	Feb-16	1.867414	5.615
Mar-12	12.0129	4.433	Mar-16	11.89468	26.28
Apr-12	34.36334	34.63	Apr-16	28.597	21.62
May-12	13.60129	13.72	May-16	15.25048	7.075
Jun-12	1.654333	5.013	Jun-16	2.120243	2.533
Jul-12	0	1.366	Jul-16	0.047742	0.6654
Aug-12	0	1.277	Aug-16	0.54901	1.111
Sep-12	0	0.8739	Sep-16	0.464427	0.4135
Oct-12	0.016774	0.1969	Oct-16	0.416803	0.3649
Nov-12	0.308	0.0978	Nov-16	1.785943	0.3757
Dec-12	0.274516	0.0656	Dec-16	2.6955	1.152
Jan-13	2.752903	0.0415	Jan-17	2.311935	0.2824
Feb-13	3.227143	0.0127	Feb-17	3.4	0.8114
Mar-13	6.70129	3.755	Mar-17	12.26258	12.4
Apr-13	25.24133	28.26	Apr-17	13.47733	6.868
May-13	6.10129	16.7	May-17	5.069032	5.544
Jun-13	3.193	5.317	Jun-17	0.005567	0.5865
Jul-13	0.25871	2.089	Jul-17	0.072452	1.015
Aug-13	0.079355	0.6403	Aug-17	0.030871	0.3153
Sep-13	0.254333	0.169	Sep-17	0.042353	2.721
Oct-13	0	0.2632	Oct-17	0.127006	0.2763
Nov-13	0.528333	0.2001	Nov-17	0.75398	1.214
Dec-13	2.35871	0.2267	Dec-17	2.499032	0.2002

APPENDIX G

Chaghasarai STATION					
Date	Observed Flow	SWAT simulated Flow	Date	Observed Flow	SWAT simulated Flow
Jan-10	2.568064	6.132	Jan-14	6.967742	5.655
Feb-10	4.702143	11.84	Feb-14	6.857143	7.249
Mar-10	33.32903	53.8	Mar-14	27.70323	22.34
Apr-10	69.28	74.11	Apr-14	83.65334	63.13
May-10	127.6677	111.5	May-14	142.5161	110.8
Jun-10	139.36	77.54	Jun-14	170.1667	91.88
Jul-10	103.1548	52.53	Jul-14	94.62581	43.65
Aug-10	52.38387	57.18	Aug-14	30.98387	35.64
Sep-10	9.832	36.1	Sep-14	11.784	33.81
Oct-10	6.439355	24.18	Oct-14	9.82258	27.62
Nov-10	6.030334	11.95	Nov-14	7.883333	18.47
Dec-10	5.600323	6.325	Dec-14	8.758064	8.765
Jan-11	6.387742	3.979	Jan-15	3.589677	3.631
Feb-11	8.08	11.49	Feb-15	13.09107	16.44
Mar-11	17.76129	48.82	Mar-15	55.07419	54.97
Apr-11	43.87667	75.69	Apr-15	90.26667	90.46
May-11	90.35162	103.4	May-15	165.0968	130.5
Jun-11	54.93	42.19	Jun-15	133.2	79.1
Jul-11	15.80645	29.82	Jul-15	69.58064	40.75
Aug-11	17.78387	34.4	Aug-15	36.85161	30.47
Sep-11	6.076667	30.06	Sep-15	16.46	24.61
Oct-11	4.828387	19.56	Oct-15	11.04548	25.78
Nov-11	5.666667	11.53	Nov-15	11.015	21.69
Dec-11	5.354839	5.972	Dec-15	3.522258	9.831
Jan-12	5.485806	3.057	Jan-16	11.15258	5.72
Feb-12	8.282069	1.69	Feb-16	12.06483	13.94
Mar-12	17.52258	2.909	Mar-16	28.0629	29.7
Apr-12	74.22	19.03	Apr-16	94.25	78.65
May-12	72.63871	51.87	May-16	242.1129	114.4
Jun-12	113.8067	93.15	Jun-16	224.1167	53.6
Jul-12	75.3871	101.7	Jul-16	81.82581	42.1
Aug-12	25.94194	96.52	Aug-16	33.09678	30.37
Sep-12	19.19	55.69	Sep-16	15.92	20.19
Oct-12	5.859355	42.88	Oct-16	25.8629	19.38
Nov-12	6.621	20.93	Nov-16	31.76167	6.948
Dec-12	4.434839	12.02	Dec-16	20.21936	3.314
Jan-13	4.705161	8.764	Jan-17	7.099032	3.453
Feb-13	8.04	14.43	Feb-17	16.99286	19.99
Mar-13	29.03226	47.22	Mar-17	15.79323	32.93
Apr-13	55.50333	78.14	Apr-17	77.235	90.1
May-13	117.7258	114.4	May-17	155.2613	64.87
Jun-13	138.3267	84.5	Jun-17	114.4567	33.59
Jul-13	45.43871	47.3	Jul-17	50.79516	20.99
Aug-13	28.06452	50.05	Aug-17	26.95	17.37
Sep-13	30.47667	27.43	Sep-17	19.24	11.6
Oct-13	8.443226	19.35	Oct-17	9.438709	9.447
Nov-13	6.81	19.23	Nov-17	9.185	3.607
Dec-13	6.591613	11.14	Dec-17	5.802903	2.053